

Department of Chemical Engineering at Worcester Polytechnic Institute

Molecular Dynamics
Studies of Polymer
Systems

Jonathan Gay
4/26/2012

Abstract

The goal of this work was to determine if molecular dynamics as represented by the United-Atom method employed by the DL_POLY2 software package could explain polymer phenomena such as melting point temperature, glass transition temperature, crystallization, and density, and assess the effect of side group length, branching, chemical structure, length of polymer, and temperature. The verified model will then serve as a confident tool in the prediction of the properties of polymeric systems. The aim was to apply molecular dynamics simulations to polymers relevant to the running shoe industry.

Acknowledgements

I would like to thank Professor N. A. Deskins and Thomas Gabry for all their help. I know I asked for a lot over the past year. I appreciate all the support, guidance, and assistance they provided.

Table of Contents

ABSTRACT	1
ACKNOWLEDGEMENTS	2
TABLE OF CONTENTS	3
TABLE OF FIGURES	6
TABLE OF TABLES	8
TABLE OF EQUATIONS	9
INTRODUCTION	10
MOTIVATION: RUNNING SHOES	10
PROJECT GOALS	10
BACKGROUND	11
POLYMERS	11
<i>Properties</i>	11
<i>Polymerization, or Growth of Polymers</i>	11
<i>Basic Structures of Polymers Examined</i>	12
<i>Degree of Polymerization</i>	13
<i>Critical Molecular weights</i>	14
<i>Branching</i>	14
<i>Crosslinking</i>	14
<i>Foams</i>	15
COMPUTATIONAL CHEMISTRY AND MOLECULAR DYNAMICS	15
<i>Basic Theory</i>	15
PREVIOUS MOLECULAR DYNAMICS SIMULATIONS OF POLYMERS	17
<i>Polymer Collapse</i>	17
<i>Temperature Effects on Density in Dense Polymer Systems</i>	17
<i>Branching Effects on Bulk Properties</i>	18
<i>Transferable Potentials for Phase Equilibria United-Atom (TraPPE-UA)</i>	18
METHODOLOGY	20
PROGRAMS	20
<i>DL_POLY</i>	20
<i>DL_FIELD</i>	21
<i>McVol</i>	21
<i>Visual Molecular Dynamics (VMD)</i>	21
UNITED ATOM FORCE FIELD	21
SIMULATIONS	25
<i>Parameters</i>	25
<i>Polymers</i>	25
<i>Polymer Chain Length</i>	25
<i>Pressure</i>	25
<i>Density</i>	26

<i>Crystallization</i>	26
<i>Melting Point</i>	26
RESULTS	27
POLYMER STRUCTURE - CHAIN LENGTH EFFECTS	27
<i>Globule Formation</i>	27
<i>Volume Calculations</i>	31
<i>Polymer System Energy</i>	33
POLYMER STRUCTURE - BRANCHING EFFECTS (300K)	34
POLYMER STRUCTURE – TEMPERATURE EFFECTS	36
DENSITY	36
<i>Pressure and Simulation Time Effects</i>	36
<i>Chain Length and Number of Chain Effects</i>	37
<i>Equilibration Effects</i>	38
<i>Branching Effects</i>	38
CRYSTALLIZATION / MELTING	39
<i>Melting Point Determination</i>	41
DISCUSSION	46
GLOBULE FORMATION.....	46
<i>Volume</i>	47
<i>Energy</i>	47
DENSITY	47
CRYSTALLIZATION/MELTING.....	47
<i>Melting Point/Glass Transition Temperature Determination</i>	48
CONCLUSIONS	49
WORKS CITED	50
APPENDIX A	52
TOTAL SYSTEM ENERGY PLOTS FOR HDPE OF VARIOUS CHAIN LENGTHS	52
APPENDIX B	58
BRANCHING EFFECTS OF POLYMER STRUCTURE	58
<i>Low Density Polyethylene (LDPE)</i>	58
<i>Polypropylene (PP)</i>	59
APPENDIX C	60
FINAL HDPE TEMPERATURE VARIATION GEOMETRIES (3000 PICoseconds)	60
APPENDIX D	63
DENSITY CALCULATIONS	63
<i>Conversions</i>	63
<i>Single Chain Simulations</i>	63
APPENDIX D	65
GLOBULE FORMATION AT VARIOUS TEMPERATURES.....	65

<i>350 Kelvin Simulation</i>	65
<i>400 Kelvin Simulation</i>	66
<i>500 Kelvin Simulation</i>	67
<i>600 Kelvin Simulation</i>	68
<i>800 Kelvin Simulation</i>	70
APPENDIX E	73
DL_POLY2 INPUT FILES.....	73
<i>CONTROL File</i>	73
<i>FIELD Files</i>	74
<i>CONFIG Files</i>	114

Table of Figures

FIGURE 1: HIGH DENSITY POLYETHYLENE (HDPE) STRUCTURE.....	12
FIGURE 2: LOW DENSITY POLYETHYLENE (LDPE) STRUCTURE.....	12
FIGURE 3: POLYPROPYLENE STRUCTURE.....	13
FIGURE 4: ETHYLENE VINYL ACETATE (EVA) STRUCTURE.....	13
FIGURE 5: CROSSLINKING AGENT DICUMYL PEROXIDE STRUCTURE.....	15
FIGURE 6: GLOBULE FORMATION TIME OF HIGH DENSITY POLYETHYLENE (HDPE) FOR VARIOUS CHAIN LENGTHS.....	27
FIGURE 7: GLOBULE FORMATION TIME OF POLYPROPYLENE (PP) FOR VARIOUS CHAIN LENGTHS.....	28
FIGURE 8: GLOBULE FORMATION TIME OF LOW DENSITY POLYETHYLENE (LDPE) FOR VARIOUS CHAIN LENGTHS.....	28
FIGURE 9: NORMALIZED GLOBULE FORMATION TIME OF HIGH DENSITY POLYETHYLENE AT VARIOUS CHAIN LENGTHS.....	29
FIGURE 10: NORMALIZED GLOBULE FORMATION TIME OF POLYPROPYLENE AT VARIOUS CHAIN LENGTHS.....	30
FIGURE 11: NORMALIZED GLOBULE FORMATION TIME OF LOW DENSITY POLYETHYLENE AT VARIOUS CHAIN LENGTHS.....	30
FIGURE 12: VAN DER WAALS VOLUME AS A FUNCTION OF CHAIN LENGTH.....	31
FIGURE 13: NORMALIZED VDW VOLUME (PER ATOM BASIS).....	32
FIGURE 14: TOTAL SYSTEM ENERGY OF HDPE FOR VARIOUS CHAIN LENGTHS.....	33
FIGURE 15: BRANCHING EFFECTS ON GLOBULE FORMATION TIME.....	34
FIGURE 16: IMAGE HDPE (130 PICOSECONDS).....	35
FIGURE 17: IMAGE OF POLYETHYLENE (130 PICOSECONDS).....	35
FIGURE 18: IMAGE OF LDPE (130 PICOSECONDS).....	35
FIGURE 19: HDPE GLOBULE FORMATION TIMES AT VARIOUS TEMPERATURES.....	36
FIGURE 20: IMAGE OF HDPE 50 CHAIN SYSTEM (100 ATOMS LONG).....	37
FIGURE 21: IMAGE OF HDPE 20 CHAIN SYSTEM (500 ATOMS LONG).....	38
FIGURE 22: IMAGE OF HDPE 100K (3000 PICOSECONDS).....	39
FIGURE 23: IMAGE OF HDPE 100K ENLARGEMENT (3000 PICOSECONDS).....	39
FIGURE 24: IMAGE OF HDPE 300K (220 PICOSECONDS).....	39
FIGURE 25: IMAGE OF HDPE 300K (340 PICOSECONDS).....	40
FIGURE 26: IMAGE OF HDPE 300K (3000 PICOSECONDS).....	40
FIGURE 27: IMAGE OF HDPE 500K (130 PICOSECONDS).....	40
FIGURE 28: IMAGE OF HDPE 800K (210 PICOSECONDS).....	41
FIGURE 29: IMAGE OF HDPE 800K (3000 PICOSECONDS).....	41
FIGURE 30: DENSITY OF HDPE AT VARIOUS TEMPERATURES.....	42
FIGURE 31: PP DENSITY DATA AT VARIOUS TEMPERATURES.....	42
FIGURE 32: PP VOLUME DATA AT VARIOUS TEMPERATURES.....	43
FIGURE 33: HDPE CONFIGURATIONAL ENERGY TEMPERATURE DATA.....	44
FIGURE 34: PP CONFIGURATIONAL ENERGY TEMPERATURE DATA.....	44
FIGURE 35: VAN DER WAALS FORCES OF HDPE AT VARIOUS TEMPERATURES.....	45
FIGURE 36: VAN DER WAALS FORCES OF POLYPROPYLENE AT VARIOUS TEMPERATURES.....	45
FIGURE 37: HDPE CHAIN LENGTH 10 PSEUDO ATOMS.....	52
FIGURE 38: HDPE CHAIN LENGTH 20 PSEUDO ATOMS.....	53
FIGURE 39: HDPE CHAIN LENGTH 50 PSEUDO ATOMS.....	53
FIGURE 40: HDPE CHAIN LENGTH 100 PSEUDO ATOMS.....	54
FIGURE 41: HDPE CHAIN LENGTH 200 PSEUDO ATOMS.....	54
FIGURE 42: HDPE CHAIN LENGTH 500 PSEUDO ATOMS.....	55
FIGURE 43: HDPE CHAIN LENGTH 1000 PSEUDO ATOMS.....	55
FIGURE 44: HDPE CHAIN LENGTH 2000 PSEUDO ATOMS.....	56

FIGURE 45: HDPE CHAIN LENGTH 3000 PSEUDO ATOMS	56
FIGURE 46: HDPE CHAIN LENGTH 4000 PSEUDO ATOMS	57
FIGURE 47: HDPE CHAIN LENGTH 5000 PSEUDO ATOMS	57
FIGURE 48: LDPE INITIAL STRUCTURE (FOUR CHAINS WITH MAIN CHAIN LENGTH OF 2000 PSEUDO ATOMS).....	58
FIGURE 49: LDPE (60 PICOSECONDS) (FOUR CHAINS WITH MAIN CHAIN LENGTH OF 2000 PSEUDO ATOMS).....	58
FIGURE 50: LDPE (310 PICOSECONDS) (FOUR CHAINS WITH MAIN CHAIN LENGTH OF 2000 PSEUDO ATOMS).....	58
FIGURE 51: LDPE (2000 PICOSECONDS) (FOUR CHAINS WITH MAIN CHAIN LENGTH OF 2000 PSEUDO ATOMS).....	58
FIGURE 52: PP INITIAL STRUCTURE (FOUR CHAINS WITH MAIN CHAIN LENGTH OF 2000 PSEUDO ATOMS).....	59
FIGURE 53: 100K	60
FIGURE 54: 200K	60
FIGURE 55: 300K	60
FIGURE 56: 350K	61
FIGURE 57: 400K	61
FIGURE 58: 500K	61
FIGURE 59: 600K	62
FIGURE 60: 800K	62
FIGURE 61: HDPE 350K (150 PICOSECONDS)	65
FIGURE 62: HDPE 350K (250 PICOSECONDS)	65
FIGURE 63: HDPE 350K (3000 PICOSECONDS)	66
FIGURE 64: HDPE 400K (90 PICOSECONDS)	66
FIGURE 65: HDPE 400K (210 PICOSECONDS)	66
FIGURE 66: HDPE 400K (3000 PICOSECONDS)	67
FIGURE 67: HDPE 500K (130 PICOSECONDS)	67
FIGURE 68: HDPE 500K (160 PICOSECONDS)	67
FIGURE 69: HDPE 500K (3000 PICOSECONDS)	68
FIGURE 70: HDPE 600K (140 PICOSECONDS)	68
FIGURE 71: HDPE 600K (150 PICOSECONDS)	69
FIGURE 72: HDPE 600K (170 PICOSECONDS)	69
FIGURE 73: HDPE 600K (200 PICOSECONDS)	70
FIGURE 74: HDPE 600K (3000 PICOSECONDS)	70
FIGURE 75: HDPE 800K (100 PICOSECONDS)	70
FIGURE 76: HDPE 800K (120 PICOSECONDS)	71
FIGURE 77: HDPE 800K (210 PICOSECONDS)	71
FIGURE 78: HDPE 800K (670 PICOSECONDS)	72

Table of Tables

TABLE 1: UNITED-ATOM TRANSFERABLE POTENTIALS FOR BOND LENGTHS.....	22
TABLE 2: UNITED-ATOM TRANSFERABLE POTENTIALS FOR BOND ANGLES.....	22
TABLE 3: UNITED-ATOM TRANSFERABLE POTENTIALS FOR TORSIONAL INTERACTIONS.....	23
TABLE 4: UNITED-ATOM TRANSFERABLE POTENTIALS FOR NON-BONDED INTERACTIONS.....	23
TABLE 5: DENSITY OF HDPE.....	36
TABLE 6: HDPE DENSITY DATA FOR DIFFERENT CHAIN LENGTHS AND NUMBER OF CHAINS	37
TABLE 7: EQUILIBRIUM/NON-EQUILIBRIUM HDPE DENSITY VALUES (G/CM ³)	38
TABLE 8: DENSITY OF FOUR CHAIN POLYMER SYSTEMS (MAIN CHAIN LENGTH 2000 ATOMS)	38

Table of Equations

EQUATION 1: FUNCTIONAL FORM OF OPLS	17
EQUATION 2: NON-BONDED INTERACTION POTENTIAL.....	24
EQUATION 3: COMBINING RULES FOR DIFFERENT SIZES OF LENNARD-JONES PARAMETERS.....	24
EQUATION 4: COMBINING RULES FOR DIFFERENT WELL DEPTHS OF LENNARD-JONES PARAMETERS.....	24
EQUATION 5: HARMONIC POTENTIAL	24
EQUATION 6: TORSIONAL INTERACTION POTENTIAL.....	24

Introduction

Motivation: Running Shoes

Running shoes provide cushioning to the foot upon impact with the ground. The most common material used in the midsole of the shoe (the part of the shoe that provides the cushioning) is ethylene vinyl acetate or EVA foam. (Shorten, 2000, p. 4) This foam has air or other gasses trapped inside the cells of the foam that upon compression, exit the cell. (Shorten, 2000, p. 12) After the shoe has left the ground, and the EVA foam is not under compression, air is drawn back into the cells. This occurs because of the elastic properties of the EVA. This cycle repeats with every step taken. The rebound time of EVA foam ranges from minutes to hours. (Wilson, 2007, p. 1372) Eventually the cells start to become permanently deformed. (Wilson, 2007, p. 1371) The foam cells draw in less air at a slower rate, hindering the full expansion to their original position. Running shoes become 'worn out' when the foam cells no longer provide a satisfactory amount of cushion.

The degradation of polymers has yet to be fully understood due to their complex chemical nature. Degradation can occur from environmental interactions such as light radiation, heat, swelling, dissolution, scission, and chemical reactions with atmospheric oxygen for instance. (Callister, Jr., 2007, pp. 655-657) During the active lifetime of a running shoe the interest would be in modeling the deformation rather than the degradation of the polymer network. As waste is becoming an increasingly important topic, efforts to use environmentally friendly polymers in running shoes have been on the rise. Modeling polymers to assess their properties is an important task towards understanding how running shoes perform and degrade with time.

Project Goals

The aim of the current work is to assess simple polymer systems that will lay the groundwork for eventually modeling complex EVA foam and its eventual deformation and degradation. Key areas for future studies include the modeling of various types of crosslinking and polymer orientations. The goal is to provide a foundation for running shoe companies to build upon. The ability to assess newly proposed polymers and their improved characteristics before experimentation will save time and reduce waste.

Background

Polymers

Polymers are large molecules of high molecular weight composed of repeating units called monomers. Most contain a high percentage of carbon and hydrogen. (Callister, Jr., 2007, p. 492)

Properties

The properties of polymers are affected by their different chemical and structural characteristics. Their composition (types of atoms, length of chains, degree of branching, etc.) determines these characteristics. For example, the degree of crystallization affects density, stiffness, strength, and ductility. The degree of crosslinking (described below) affects the stiffness, and the chemical makeup of the polymer affects the melting and glass transition temperatures. (Callister, Jr., 2007, p. 489)

Polymerization, or Growth of Polymers

Addition Polymerization

Addition polymerization usually occurs through radical addition, where an initiator molecule, usually peroxide, is degraded to produce two radicals. These radicals attack the double bonds of short molecules, in the case of polyethylene, an ethylene molecule, forcing an electron from the double bond to become an unpaired on the opposite side of where the peroxide attacked. This unpaired electron (radical) can now attack an ethylene molecule on its own, and continue the polymer growth. The unpaired electron on the carbon atom attacks the double bond of the neighboring ethylene molecule, creating a carbon-carbon single bond. This forces the other electron previously participating in the double bond to the other side of the molecule, opposite of the attack. This in turn creates another unpaired radical electron which continues to propagate the chain. (Wade Jr., 2009)

Condensation polymerization

Condensation polymerization forms polymers through the elimination of a small molecular weight byproduct when two reactant species come together. The reactant species can be the same or different molecules. The number of reactive sites each building block molecule has determines the type of polymer that can result from polymerization. Building block molecules with two reactive sites, termed bi-functional, form linear chains. A molecule with only one reactive site terminates the chain, whereas molecules with three or more reactive sites, tri-functional or higher functional monomers have the ability to form branching, crosslinks, and polymer networks. Typically condensation polymerization reactions are slower than those of addition polymerization. This type of polymerization also tends to produce lower molecular weight polymers. (Callister, Jr., 2007, p. 593)

Ring opening polymerization

Ring opening polymerization is a process that involves breaking open a cyclic ring to grow the polymer. This progression of chain growth can employ techniques from both types of polymerization described above (Davis, 2004, p. 44).

Basic Structures of Polymers Examined

Polyethylene

Polyethylene is the most basic of olefinic polymers, consisting of the repeating unit $-(C_2H_4)-$. This polyolefin is a homopolymer, consisting of only one type of repeating unit. (Callister, Jr., 2007, p. 496) Figure 1 below, shows the basic structure of polyethylene. Carbon atoms make up the backbone of the chain and are colored grey. Hydrogen atoms are colored white.

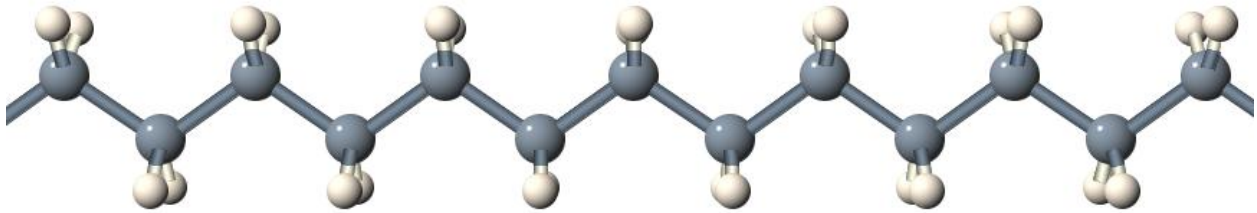


Figure 1: High Density Polyethylene (HDPE) Structure

Branched Polyethylene, or Low Density Polyethylene (LDPE)

Low density polyethylene is a branched version of polyethylene, where side chains extend out from the main chain. Figure 2 below is an image of LDPE where only the carbon atoms are shown.

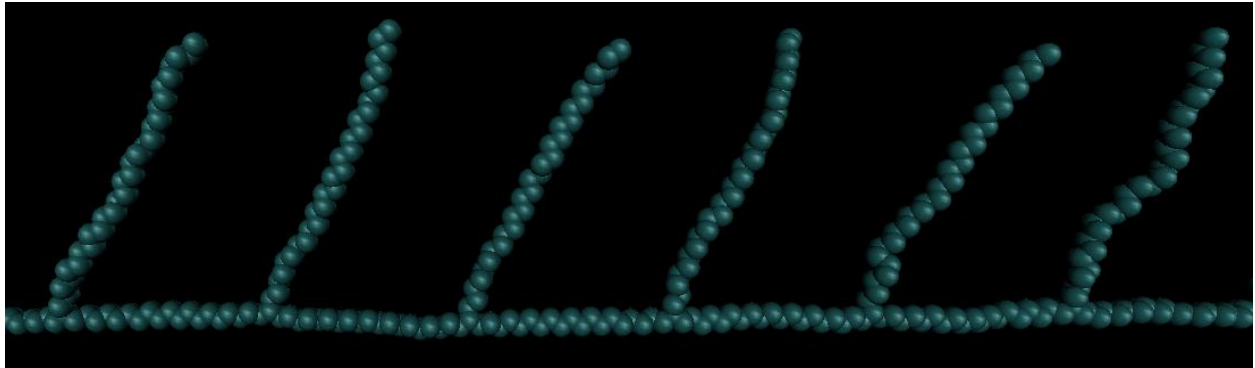


Figure 2: Low Density Polyethylene (LDPE) Structure

Polypropylene

Polypropylene is another olefinic polymer. From the basic polyethylene structure, one of the substituent hydrogen molecules is replaced with a methyl group. The repeating unit is $-(C_2H_3CH_3)-$. This polyolefin is a homopolymer as polyethylene is, consisting of only one type of repeating unit. (Callister, Jr., 2007, p. 496) Figure 3 below shows the basic structure of polypropylene. The carbon atoms are colored grey and the hydrogen atoms are colored white.

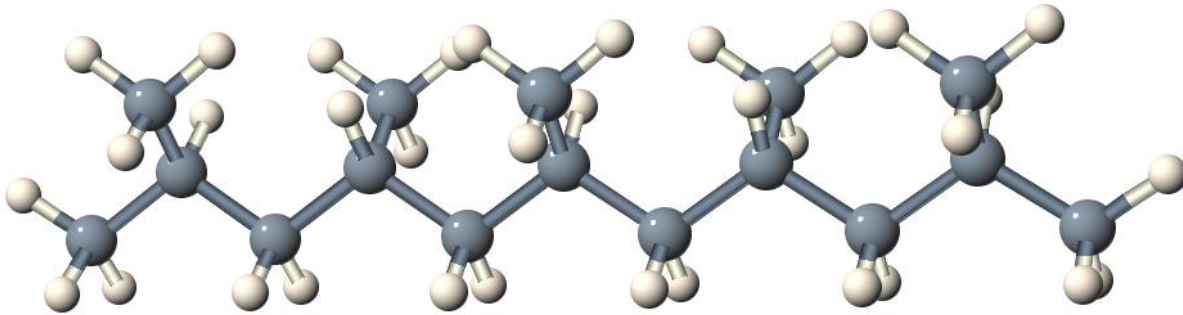


Figure 3: Polypropylene Structure

Ethylene Vinyl Acetate

Ethylene vinyl acetate is a copolymer. This term refers to a polymer chain with different repeating units (Callister, Jr., 2007, p. 495). The two repeating units are ethylene $-(C_2H_4)-$ and acetate $-(C_2O_2H_3)-$. Running shoes typically have 18 percent by weight vinyl acetate, with the remainder being ethylene. (Verdejo & Mills, 2002, p. 582) Figure 4 below shows the basic structure of ethylene vinyl acetate with one acetate group. The carbon atoms are colored grey, the hydrogen atoms are colored white, and the oxygen atoms are colored red.

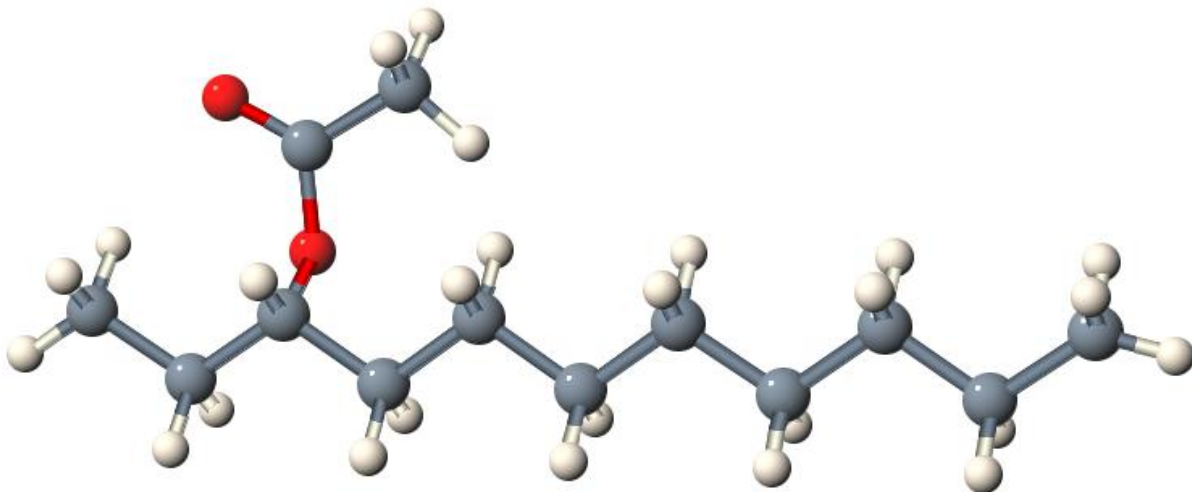


Figure 4: Ethylene Vinyl Acetate (EVA) Structure

Degree of Polymerization

The degree of polymerization, DP, describes the number of repeat units or monomers that have joined together to form a polymer chain. The degree of polymerization for a polymer is given by the equation $DP = M_n/m$, where M_n is the number average molecular weight of the given sample and m is the

molecular weight of the monomer. The number average molecular weight is a weighted average representing the molecular weight of the most abundant chains. For a given polymer sample, the degree of polymerization is the average number of monomers per polymer chain. (Callister, Jr., 2007, p. 498)

Critical Molecular weights

The critical molecular weight of a polymer is the minimum molecular weight that a polymer needs to have to exhibit its steady state bulk properties. At this molecular weight the chain dynamics cross over from free (or Rouse) to entangled (or reptation). Free chain dynamics explain the unattached nature of the polymers. They are free to move and slide over other chains without much hindrance. Entangled dynamics explain chains that are of a certain length where interactions with other neighboring chains greatly affect their movement. The chains are considered intertwined, as they are not able to freely move. (Drzewinski & van Leeuwen, 2006) Polymer chains with less than the critical molecular weight have transient properties. (Kausik, Mattea, Fatkullin, & Kimmich, 2006) Just as ethane, butane, and octane are essentially short chains of polyethylene and have different properties, polymer chains of different lengths have different properties as well. Only once the chains exceed the threshold length (or mass) known as the critical molecular weight, do they start to exhibit consistent properties. At this length the tangled nature of the chains allows the van der Waals forces to act steadily as the chains are hindered from moving freely over each other. Van der Waals forces are the long range attractive forces that act on neighboring molecules. Critical molecular weights are different for each polymer. Polymers exhibiting more flexible behaviors and minimal branching have much higher critical values than those with rigid backbones and high degrees of branching which promote tangling.

Branching

Branching is the term used for polymers that are not linear. Branched polymers are those that have multiple secondary chains that extend out from the main chain. (Callister, Jr., 2007, p. 502) Polymer branching occurs when monomers have more than two reactive sites, or are tri-functional or multifunctional. (Callister, Jr., 2007, p. 593) When the monomers have these unique properties, side reactions can occur at multiple points during polymer formation resulting in branching. The higher the degree of branching, the more the packing efficiency is reduced, effectively lowering the polymer density. (Callister, Jr., 2007, p. 502)

Crosslinking

Crosslinked polymers are created when adjacent chains are fused together by covalent bonds. The more places that neighboring chains are linked together, the higher the degree of crosslinking the polymer has. When polymers become highly crosslinked, they assume a three-dimensional structure and are termed network polymers. (Callister, Jr., 2007, p. 503)

Vulcanization was the first form of synthetic crosslinking. Natural and synthetic rubber when heated with sulfur form sulfur bridges or links between the long polymers. Vulcanization treats unsaturated polymers where the double bond in the backbone of the chain is broken and bonds to the sulfur crosslinking chain. (Encyclopedia Britannica, 2012, p. 1) These links are covalently bonded and effectively rebound the shape of the material after an induced stress, giving it elastic properties. (Encyclopedia Britannica, 2012, p. 1) (Odian, 2004, p. 740)

Unfortunately this basic method of vulcanization crosslinking does not work for saturated polymers like EVA or polyethylene. Organic peroxides are used to crosslink such macromolecules without double bonds. Peroxides when heated form radicals that are able to attack the backbone of saturated polymers and create sites for crosslinking. A common organic peroxide crosslinking agent for EVA is dicumyl peroxide shown in Figure 5 below. (Arkema, 2009, p. 5)

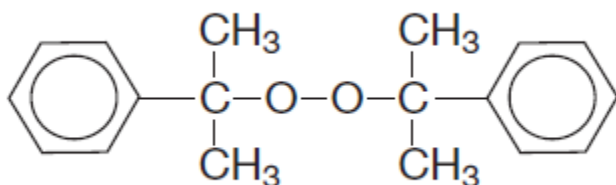


Figure 5: Crosslinking agent Dicumyl Peroxide Structure

Foams

Foams are expanded plastics that are more rigid than dense polymers at any given weight. Foams collapse under impact or compressive stresses, but are able to absorb much of the energy transferred to them, a basis reasoning for their use as cushioning agents in running shoes. Foams can be produced by injecting gasses into a quantity of polymers in the liquid state. Upon cooling, the plastic traps the gasses within the network forming a foam. (Encyclopedia Britannica, 2012)

Computational Chemistry and Molecular Dynamics

Simulations are important in the chemical industry as precursors to industrial change. Simulations of proposed processes are needed to assess changes in current processes or for the initialization of new ones. Computational chemistry and molecular dynamic simulations are used to examine the physical properties of molecular systems to determine the possibility of manufacture or implementation. Using these methods the individual atoms or molecules are simulated. (The NSF Blue Ribbon Panel on Simulation-Based Engineering Science, 2006)

Basic Theory

Computational chemistry, sometimes called theoretical chemistry or molecular modeling, combines quantum mechanics theory with the simplifying approximations of a model to solve practical problems. (Cramer, 2002, p. 2) The observable chemical properties of a system are fundamentally described by the theorems of quantum mechanics. (Cramer, 2002, p. 4)

The minimum input needed to model an isolated molecule is the types of component atoms and their relative positions. (Cramer, 2002, p. 5) Molecules are constantly in motion (bond stretching, bond rotation) and rarely at any given point have the same exact geometry as other molecules of the same type within the system. (Callister, Jr., 2007, p. 501) For the model to more closely represent actuality therefore, all molecular geometries are captured by molecular dynamics into what is known as a complete potential energy surface (PES). (Cramer, 2002, p. 6) Molecular dynamics simulations attempt

to 'map' the PES for given molecules to find local energy minima, or the most stable geometric configurations. (Cramer, 2002, p. 5)

Molecular dynamics simulation involves step-by-step solutions of Newton's equations of motion. It uses atomic coordinates, or the relative positions of the atoms, comprised of inter-atomic distances, bend angles, and torsion angles, to calculate the potential energy of the molecule. (Allen, 2004, p. 2) The simulation runs through a range of each of these parameters to find the optimum geometry of the molecule, in which it has the lowest potential energy. This range of each of the parameters is defined by the force field potential used in the simulation. There are different force fields to choose from, each working best for different types of molecular systems. Some of them are described below.

Inaccurate properties of the bulk system result from simulations of small numbers of molecules, as a large part of them comprise the surfaces. To address this, periodic boundary conditions are introduced that surround the sample simulation box with replicas on all sides. The system becomes much larger and properties are able to be measured with the entirety of the system encapsulated with mirror images.

The current work utilizes molecular modeling as defined by Cramer (p4). The aim is "to focus on a target system having a particular chemical relevance (e.g., for economic reasons) and to be willing to sacrifice a certain amount of theoretical rigor in favor of getting the right answer in an efficient manner." (Cramer, 2002, p. 4) Many simulations are based around simplifying approximations that decrease the time it takes for the computer to work through the calculations. For example, harmonic potentials are used to describe bonds and angles, but are commonly replaced by fixed values to save computational time. One simplification used in the current work, as well as in many polymer modeling papers, is the United-Atom method. This method groups together multiple atoms into a pseudo atom. The number of parameters mentioned earlier, such as bond lengths and angles, therefore, decreases significantly as the number of 'atoms' in the system is reduced.

In molecular dynamics simulations, force field denotes the parameters of the potential used to calculate the forces acting on the atoms of the system being modeled. Different atom types are described with various defining parameters such as bonds, angles, dihedrals, and long-range interactions based on the particular surrounding environment of each atom. One such force field developed by William L. Jorgensen is known as OPLS (Optimized Potential for Liquid Simulations) force field, shown below in Equation 1. This force field describes the velocities of the atoms within the system through summations of the bonds, angles, torsions, and Lennard-Jones potentials. (Marcon, Vehoff, & Ghiringhelli, 2007) In Equation 1, b is the bond length, θ is the bond angle, b_0 and θ_0 are the equilibrium values, K_b and K_θ are the force constants, ω is the dihedral angle and V_n the corresponding force constant, and γ is the phase angle. The parameters r_{ij} , ϵ_{ij} , σ_{ij} , q_i , and q_j are the 'atom' separation, Lennard-Jones well depth, Lennard-Jones size, and partial charges, respectively, for the pair of interaction sites i and j . (Duan, et al., 2003)

$$\begin{aligned}
V(\{\vec{r}_N\}) = & \sum_{bonds} \frac{1}{2} k_b (r - r_0)^2 \\
& + \sum_{angles} k_\theta (\theta - \theta_0)^2 \\
& + \sum_{torsions} \frac{1}{2} V_n [1 + \cos(n\omega - \gamma)] + \sum_{i=1}^{N-1} \sum_{j=i+1}^N \left\{ 4\varepsilon_{ij} \left[\left(\frac{\sigma_{ij}}{r_{ij}} \right)^{12} + \left(\frac{\sigma_{ij}}{r_{ij}} \right)^6 \right] + \frac{q_i q_j}{4\pi\varepsilon_0 r_{ij}} \right\}
\end{aligned}$$

Equation 1: Functional Form of OPLS

Lennard-Jones potentials are used to approximate the interactions between two neutral molecules. These potentials take into account the short range Pauli Repulsion forces as well as the long range van der Waals attractive forces from dipole-dipole interactions. Lennard-Jones potentials are able to be transferred from molecule to molecule as they define a single functional group and their non-bonded interactions. They are therefore able to be incorporated into larger more complex molecules that have substituent groups corresponding to those previously defined by the potentials. In the United-Atom force field the transferability of these potentials is known as “transferable potentials for phase equilibria” (TraPPE-UA). (Kamath, Robinson, & Potoff, 2005, p. 46)

Previous Molecular Dynamics Simulations of Polymers

Polymer Collapse

Zhan and Mattice examined simulations of Poly (1, 4-trans-butadiene). Simulations were run to calculate the volumes and densities of this polymer in a vacuum with no periodic boundary conditions and also with periodic boundary conditions in two planes, leaving the third dimension at a large value to represent infinite space. In their findings the polymer exhibited a globular structure when left to equilibrate in a vacuum for 1500 picoseconds. Simulations with periodic boundary conditions in two dimensions forced the polymer into a coil or thin film. They concluded that this was a result of secondary bonding interactions with mirror images of the polymer in adjacent cells. (Zhan & Mattice, 1994)

Temperature Effects on Density in Dense Polymer Systems

The structures and equilibrium properties of dense polyethylene polymer systems through the use of Monte Carlo simulations have been simulated. Employed was a new technique using rigid bonds and bond angles. The range of chain lengths studied were 10-60 carbon atoms long with systems ranging from 3-20 chains. Through simultaneous simulation of a constant volume configurational simulation and an isobaric-isothermal simulation, the most accurate densities of dense polymeric systems were obtained. Lower densities were reported compared to literature when simulating a single chain of polyethylene 60 segments long. Simulations of three polyethylene chains of 60 segments long provided more accurate density data. The simulations of density values ranging from 0-200 degrees centigrade (273-473K) produced a trend that matched the experimental data. The simulations followed the experimental data trend of decreasing density with increasing temperature. (de Pablo, Laso, & Suter, 1992)

The condensed –phase optimized molecular potentials for atomistic simulation studies (COMPASS) force field was used for the molecular systems of myo- and neo-inositol. The study examined the heat of sublimation, density, melting point, and glass transition temperature. The melting point and glass transition temperature plots were defined by cell volume as a function of temperature. Melting point determination utilized system models in the crystalline state, while glass transition temperature determination made use of system models in the amorphous state. Using the plots, the values for these properties were determined by sudden shifts in slope. Values obtained for these properties matched well to experimental data found in literature. (Watt, Chisholm, Jones, & Motherwell, 2004)

Chain dynamics of polymer melts confined to micrometer thick layers were studied. Properties of the polymer melts restricted to the film layer were different than those of the bulk polymer melt. Polymers of molecular weights below the critical value in the confined space were shown to change over from Rouse to reptation dynamics. (Kausik, Mattea, Fatkullin, & Kimmich, 2006) An explicit study of the cross over from Rouse to reptation dynamics in polymers developed a simple model for a one-dimensional chain. The model focused on hernia annihilation and creation which allowed the links of the chain to change between slack and taut. The new model allowed the interchange rate to increase significantly from previous models making the study of the cross-over behavior possible. (Drzewinski & van Leeuwen, 2006)

Branching Effects on Bulk Properties

Rheological properties of polymer melts were studied for polyethylene chains of varying molecular architecture. Linear, star, H-shaped, and comb-shaped structures were used to examine the bulk properties. Branched molecules were found to differ in properties from linear chains of the same molecular weight in the area of viscosity. The study concluded however, that despite the property changes with shape variance, the rheological properties will be most affected by the chain length and degree of branching. (Jabbarzadeh, Atkinson, & Tanner, 2003)

Transferable Potentials for Phase Equilibria United-Atom (TraPPE-UA)

The TraPPE-UA force field was used to model branched alkanes. Lennard-Jones interaction parameters for methine and quaternary carbon groups were added to the model. Critical temperatures and saturated liquid densities were used to optimize these parameters to fit the force field model. The vapor-liquid coexistence curves (VLCC) were then determined for small alkane isomers. Densities were studied using the isobaric-isothermal ensemble. The TraPPE-UA force field was concluded to under predict second virial coefficients, and show small deviations from experimental data of saturated vapor pressures and densities for normal alkanes. The force field also slightly over predicted the critical temperatures of the larger branched alkanes. (Martin & Siepmann, 1999)

The TraPPE-UA force field was extended to include parameters for the functional groups ether, glycol, ketone, and aldehyde. The parameters were optimized using vapor-liquid coexistence curves. Small molecules with the functional groups were simulated for determination of a variety of properties. The simulations resulted in very close fits to experimental data for critical temperatures and normal boiling temperatures. (Stubbs, Potoff, & Siepmann, 2004)

The TraPPE-UA force field was assessed through simulations of carboxylate esters. Partial charges were taken from the optimized potentials for liquid simulations (OPLS) force field. The model was used to determine vapor-liquid coexistence curves, vapor pressures, and critical temperatures, saturated liquid densities, and critical densities of four esters studied. The critical densities and azeotrope of methyl acetate and methanol were both in very close agreement with experimental data. Pure component vapor pressures were over predicted which resulted in the offset of pressure-composition diagrams. The diagrams did show good qualitative trends. (Kamath, Robinson, & Potoff, 2005)

Methodology

Programs

DL_POLY

“DL_POLY is a parallel molecular dynamics simulation package developed at Daresbury Laboratory.”
(DL_Poly2 user manual)

Input Files

Several input files are needed for the simulations and are described below.

The FIELD file

The FIELD file defines the nature of the molecular forces governing the molecules being modeled. This file contains force field information partitioned into three categories; general information, molecular descriptions, and non-bonded interaction descriptions.

The CONFIG file

The CONFIG file contains the initial coordinates of the molecule. The atom entries of this file with specified coordinates correspond to the FIELD file atom entries, so that together, they construct all the parameters needed to run the DL_POLY simulation.

The CONTROL file

The CONTROL file is responsible for defining the design system parameters and variables. This file specifies the temperature, pressure, timestep, time duration desired for geometry optimization/equilibration, the job time length, etc.

Output Files

The DL_POLY program produces output files from completed simulations described below.

The HISTORY file

“The HISTORY file is the dump file of atomic coordinates, velocities, and forces.” (DL_Poly2 user manual)
This file contains the coordinates, velocities, and forces at each timestep interval specified in the CONTROL file.

The REVCON file

The REVCON file produces the final atomic coordinates, velocities, and forces. It can be used to restart or continue a simulation. In the current work, the REVCON file is used to assess final geometric configurations along with occupying volume and box volume used in density calculations.

The STATIS file

The STATIS file is a collection of energy data from the simulation recorded for each timestep interval specified in the CONTROL file.

The REVIVE file

The REVIVE file is an accumulation of statistical results and is to be renamed as REVOLD and used as an input if a continuation of a simulation is desired.

The OUTPUT file

The OUTPUT file includes specifications on force fields and simulation control gathered from the CONTROL and FIELD file inputs. This file relays simulation progress, a summary of statistical data which includes the diffusion coefficients, a sample of the final geometric configuration, and radial distribution functions.

DL_FIELD

DL_FIELD is a program designed by Daresbury Laboratory intended to assist in the use of DL_POLY programs. The program creates CONFIG, CONTROL, and FIELD input files for DL_POLY from the user's simple atomic configuration in xyz form. DL_FIELD is able to utilize CHARMM and AMBER force field files in the creation of the input files needed for DL_POLY.

McVol

McVol is a program used in the determination of the volume occupied by a molecule. The program is used in the evaluation of configurational volume to assess changes in volume resulting from shape changes during simulation. The program uses radii of a given distance specified by the user around each atom. In polymer simulations the chains fold in on one another. As this occurs, the radius around each atom becomes slightly overlapped, thus decreasing the calculated volume. A straight chained polymer therefore would have the highest calculated volume.

Visual Molecular Dynamics (VMD)

VMD is a program used to view the simulations. The program converts the data of the HISTORY file of DL_POLY2 into a motion picture of the molecular system.

United Atom Force Field

The united atom method was employed as the program DL_POLY2 could not handle large polymer systems. The computational time required to calculate all required bond energies etc. for each methylene/methyl/methionine group increases as the hydrogen atoms in these groups add to the number of bond angles and dihedrals. These extra attributes dramatically increase the amount of calculations that DL_POLY2 needs to perform and therefore increase computational time excessively to the point where computational chemistry for molecular dynamics purposes becomes senseless. The united atom method groups the carbon hydrogen groups commonly found in the main chain backbone of vinyl polymers. Methyl, methylene, and methionine groups or singular carbon atoms without hydrogen are lumped into one pseudo-atom with a set of its own potentials and parameters. Bond lengths are fixed. Atom mass and charge, angles, dihedrals, Lennard-Jones potentials, and atomic coordinates are still specified. Dihedrals are specified using optimized potentials for liquid simulations (OPLS force) force field data. (Kamath, Robinson, & Potoff, 2005, p. 47)

Force field data known as TraPPE-UA was used for this work. (Kamath, Robinson, & Potoff, 2005, p. 47) (Martin & Siepmann, 1999) (Stubbs, Potoff, & Siepmann, 2004)

Bond	Bond Length, r_0 (Å)
$\text{CH}_x\text{-CH}_y$	1.54
$\text{CH}_2=\text{CH}$	1.33
C-CH_x	1.52
O-H	0.945
C-O	1.344
O-CH_x	1.41
CH=O	1.217
C=O	1.229

Table 1: United-atom transferable potentials for bond lengths

United-atom transferable potentials for bond lengths are shown in Table 1 above. Bond lengths are specified for various types of connected atoms. Values are reported in angstroms.

Bond Angle	θ_0 (degrees)	k_θ/k_b (kcal/mol)
$\angle \text{CH}_x\text{-CH}_2\text{-CH}_y$	114	124.20
$\angle \text{CH}_x\text{-CH-CH}_y$	112	124.20
$\angle \text{CH}_x\text{-C-CH}_y$	109.47	124.20
$\angle \text{C-O-CH}_3$	115	124.20
$\angle \text{O-C=O}$	125	124.20
$\angle \text{O-C-CH}_3$	110	140.30
$\angle \text{O=C-CH}_3$	125	124.20
$\angle \text{CH}_3\text{-O-H}$	108.5	110.09
$\angle \text{CH}_x\text{-CH}_y\text{-O}$	112	99.96
$\angle \text{CH}_x\text{-O-CH}_y$	112	120.03
$\angle \text{CH}_x\text{-C(=O)-CH}_y$	117.2	124.20
$\angle \text{CH}_x\text{-CH=O}$	121.4	124.20

Table 2: United-atom transferable potentials for bond angles

United-atom transferable potentials for bond angles are shown in Table 2 above. Bond lengths are specified for various types of connected atoms. Values are reported in degrees.

Torsional Interactions	c_0/k_b (kcal/mol)	c_1/k_b (kcal/mol)	c_2/k_b (kcal/mol)	c_3/k_b (kcal/mol)
$\text{CH}_x\text{-O-C=O}$	9.3717	4.3599	4.0917	-0.3048
$\text{CH}_x\text{-O-C-CH}_y$	0.0000	4.2884	4.1692	0.3921
$\text{CH}_2=\text{CH-O-C}$	0.0000	3.3743	3.1080	0.1719
CH-O-C-CH_x	-0.0288	1.9735	1.0347	-0.2752
$\text{CH}_y\text{-CH}_x\text{-C=O}$	4.0451	-1.4644	0.1149	-0.5827
$\text{CH}_y\text{-CH}_x\text{-O-C}$	0.0000	1.4414	0.3254	1.1093
$\text{CH}_x\text{-CH}_2\text{-CH}_2\text{-CH}_y$	0.0000	0.6658	-0.1355	1.5725
$\text{CH}_x\text{-CH}_y\text{-O-CH}_z$	0.0000	1.4414	-0.3254	1.1093
$\text{CH}_x\text{-CH}_2\text{-CH}_2\text{-O}$	0.0000	0.3510	-0.1060	1.5300
$\text{O-CH}_2\text{-CH}_2\text{-O}$	1.0000	0.0000	-0.5000	2.0001
$\text{CH}_x\text{-CH}_y\text{-C=O}$	4.0451	-1.4644	0.1149	-0.5827
$\text{CH}_x\text{-CH}_2\text{-CH-CH}_y$	-0.4989	0.8520	-0.2223	0.8769
$\text{CH}_x\text{-CH}_2\text{-C-CH}_y$	0.0000	0.0000	0.0000	0.9167
$\text{CH}_x\text{-CH-CH-CH}_y$	-0.4989	0.8520	-0.2223	0.8769

Table 3: United-atom transferable potentials for torsional interactions

United-atom transferable potentials for torsional interactions are shown in Table 3 above. Torsional interactions are specified for various types of connected atoms. Values are reported in kcal/mol.

Non-Bonded Interactions	Molecule Type	σ Length (Å)	ϵ/k_B (kcal/mol)	q (e)
$\text{CH}_3(\text{sp}^3)$	ether/alcohol/aldehyde	3.75	0.1947	$0.25^a/0.265^b/-0.043^c$
$\text{CH}_2(\text{sp}^3)$	ether/alcohol/aldehyde	3.95	0.0914	$0.25^a/0.265^b/-0.043^c$
$\text{CH}(\text{sp}^3)$	ether/alcohol	4.33	0.0199	$0.25^a/0.265^b$
$\text{C}(\text{sp}^3)$	ether/alcohol	5.8	0.0010	$0.25^a/0.265^b$
$\text{CH}_3(\text{sp}^3)$	all other	3.75	0.1947	0
$\text{CH}_2(\text{sp}^3)$	all other	3.95	0.0914	0
$\text{CH}(\text{sp}^3)$	all other/aldehyde	4.68	0.0199	$0/-0.043^c$
$\text{C}(\text{sp}^3)$	all other/aldehyde	6.4	0.0010	$0/-0.043^c$
O	ether	2.8	0.1093	-0.5
O	alcohol	3.02	0.1848	-0.7
H	alcohol		0.0000	0.435
$\text{CH}(\text{sp}^2)$	aldehyde	3.52	0.1073	0.525
$\text{O}(\text{sp}^2)$	aldehyde	3.05	0.1570	-0.482
$\text{C}(\text{sp}^2)$	ketone	3.82	0.0795	0.424
$\text{O}(\text{sp}^2)$	ketone	3.05	0.1570	-0.424

Table 4: United-atom transferable potentials for non-bonded interactions

United-atom transferable potentials for non-bonded interactions are shown in Table 4 above. Lennard-Jones potentials and atomic charges for various atoms are specified for non-bonded interactions. Values for Lennard-Jones size (σ) are in angstroms, Lennard-Jones well depth (ϵ) is in kcal/mol, and partial charges (q) are in units of electron volts. ^a For sites adjacent to the ether oxygen. ^b For sites adjacent to the alcohol oxygen. ^c For sites adjacent to the aldehyde carbon.)

Non-bonded interactions are described by Equation 2 below, where r_{ij} , ϵ_{ij} , σ_{ij} , q_i , and q_j are the 'atom' separation, Lennard-Jones well depth, Lennard-Jones size, and partial charges, respectively, for the pair of interaction sites i and j .

$$U(r_{ij}) = 4\epsilon_{ij} \left[\left(\frac{\sigma_{ij}}{r_{ij}} \right)^{12} - \left(\frac{\sigma_{ij}}{r_{ij}} \right)^6 \right] + \frac{q_i q_j}{4\pi\epsilon_0 r_{ij}}$$

Equation 2: Non-bonded Interaction Potential

Lorentz-Berthelot rules were used as shown below in Equation 3 and Equation 4 to calculate van der Waals interactions for other combinations of atoms not specified in Table 4 above. (Kamath, Robinson, & Potoff, 2005, p. 47)

$$\sigma_{ij} = \frac{\sigma_{ii} + \sigma_{jj}}{2}$$

Equation 3: Combining rules for different sizes of Lennard-Jones parameters

$$\epsilon_{ij} = \sqrt{\epsilon_{ii} * \epsilon_{jj}}$$

Equation 4: Combining rules for different well depths of Lennard-Jones parameters

Bond angle bending is controlled by a harmonic potential shown in Equation 5 below. θ is the measured bond angle, θ_0 is the equilibrium bond angle and k_θ is the force constant.

$$U_{angle} = \frac{k_\theta}{2} (\theta - \theta_0)^2$$

Equation 5: Harmonic Potential

Torsional interactions separated by three bonds are described by Equation 6. ϕ is the dihedral angle and c_i are the Fourier constants listed in Table 3.

$$U_{torsion} = c_0 + c_1[1 + \cos(\phi)] + c_2[1 - \cos(2\phi)] + c_3[1 + \cos(3\phi)]$$

Equation 6: Torsional Interaction Potential

(Kamath, Robinson, & Potoff, 2005, p. 48)

Simulations

Parameters

A simulation time for the polymer chains of 1500 seconds was chosen as the minimum run time based on the 1994 paper Molecular Dynamics Simulation of the collapse of Poly(1,4-trans-butadiene) to a globule and to a thin film by Zhan and Mattice. This time duration provides a sufficient time for the system to reach steady state. (Zhan & Mattice, 1994)

The time step of the simulation controls the time value jump between each stepwise calculation. The larger the time step, the faster the simulations are able to reach the desired job end time, but the larger the resulting error in data extracted from the simulation. Larger time steps of 5 fs have been shown to result in dramatic energy drifts. (Izaguirre, Reich, & Skeel, 1999, p. 9853) The time step used for all simulations in the current work was 1 fs.

Various temperatures were used in the simulations of the current work. To assess temperature related trends, simulations of system temperatures ranging from 100K to 800K were used. The extremes were simulated to extrapolate more accurate mid-range temperature data to more clearly show the trends, and not used in explicit value retrieval. Molecular dynamics simulation temperatures have been shown to deviate from actual temperature, (Jobic, Smirnov, & Bougeard, 2001), which is a compounding reason for the broad range of temperatures used in the current work. A far-reaching series of temperatures was used to encompass the entirety of each of the trends examined.

A NVT simulation, known as a canonical ensemble, is based on the temperature and volume of the system having specified average values. A NPT simulation, known as an isothermal-isobaric ensemble, is based on the pressure and temperature of the system having a specified average values, while the volume is able to fluctuate. (Hunenberger, 2005, p. 111)

Polymers

Four polymer types were simulated, straight chained polyethylene or high density polyethylene (HDPE), branched polyethylene or low density polyethylene (LDPE), polypropylene (PP), and ethylene vinyl acetate (EVA). Geometries, coordinates, and force field data (CONFIG and FIELD files) were developed for various lengths of the main chain ranging from 10 pseudo atoms long (a degree of polymerization of 5 – DP of 5) to 5000 pseudo atoms long (a degree of polymerization of 2500 – DP of 2500).

Polymer Chain Length

To assess how chain length affects polymer structure, NVT simulations of each chain length for a given polymer type were run. To isolate the singular molecular chain, the simulations were performed with no periodic boundaries as a single polymer alone in space. This eliminated the possibility of mirror chain interactions between adjacent cells as well as decreased the simulation time. The simulations were run at 300K for 3000 picoseconds to fully reach steady state equilibrium.

Pressure

To determine whether a pressure difference of 1atm changed the density of polymer, two simulations were run for polyethylene with chain lengths of 2000 pseudo atoms. The precursor NVT simulation

equilibrated the 1 chain polymer system for 3000 picoseconds at 300K and 0atm. Following this, the first NPT simulation was run at 0atm for 1500 picoseconds, and the second NPT simulation at 1atm for the same length of time.

Density

To examine the density difference between single and multiple polymers chain systems, a single polymer with a chain length of 2000 pseudo atoms, and four chains of the same length were each run for high density polyethylene and polypropylene. NVT simulations were run for 3000 picoseconds with no periodic boundary conditions to equilibrate the system. NPT simulations were then run for 1500 picoseconds using thermostat and barostat relaxation times of 0.5fs for both. Simulations were run at 300K and 0atm.

Crystallization

Polymer systems of HDPE were simulated at various low temperatures to assess the degree of ordering among the chains. Four chains of 2000 pseudo atoms were examined at temperatures as low as 100K. Systems of 20 chains 500 pseudo atoms in length, 25 chains 200 pseudo atoms in length, and 50 chains 100 pseudo atoms in length were also studied. The chains were initially linear and adjacent with the low temperatures held constant from the beginning of the simulations. Another series of simulations was run where the system of 50 chains 100 pseudo atoms in length was initially equilibrated at 1000K to imitate a liquid polymer melt. The temperature was slowly decreased in each subsequent simulation which was a continuation of the last.

Melting Point

To evaluate the melting point of high density polyethylene and polypropylene, NVT simulations of four chains each of 2000 pseudo atoms in main chain length were run for various temperatures surrounding their respective experimental melting points found in literature. These simulations were run for 3000 picoseconds with no periodic boundary conditions to equilibrate the system. The final geometries retrieved from the REVCON files were then used to start new NPT simulations. These simulations were run for 1500 picoseconds at each respective temperature and at 0atm. The temperatures ranged from 100K to 800k and clustered around the polymer type's experimental melting point.

High density polyethylene polymer systems of a larger number of macromolecules were simulated. Systems of 50 chains 100 pseudo atoms in length, 25 chains 200 pseudo atoms in length, and 20 chains 500 pseudo atoms in length were simulated.

Results

Polymer Structure - Chain Length Effects

HDPE, LDPE, and PP molecules with main chain lengths ranging from 10 to 5000 pseudo atoms long were simulated each for 3000 picoseconds with time steps of 0.01 picoseconds. Each polymer simulation started with a straight chain molecule. Using no periodic boundary conditions, the polymers collapsed in on themselves forming globules.

Globule Formation

Globule formation times were qualitatively extracted through visual methods by viewing the HISTORY output files of DL_POLY using the program VMD. Globule formation was determined to be the initial point of the chain coming together.

A range of HDPE, PP, and LDPE polymer lengths were simulated for 3000 picoseconds at 300K and 0 atm. Figure 6, Figure 7, and Figure 8 below, display globule formation times for various lengths of polymer chains. The plots show a general trend that as the length of the polymer increases, the time to form a globule also increases.

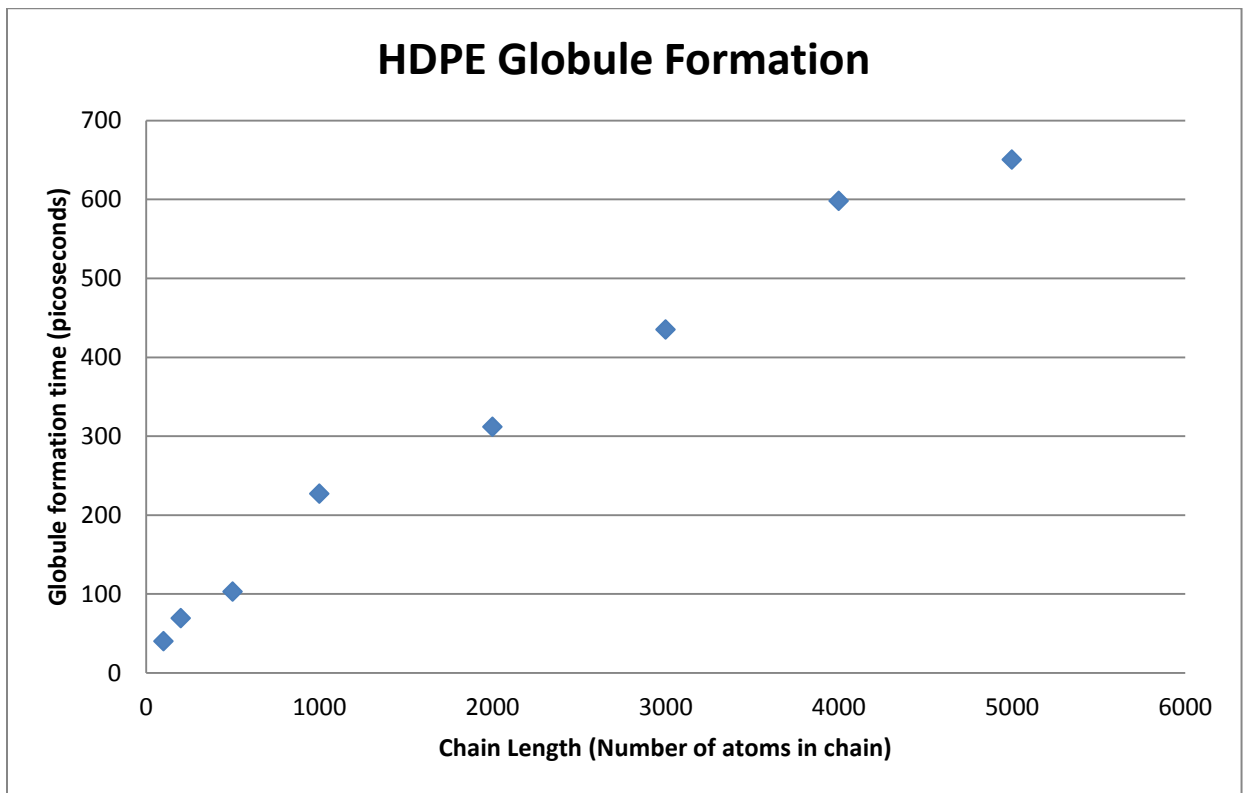


Figure 6: Globule Formation Time of High Density Polyethylene (HDPE) for various chain lengths

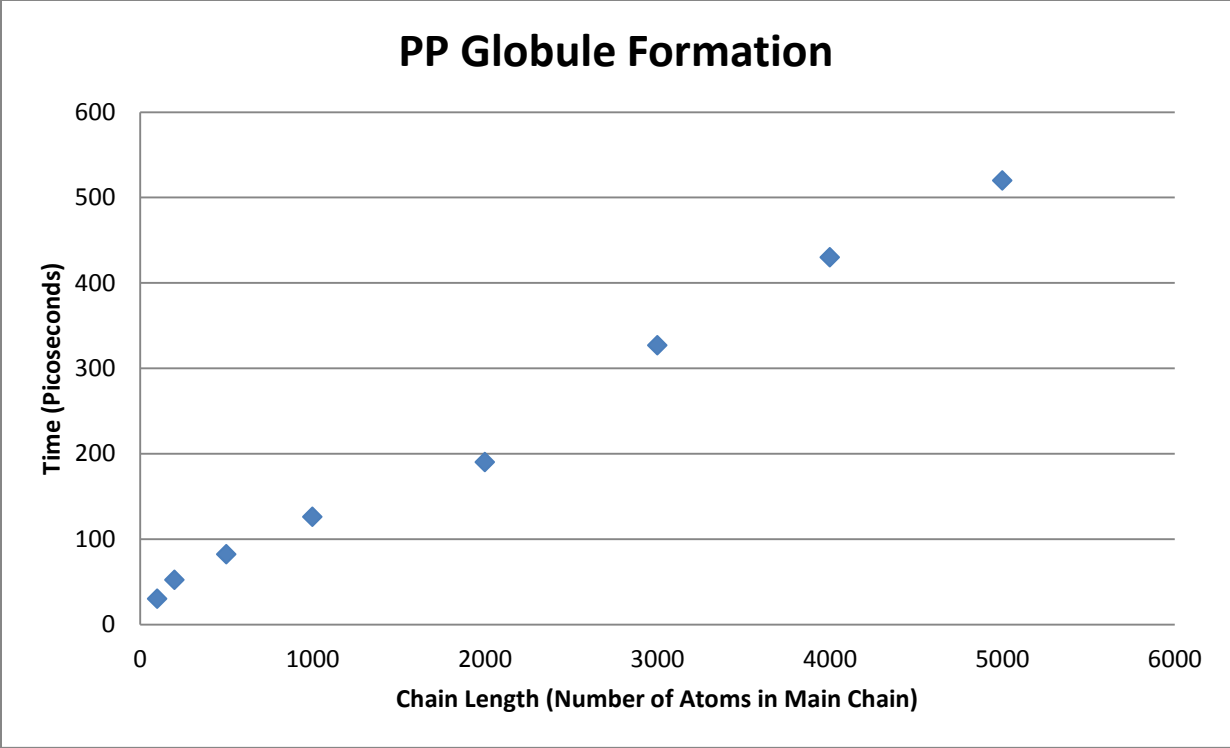


Figure 7: Globule Formation Time of Polypropylene (PP) for various Chain Lengths

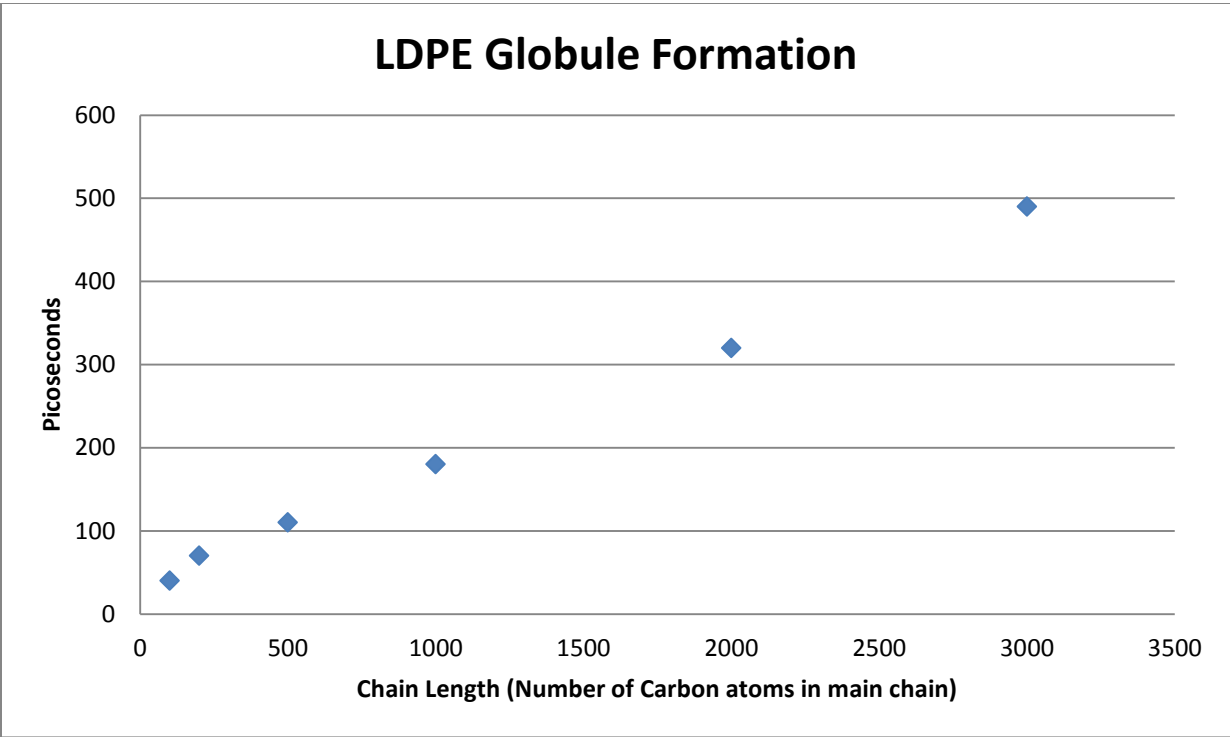


Figure 8: Globule Formation Time of Low Density Polyethylene (LDPE) for various Chain Lengths

Figure 9, Figure 10, and Figure 11 are a different interpretation of the data shown above. The following plots display the globule formation time of HDPE, PP, and LDPE on a per atom basis. The simulations were run at 300K and 0atm for 3000 picoseconds. Each plot levels off and reaches a steady state value. This shows that as the chain length increases over a certain point, the globule formation time on a per atom basis becomes constant.

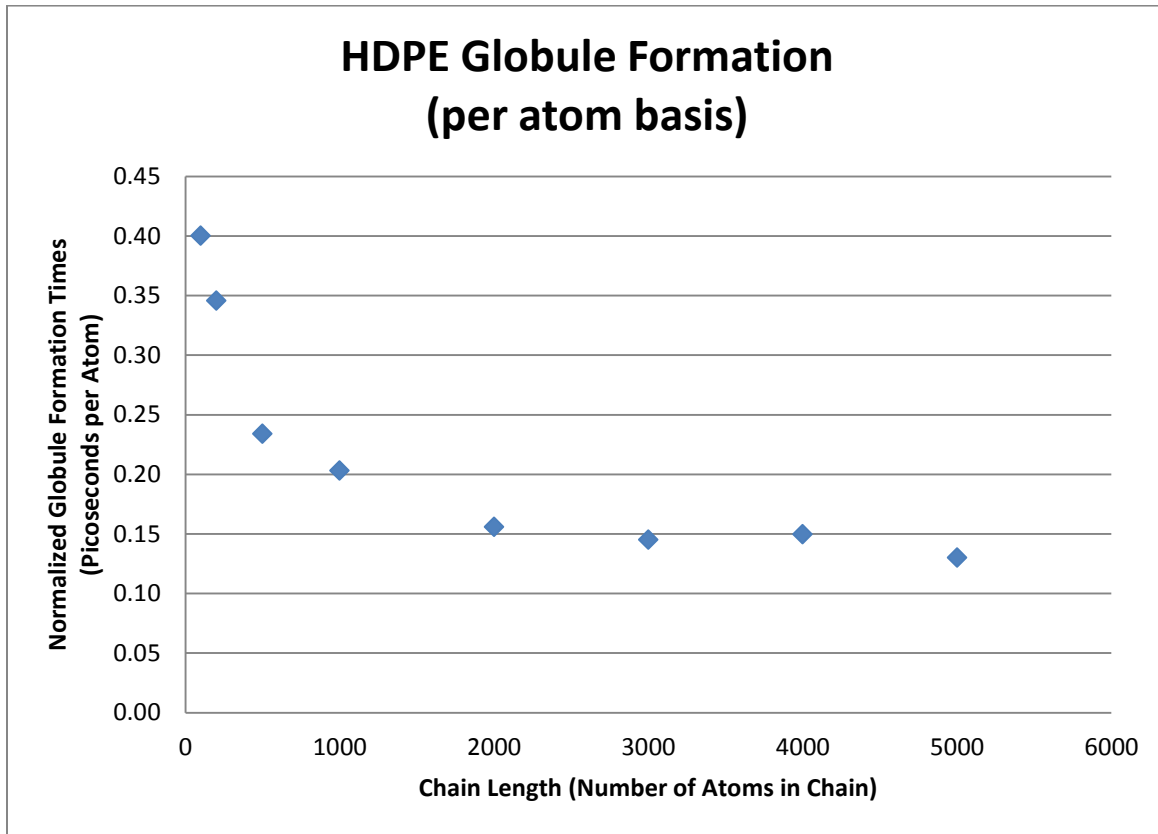


Figure 9: Normalized Globule Formation Time of High Density Polyethylene at various Chain Lengths

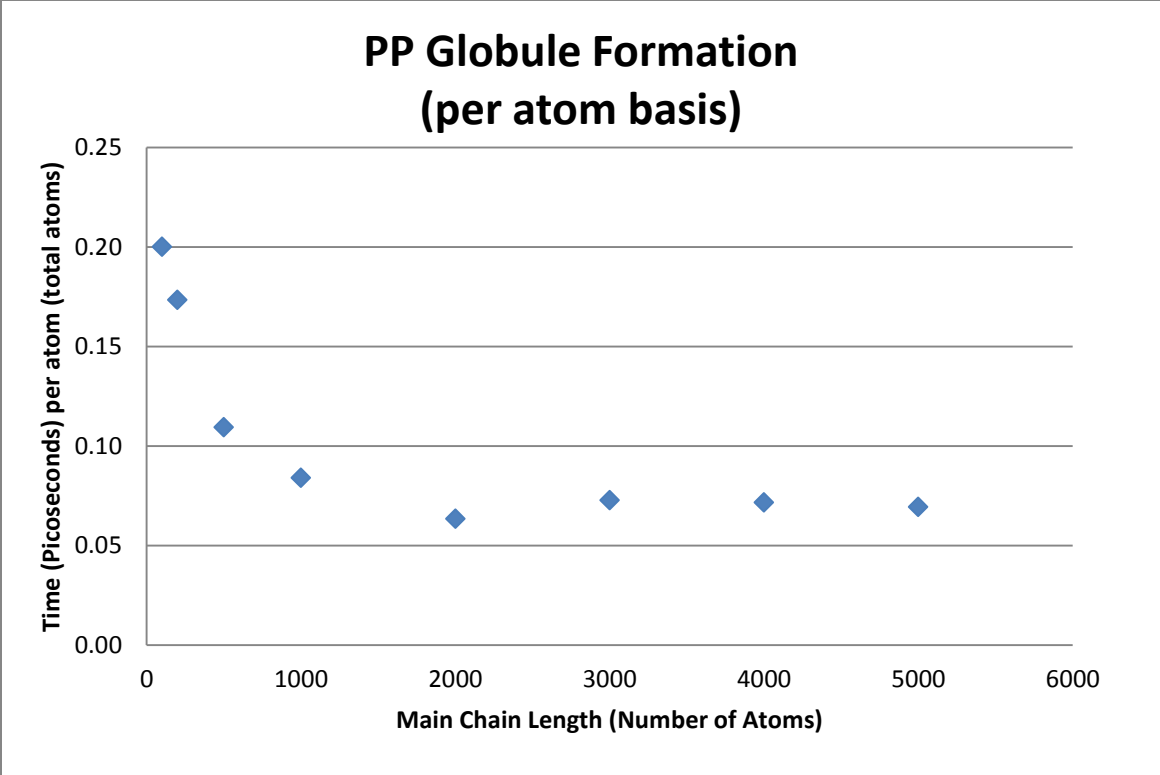


Figure 10: Normalized Globule Formation Time of Polypropylene at various Chain Lengths

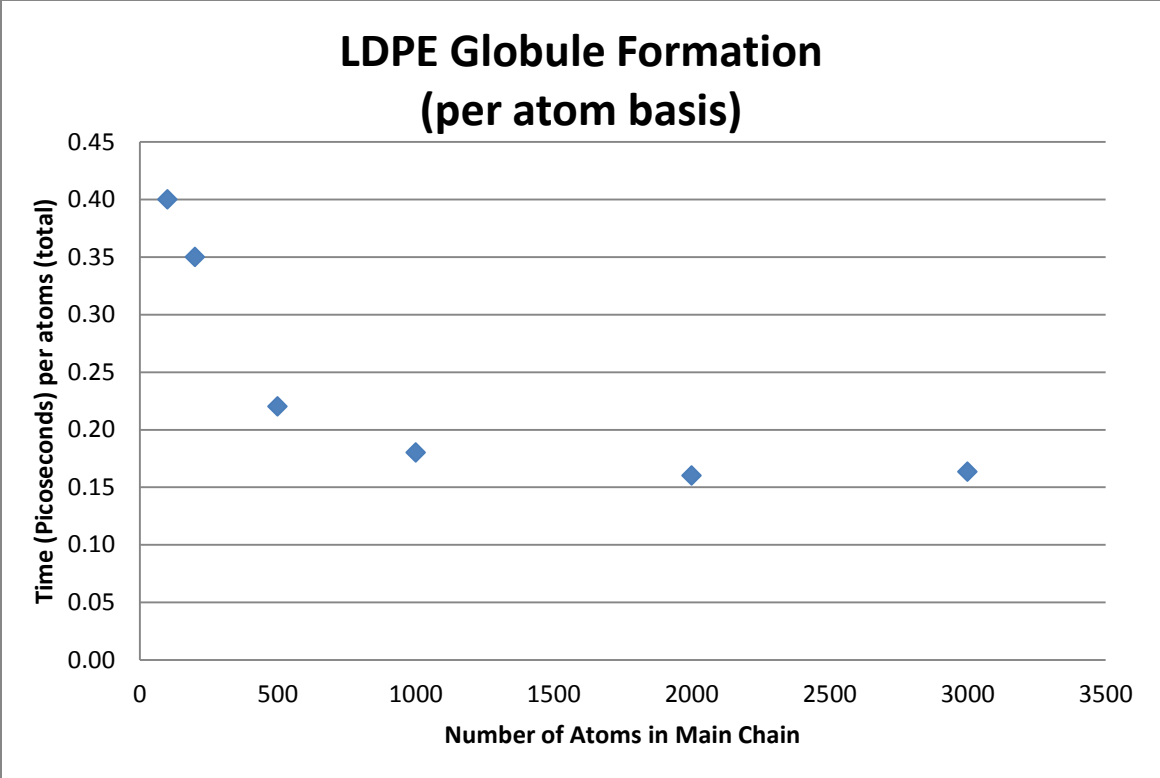


Figure 11: Normalized Globule Formation Time of Low Density Polyethylene at various Chain Lengths

Volume Calculations

The volume occupied by the polymer using a 1.9 angstrom radius around each united atom was calculated using the McVol program. Figure 12 below shows high density polyethylene chains of various lengths simulated with no periodic boundary conditions at 300K and 0atm for 1500 picoseconds. These simulations produced globule-type structures. As the chain length increases, the van der Waals volume increases.

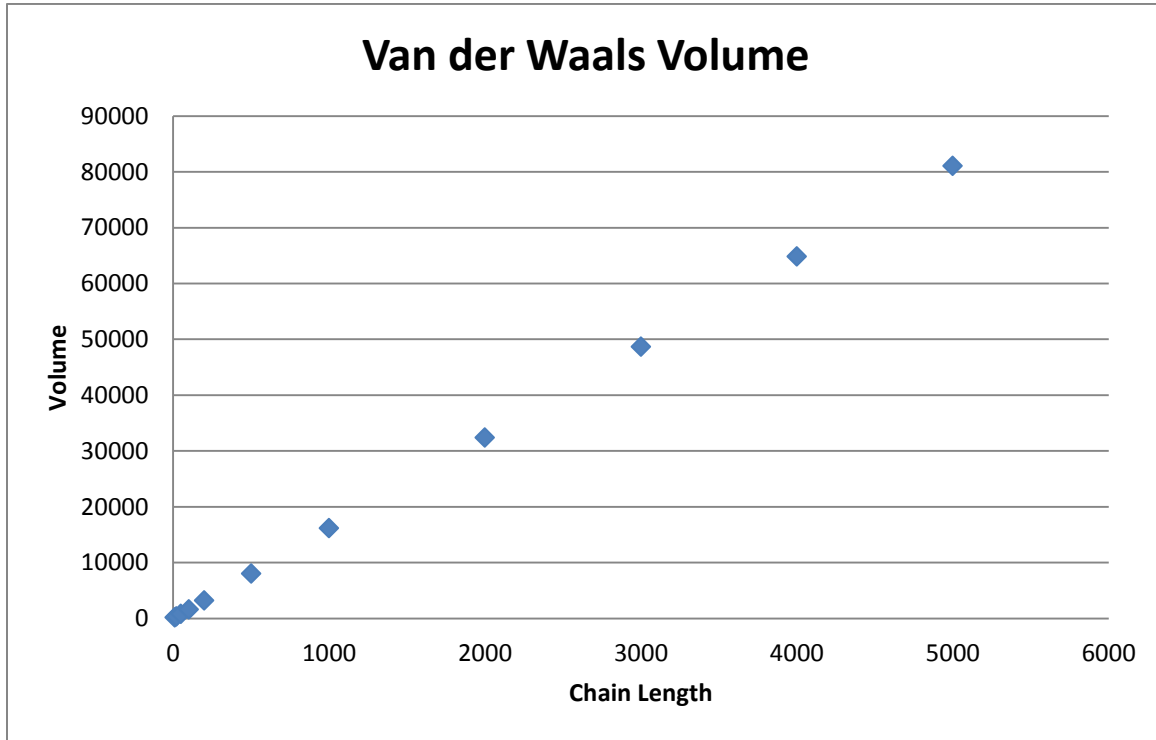


Figure 12: Van der Waals Volume as a function of Chain Length

Figure 13 below, shows the van der Waals volume data for the same set of simulations on a per atom basis. The volume per atom drops significantly as the chain length increases. When the polymer chain becomes a certain length, the volume per atom reaches a constant value.

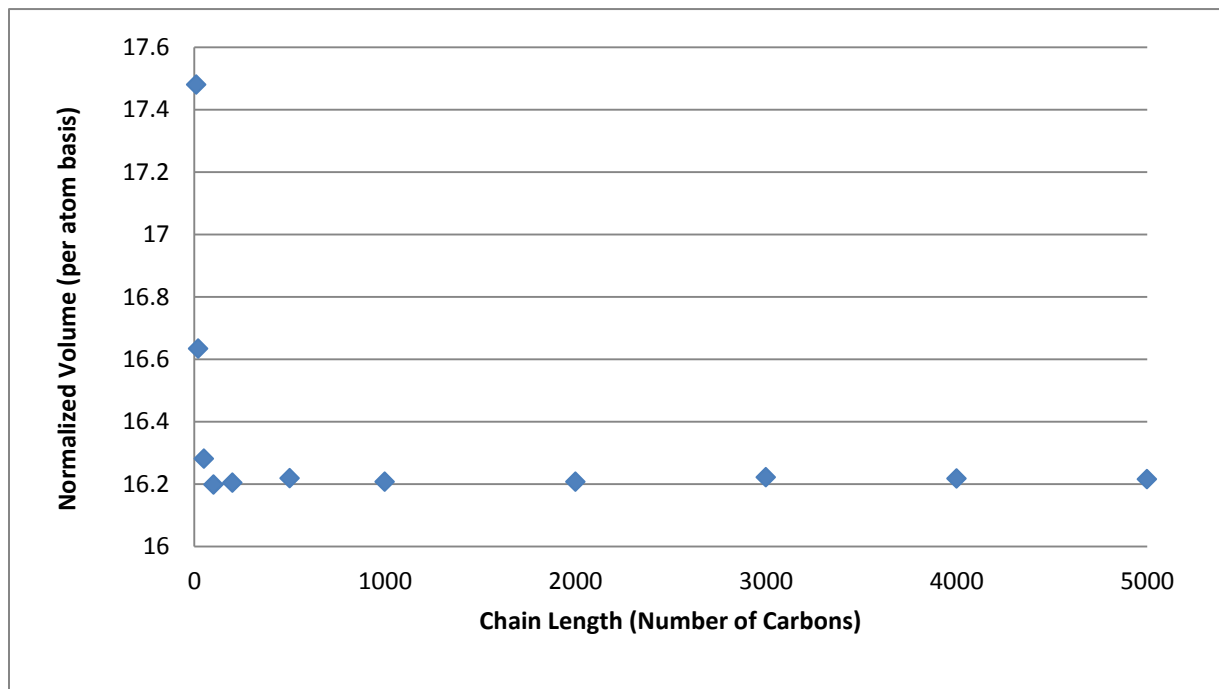


Figure 13: Normalized VDW Volume (per atom basis)

Polymer System Energy

The total system energy of high density polyethylene chains was simulated under no periodic boundary conditions at 300K and 0atm for 1500 picoseconds and was plotted in Figure 14. Globule formation occurred at the intersection of the curved and straight lines. The polymer chains reached a minimum energy state after re-orienting to a globule formation from the straight chain construction established in the initial coordinates. As the chain length increases, a significant initial reduction in energy becomes more and more prominent. Individual energy plots for each chain length can be found in Appendix A. The key to the right of Figure 14 corresponds to chain length in terms of pseudo atoms.

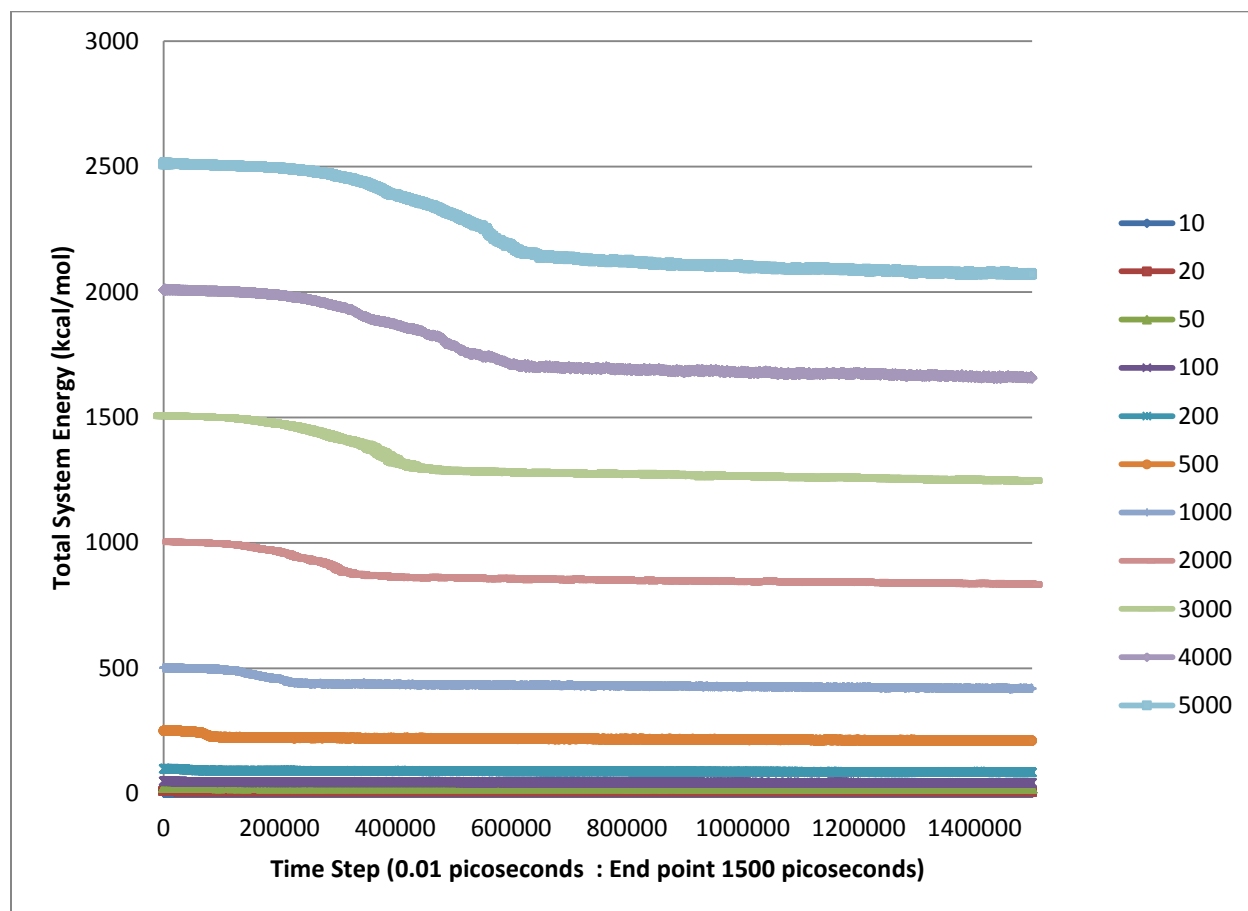


Figure 14: Total System Energy of HDPE for various chain lengths

Polymer Structure - Branching Effects (300K)

Figure 15 below shows the globule formation times of HDPE, PP, and LDPE on a per atom basis. Four chains of 2000 pseudo atoms in main chain length of each polymer type were simulated at 300K and 0atm for 3000 picoseconds. The figure shows a dramatic drop in time per atom between the non-branched HDPE and the side group/branched polymers PP and LDPE.

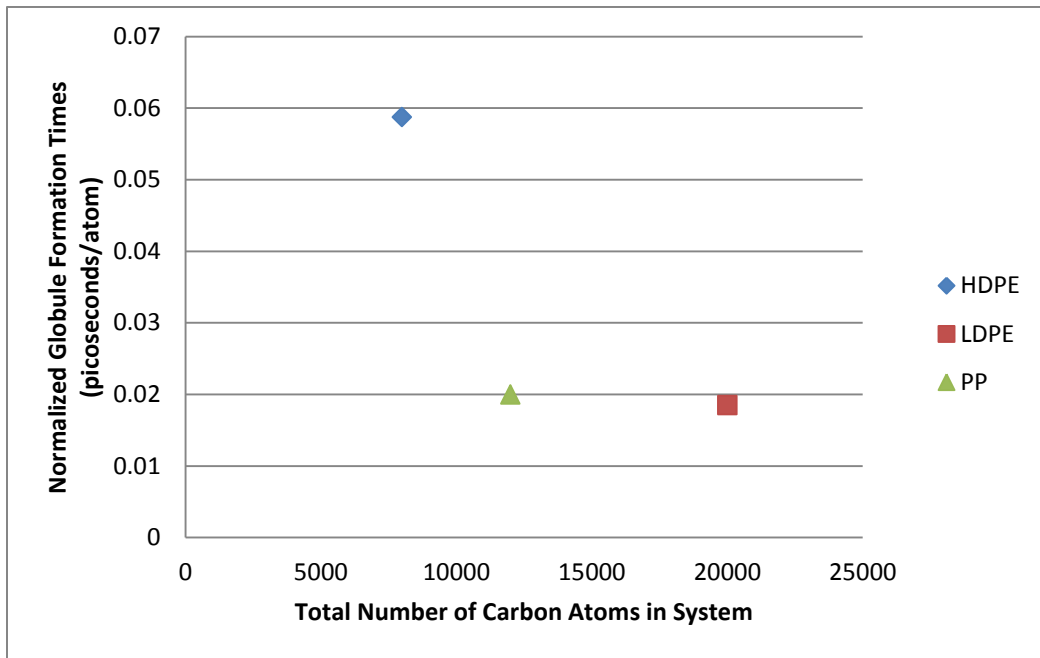


Figure 15: Branching Effects on Globule Formation Time

Figure 16, Figure 17, and Figure 18 are images of HDPE, PP, and LDPE simulations at 130 picoseconds during a 3000 picosecond simulation at 300K and 0atm for each. The scrunching of the chains is more prevalent with increased branching. As branching is increased, the lateral movement of the entire chain is decreased. The straight chains of HDPE show the complete lengths of the chains folding in on themselves to form a globule, whereas the chains of LDPE are seen to climb in on themselves in an elastic-like manner.

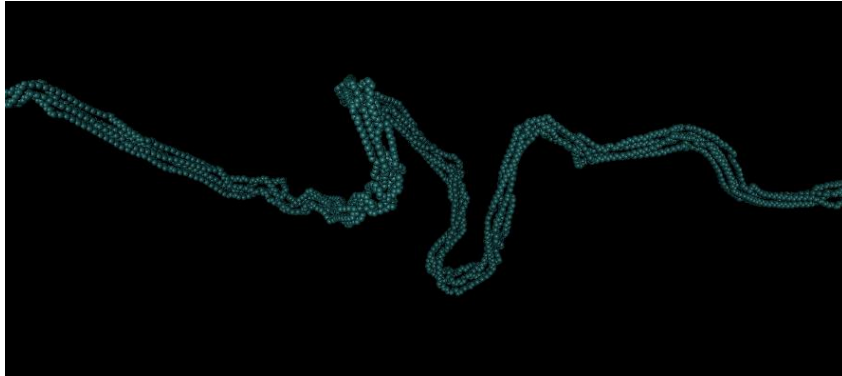


Figure 16: Image HDPE (130 picoseconds)

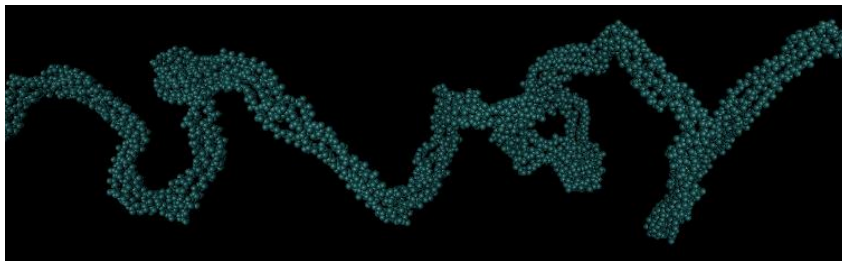


Figure 17: Image of Polyethylene (130 picoseconds)

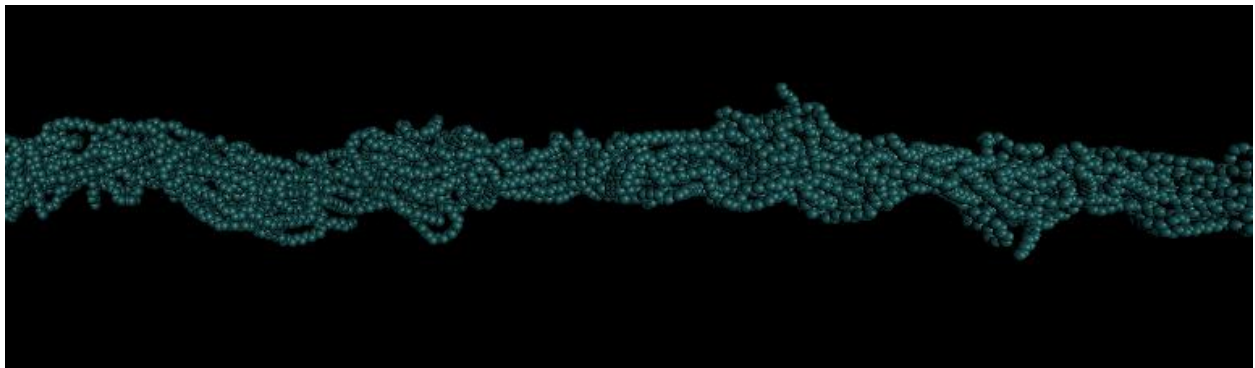


Figure 18: Image of LDPE (130 picoseconds)

Polymer Structure – Temperature Effects

Figure 19 below shows globule formation times for HDPE at various temperatures. The simulations were of four chains of 2000 pseudo atoms run for 3000 picoseconds at 300K and 0atm. As the temperature of the system was increased the time for the polymer to ball up and assume a globule shape decreased.

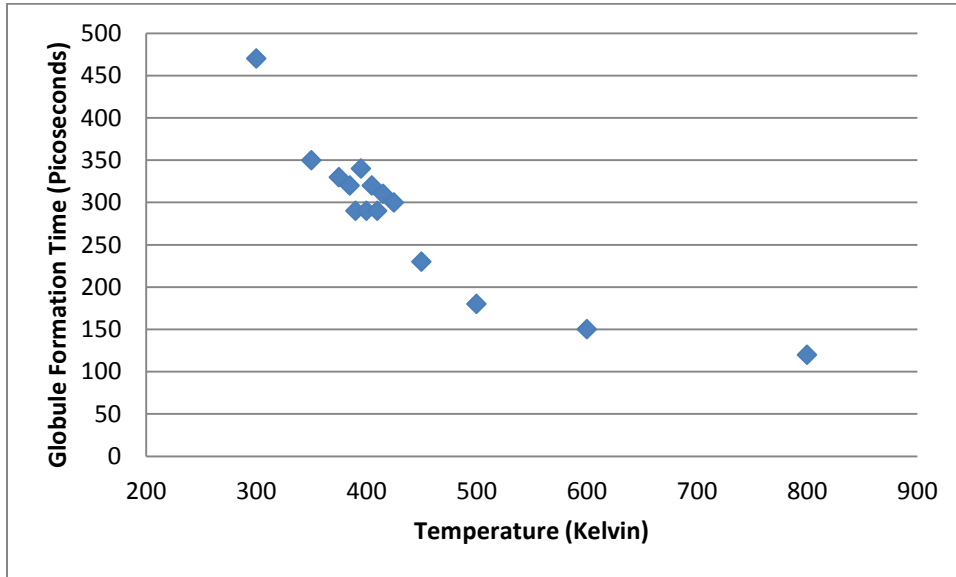


Figure 19: HDPE Globule Formation Times at Various Temperatures

Density

Pressure and Simulation Time Effects

Table 5 below shows the effect of simulation time, pressure, and chain length on the density of the polymer system. Simulations were run for single polymer systems at 300K. Experimental density of HDPE (0% branching; molecular weight 83100 ^g/_{mol}) is 0.947g/cm³. (Liu, Wang, & He, 2002)

Column	1	2	3	4
Simulation Duration (picoseconds)	150	1500	1500	1500
Polymer Chain Length (Number of Carbons)	1000	1000	1000	2000
Pressure (atm)	0	0	1	0
Temperature (Kelvin)	300	300	300	300
Density	1.0612	0.873	0.867	0.868

Table 5: Density of HDPE

Table 5 above, shows that for different simulation times (column 1 and 2), the longer simulation resulted in the more accurate density calculation. Pressure differences (column 2 and 3) had little effect on the density of the system, although the simulation with 0atm pressure was closer to literature values. The length of the polymer chain (columns 3 and 4) also had an insignificant effect on the density of the system.

Chain Length and Number of Chain Effects

Simulations shown in Table 6 were run for 3000 picoseconds at 300K and 0atm. Table 6 displays the density data for simulations of different chain lengths and quantities. Despite the previously stated findings of the critical molecular weight being 2000 carbons long for HDPE (Figure 6), the simulations of the chains of 100 and 200 pseudo atoms long produced the most accurate density data.

Number of Chains	1	4	25	50
Chain Length – Number of Atoms	2000	2000	200	100
Density (g/cm ³)	0.868	0.886	0.951	0.944

Table 6: HDPE density data for different chain lengths and number of chains

Figure 20 and Figure 21 below, are images of HDPE for a 50 chain system of 100 pseudo atoms long and a 20 chain system of 500 pseudo atoms long respectively. The images were taken during 3000 picosecond long NPT simulations at 300K and 0atm. Voids can be seen in Figure 21 in the simulation of a longer chain system of lesser quantity.

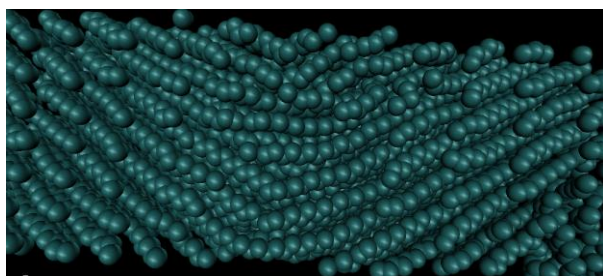


Figure 20: Image of HDPE 50 Chain System (100 atoms long)

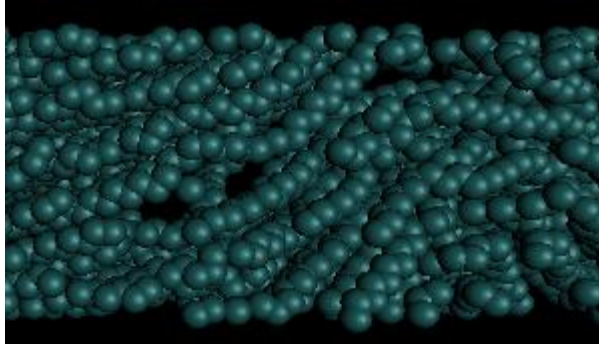


Figure 21: Image of HDPE 20 Chain System (500 atoms long)

Equilibration Effects

Initial NVT and NPT simulations in Table 7 were run for 3000 picoseconds at 300K and 0atm. Subsequent continuation simulations (NPT post equilibration) were run for 1500 picoseconds at 300K and 0atm. Table 6 Table 7 displays the results of six simulations that assessed the effects of equilibrating the system before running a NPT simulation to calculate the density. Equilibration is shown to affect the density minimally.

Type of Simulation	NPT - (no NVT equilibration)	NPT – (with NVT equilibration)
HDPE 50 Chains – 100 atoms long	0.942	0.944
HDPE 25 Chains – 200 atoms long	0.948	0.951

Table 7: Equilibrium/non-equilibrium HDPE density values (g/cm³)

Branching Effects

Densities of HDPE, PP, and LDPE are shown in Table 8. Simulations were performed for four chain systems at 300K and 0atm for 3000 picoseconds. A general trend can be seen where density increases with decreasing branching.

Polymer Type	HDPE	PP	LDPE
Density (g/cm ³)	0.886	0.845	0.734

Table 8: Density of Four Chain Polymer systems (main chain length 2000 atoms)

Crystallization / Melting

A series of simulations were run at various temperatures under no periodic boundary conditions. Four chains of HDPE with chain lengths of 2000 pseudo atoms comprised each system. Each simulation was run at 0atm for 3000 picoseconds.

Figure 22 and Figure 23 below show a low temperature simulation which resulted in the polymer chains aligning themselves into ordered structures.

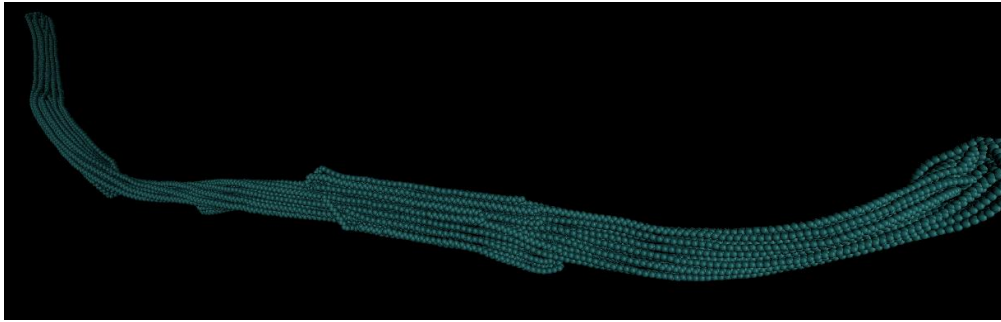


Figure 22: Image of HDPE 100K (3000 picoseconds)

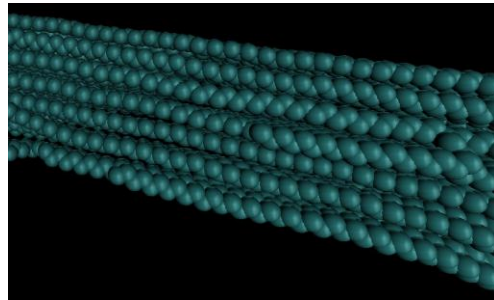


Figure 23: Image of HDPE 100K enlargement (3000 picoseconds)

Figure 24, Figure 25, and Figure 26 show room temperature simulations at 300K. These resulted in the formation of a globular structure. The chains stayed together in the globule formation process as seen in Figure 25.

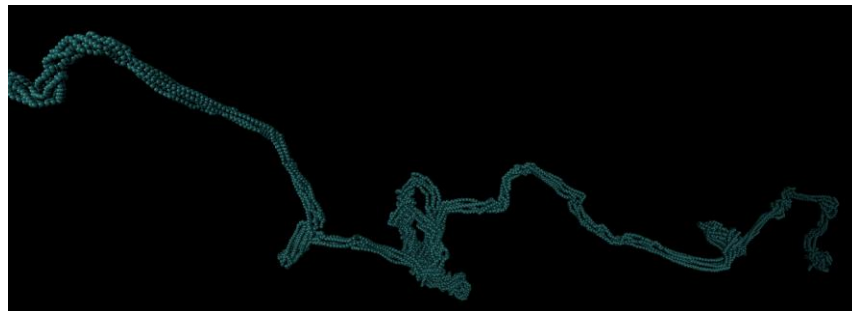


Figure 24: Image of HDPE 300K (220 picoseconds)



Figure 25: Image of HDPE 300K (340 picoseconds)

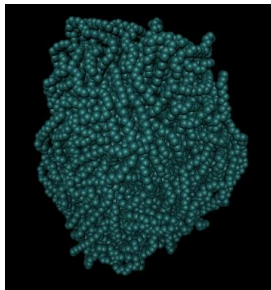


Figure 26: Image of HDPE 300K (3000 picoseconds)

As the temperature starts to increase, the chains do not stay together as well as seen by the large chain separation in Figure 27. Figure 28 and Figure 29 show singular chains stemming out from the globule which have parted from group of four from which they started.

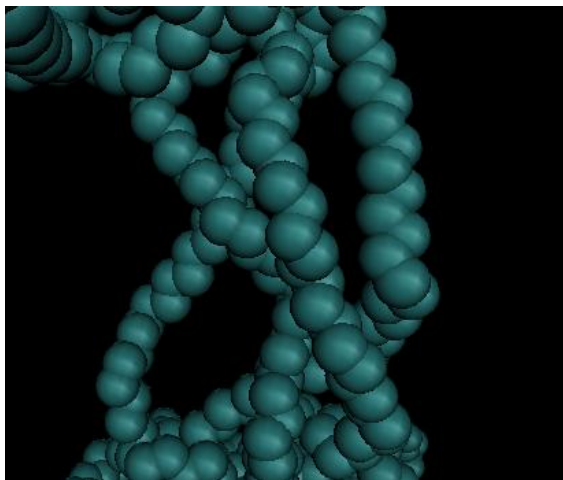


Figure 27: Image of HDPE 500K (130 picoseconds)

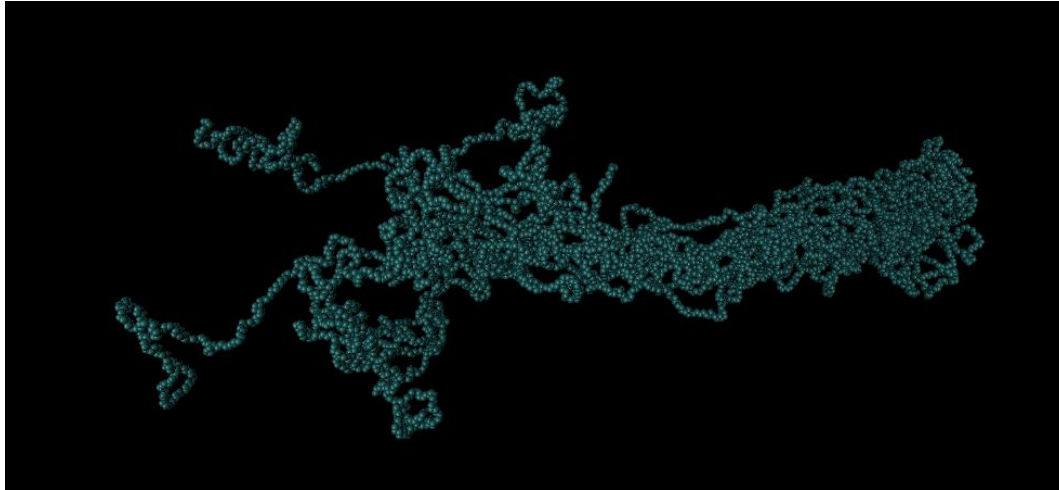


Figure 28: Image of HDPE 800K (210 picoseconds)

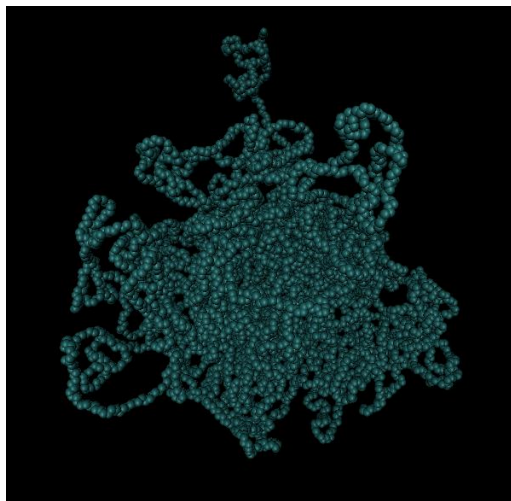


Figure 29: Image of HDPE 800K (3000 picoseconds)

Melting Point Determination

Density data for HDPE and PP at various temperatures are shown in Figure 30 and Figure 31 below. Four chains of 2000 pseudo atoms in length were simulated (NVT) for 3000 picoseconds with no periodic boundary conditions to equilibrate the system and then run (NPT) for an additional 1500 picoseconds. The pressure for all simulations was 0 atm. The melting point/glass transition temperatures were estimated by the vertical dotted lines placed between the two density values of differing slopes. The glass transition temperature is estimated for HDPE in Figure 30 as the system is mostly amorphous, while the melting point is estimated for PP in Figure 31 as the system is more crystalline.

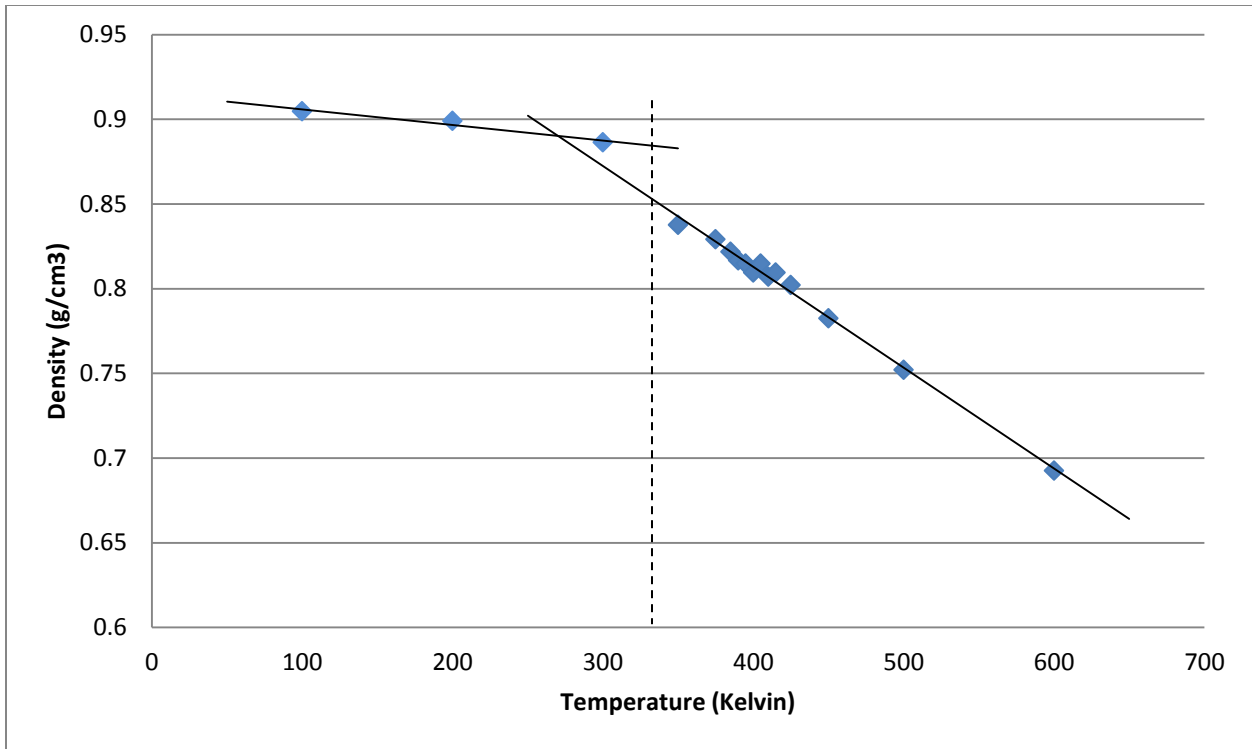


Figure 30: Density of HDPE at various temperatures

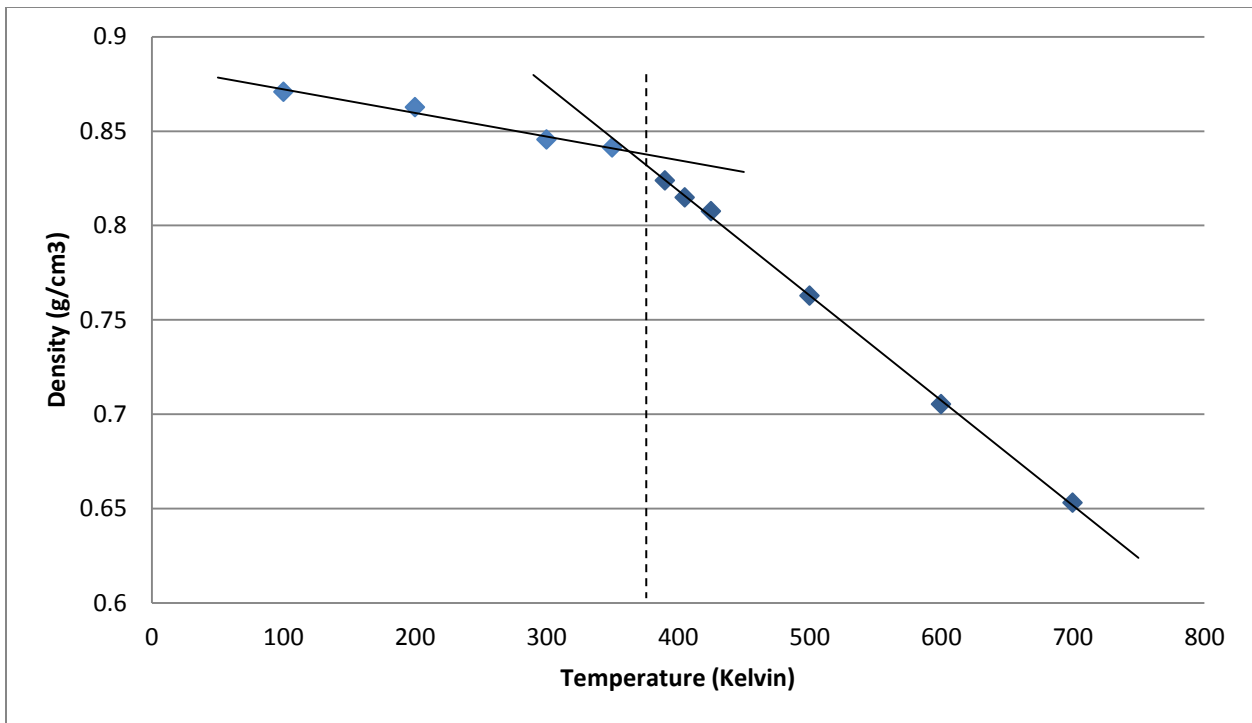


Figure 31: PP Density Data at Various Temperatures

Figure 32 below shows the volume data for polypropylene extracted from Figure 31. The plot shows a change in expansion rate of the polymer system when plotted for various temperatures.

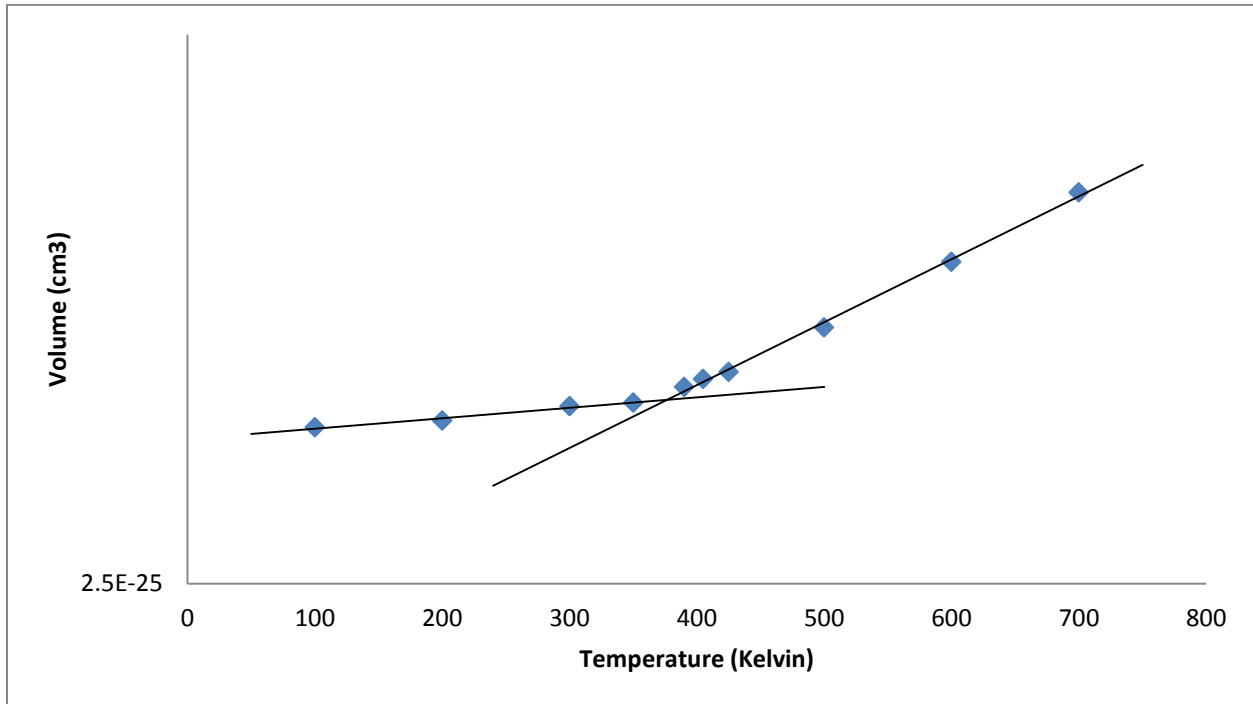


Figure 32: PP Volume data at various temperatures

Four chains of HDPE and PP were simulated for 3000 picoseconds at 0 atmospheres for various temperatures around the respective melting points of each polymer. Figure 33 and Figure 34 below, show the configurational energy change with increasing temperature. Figure 35 and Figure 36 below, show the van der Waals forces plotted against temperature. A slight inflection point can be seen around the melting temperatures of each polymer for these two types of system energy.

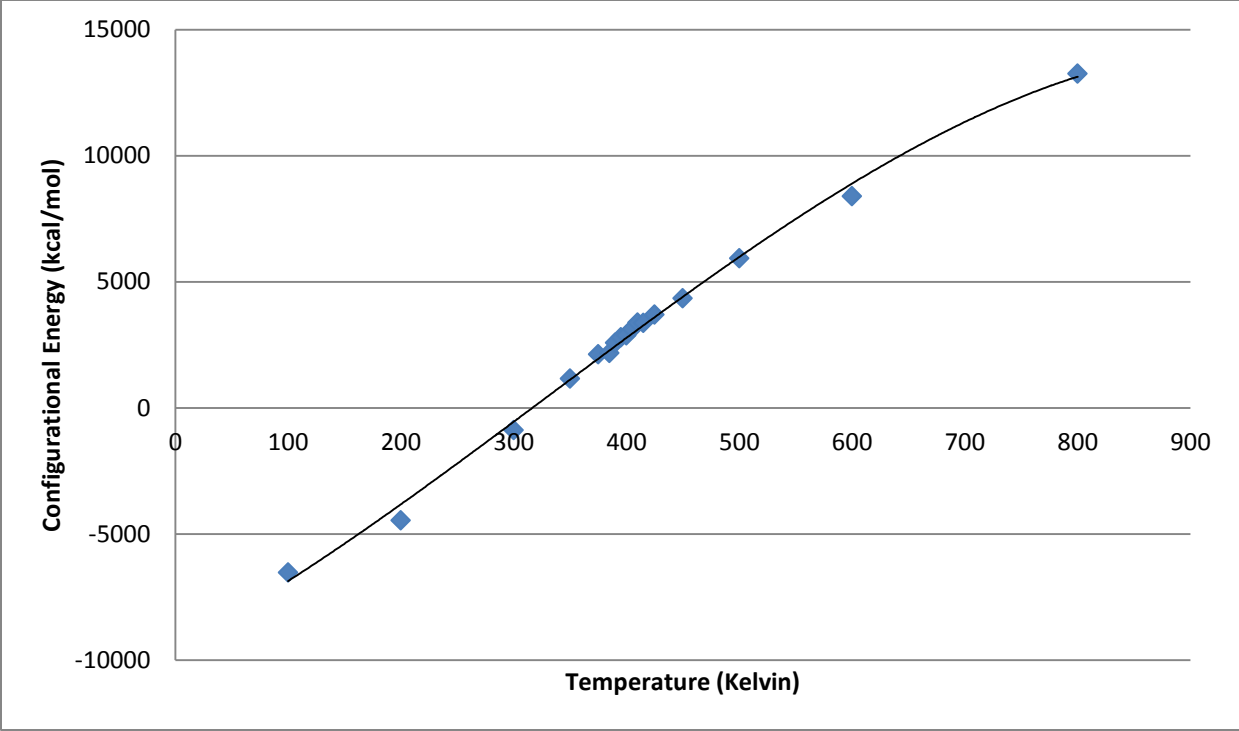


Figure 33: HDPE Configurational Energy Temperature Data

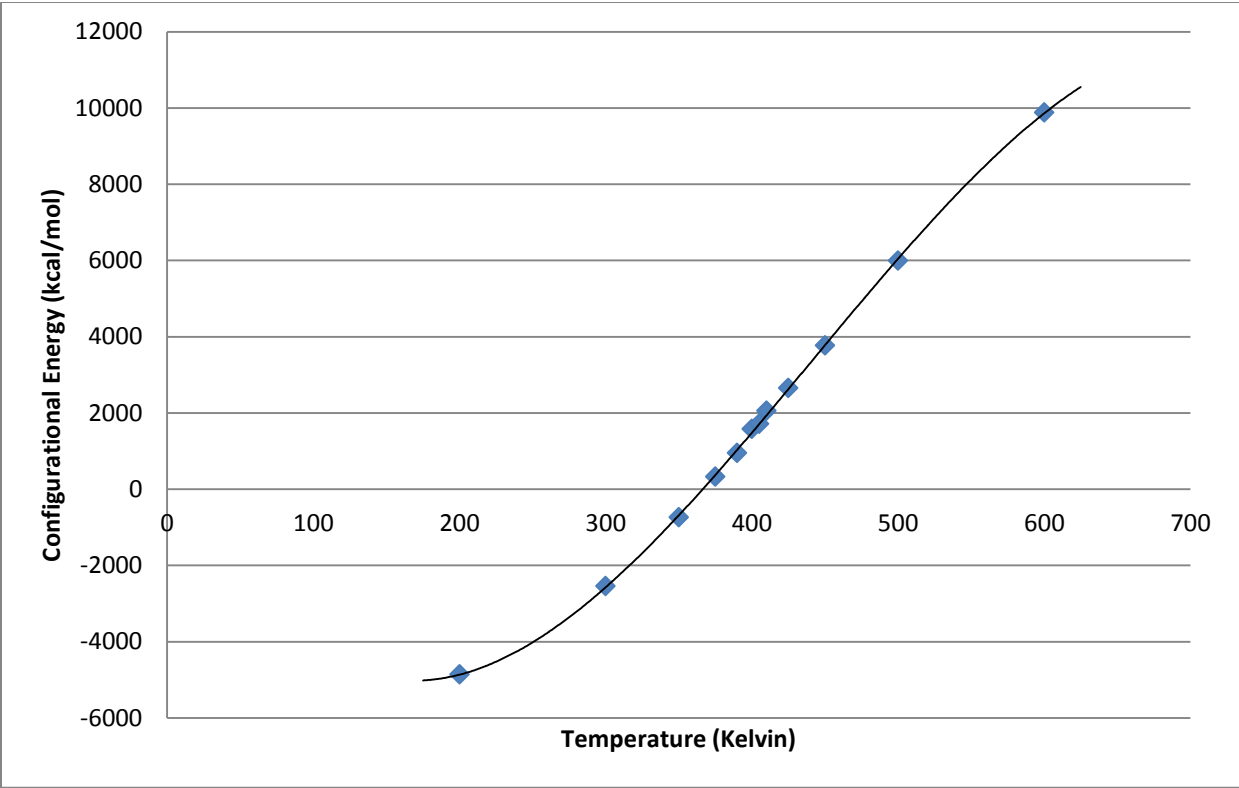


Figure 34: PP Configurational Energy Temperature Data

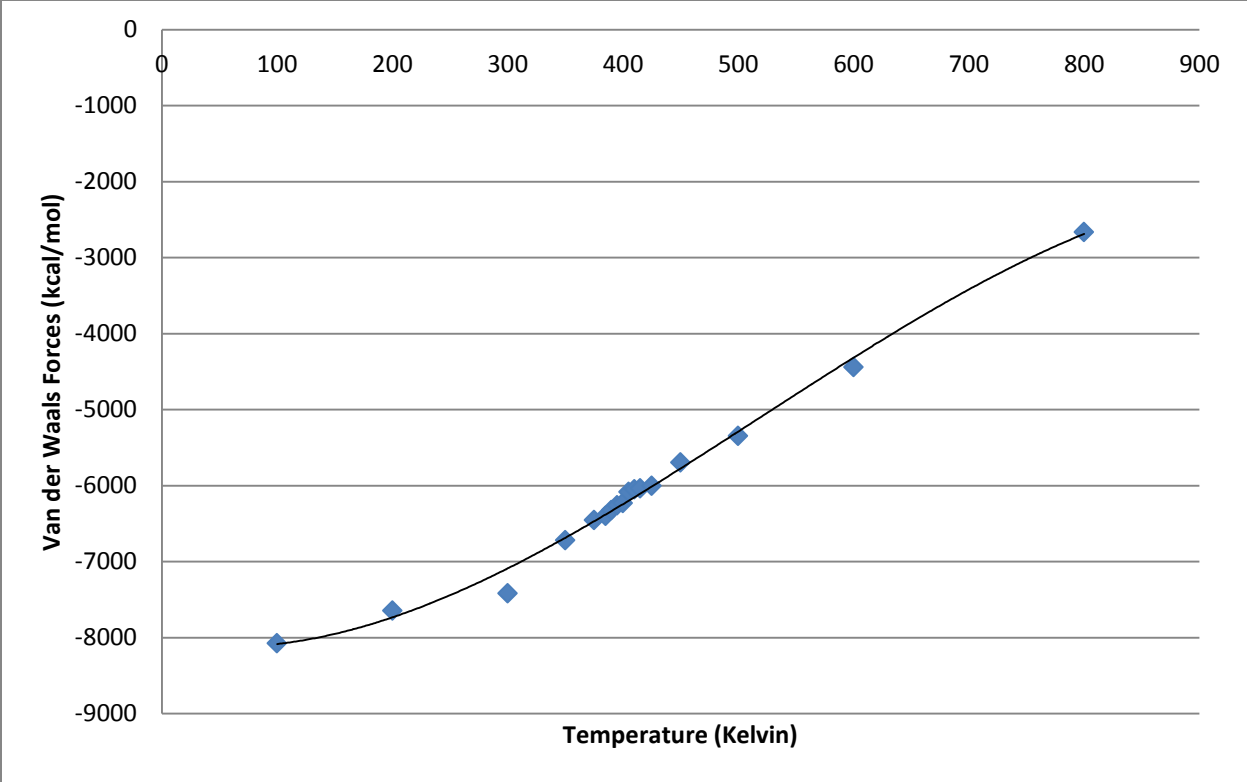


Figure 35: Van der Waals Forces of HDPE at Various Temperatures

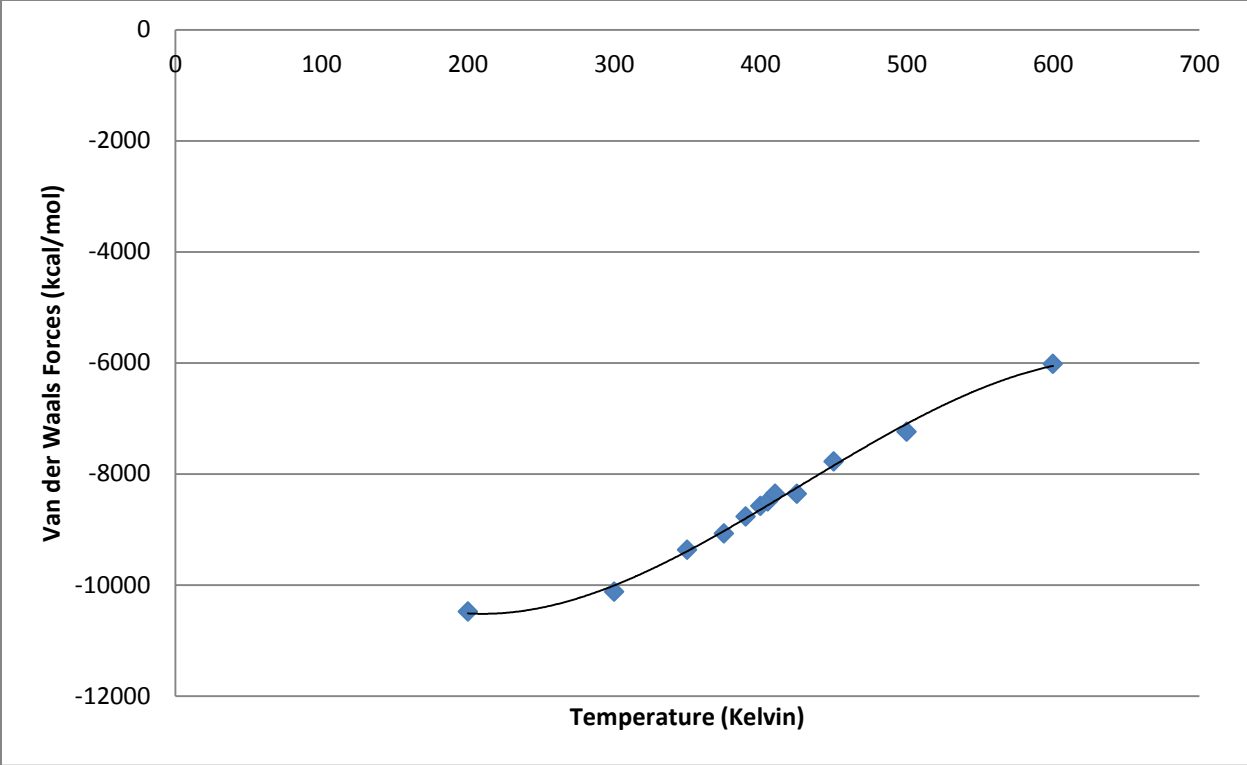


Figure 36: Van der Waals Forces of Polypropylene at Various Temperatures

Discussion

Globule Formation

As the time values were visually determined they are therefore approximate. The CONTROL file specifies the number of steps recorded to the HISTORY file. In order to keep the HISTORY file to a reasonable size, the steps logged were taken every X amount of steps. For longer simulations, this number increased. For a three million step simulation, steps recorded every 10,000 steps would produce 300 entries in the HISTORY file. Depending on the fraction of steps recorded, the instant that the globule may have appeared to form could possibly be some time after the actual formation. The globule formation times were used to assess trends and should not be taken as exact formation times.

Exact globule formation times could be more accurately determined through recording a larger percentage of the simulation steps. Using the coordinates of the HISTORY file, the McVol program could also be employed to calculate the volume of the molecule at every step. A more exact globule formation time could then be extracted based on the volume change. This would be a very tedious and time consuming process, and so was not used for the general purposes of this work.

The energy data was referenced when determining the globule formation times. The intersection of the curved dramatic energy drop with the linear, such as seen in Figure 14, also describes the globule formation time. The values extracted from the energy graph such as this were on the same level of accuracy as visual interpretation.

Figure 6, Figure 7, and Figure 8 display the globule formation times at various chain lengths. As chain length increases, so does the time it takes to form a globule. This is expected as the ends of long chains are further from each other than the ends of short chains, and so will take longer to come together as there is a greater distance to travel.

Figure 9, Figure 10, and Figure 11 display the globule formation times on a per atom basis. These plots show that as the size of the chain increases, the globule formation times on a per atom basis achieve constant values. When a constant value is reached, the van der Waals forces act proportionally on each atom in the polymer. This means that there is a minimum chain length for the van der Waals forces to be consistent. The minimum chain length corresponds to the critical molecular weight of a polymer.

The critical molecular weight values extracted from the plots were approximately 2000, 1700, and 1500 pseudo atoms long for HDPE, PP, and LDPE respectively. As HDPE is the most flexible out of the polymers tested, it is expected that the critical molecular weight will be highest, and therefore the chain length will be longest as it does not have side groups. The side groups of polypropylene stiffen the chain making it more rigid, promoting entanglement and van der Waals attractive forces. The branching of LDPE entangles the chain to an even higher degree, promoting van der Waals attractive forces also. As a result, polymer chains of 2000 pseudo-atoms long formed the standard chain length for all subsequent simulations in this work.

Figure 15 shows the effects of branching on globule formation time. The plot shows that globules are formed much more quickly when the chains have any amount of side groups or degree of branching.

The dramatic drop in time from the HDPE to the fairly equal values of both polypropylene and LDPE demonstrates this. The HDPE molecules are able to slide over one another more easily than the branched molecules do. The branching helps promote quicker globule formation due to increased entanglement of the chains.

Volume

The volume on a per atom basis shown in Figure 13 reaches an asymptotic value as the chain length increases beyond a certain point. The van der Waals forces from other parts of the chain promote bond angle bending to wrap the polymer in tightly and form a globule. The straight chain volume is larger than the volume of the globule. This can be seen as the shorter chains have larger volumes and are not able to collapse in on themselves to form globules but instead remain quite straight. The spheres encompassing each pseudo atom have large radii as specified by the McVol program. These radii are able to overlap and do so when attractive van der Waals forces bring distant parts of the chain together. The folding and tangling process promotes overlapping and therefore a decrease in volume. As bond angles can only vary so much, shorter chains are not able to exhibit McVol radii overlap, and therefore display a larger volume per atom.

Energy

The total system energy plot of HDPE, Figure 14, shows that as the chain length increases, the difficulty in maintaining a linear chain also increases. The energy needed to keep the polymer chain in this straight state is much higher and so becomes increasingly less ideal. This is described by the initial dramatic energy drop followed by the steady state straight line with minimal slope. The straight chain reaches a much lower energy state upon formation of a globule which occurs at the end of the dramatic energy drop. The globule undergoes a steady state energy minimization as it reorients itself to find the most stable conformation. This reorientation is described by the straight part of the line with minimal slope on the energy plot.

Density

The results in Table 6 show that the number of chains simulated is more important than the length of chain. The more chains that are simulated, the closer the density becomes to the actual value. The shorter polymers with the larger number of simulated chains were able to fill the simulation box more thoroughly as seen in Figure 20, depicting a more accurate polymeric environment with more precise bulk properties. The 1 and 4 chain systems may have created voids within the simulation box due to a large degree of chain folding, which resulted in a decreased density.

The results from Table 8 show an accurate trend. HDPE has a higher density than LDPE. The side groups and branching do not allow adjacent chains to lie as closely to one another as would linear chains. The inefficient packing results in voids within the system, effectively lowering the density.

Crystallization/Melting

Qualitative observations of crystallization and melting were made when running simulations at various temperatures.

Figure 22 and Figure 23 show crystallization. Four polymer chains were initially simulated at 100K for 3000 picoseconds. The figures reveal that the chains folded over onto one another in an ordered manner multiple times.

Figure 28 and Figure 29 depict melting as there are singular chains extending out from the center. The increased energy in the system has overpowered the attractive van der Waals forces allowing the chains to move independently. Only the bulk of the globule has enough mass to keep the chains centered in a globule type sphere, but they are held together much less tightly than the globules simulated at lower temperatures.

Melting Point/Glass Transition Temperature Determination

Figure 30 and Figure 31 show the densities of HDPE and polypropylene respectively as a function of temperature. Two lines were drawn on each figure that represented the general sloped trend of the data. A third dotted line was drawn in the middle of the two density values at the intersection of the two previous lines. This dotted line describes the melting points for crystalline systems and the glass transition temperatures for amorphous systems. Both systems were comprised of four chains and could be described to have portions of both crystalline and amorphous. As mentioned earlier, the temperatures of molecular simulations may not correspond perfectly to those in the lab. (Jobic, Smirnov, & Bougeard, 2001) For this added reason, the current work is more interested in the qualitative results produced by the simulations. The 'melting point' therefore of polypropylene is seen to be higher than that of HDPE which is expected. The methyl side groups of polypropylene act as barriers that hinder chain slippage and promote entanglement.

The intersection of the two lines with the dotted line describes the breaking point of the attractive van der Waals forces. Figure 32 displays the volumes of PP at various temperatures and can be thought of as the distances between neighboring molecules. This plot demonstrates how the VDW forces have a certain distance where the attraction is fairly consistent. When adjacent molecules exceed this distance, the attraction diminishes quickly, as seen by the rapid volume expansion, and therefore rapid separation of adjacent chains.

The melting point values for both plots are lower than literature values. These simulations were performed with four chains of 2000 pseudo atoms in length. As mentioned earlier in regards to density, simulations with larger numbers of molecules proved to be more accurate. As the melting points were calculated via a density change method, simulations with larger numbers of molecules may provide more precise results.

Figure 33 and Figure 34 show the configurational energy of a four chain system of HDPE and PP respectively. Figure 35 and Figure 36 show the van der Waals attractive forces of the same HDPE and PP systems. The slight inflection point shows the energy change corresponding to chain slippage or melting. The inflection point may have been more defined if simulations of a larger number of polymers were used.

Conclusions

The phenomenon of crystallization was qualitatively observed in the low temperature simulations. Chains were seen to form ordered structures through folding. Melting was also qualitatively observed at high temperatures. Chains were seen to separate from the four adjacent chains from which they initially started.

In agreement with Zhan & Mattice, globule formation was seen in all polymers simulated at temperatures at and above 300K. This depicted van der Waals attractive forces as a result of dipole-dipole interactions. As temperatures increased the chains were seen to break away from the central globules, showing that the increased energy of the system overpowered the attractive forces.

Physical properties were seen to differ between polymers of branched and linear structures. This was in accordance with the findings of Jabbarzadeh et al. The trend of critical molecular weights of all polymers modeled was accurately predicted. Polymers with the least branching exhibited the largest values, while polymers with the most branching displayed the lowest values.

The TraPPE-UA force field did accurately predict the density of high density polyethylene at room temperature, when simulated with a large number of chains. The simulations with four chains at and over the critical molecular weight had densities that deviated from experimental data more so than much shorter chains simulated with a large quantity. The density values corresponded to experimental data. This concludes that the number of chains in the simulation is more important than the length of the chains when studying density of a polymeric system. The current work used longer polymer chains and a larger number of chains during density simulations and expectedly reported densities more accurate than those of de Pablo et al.

Various accurate polymer property trends were observed in the current work. It is concluded that the same trends can be witnessed with a wide variety of polymer systems including those of special interest to the running shoe industry. Careful considerations need to be made in choosing how to model polymer systems of importance. Optimizations of these design parameters will produce more accurate data for predicted properties. Exploration of other force fields not used in this work may provide more precise values for both the properties examined in this work and other properties useful in assessing running shoe polymers.

Works Cited

- Allen, M. P. (2004). Introduction to Molecular Dynamics Simulation. *Computational Soft Matter: From Synthetic Polymers to Proteins, Lecture Notes*, 1-28.
- Arkema. (2009). *Organic Peroxides*. Retrieved January 19, 2012, from Dupont: <http://www.arkema-inc.com/literature/pdf/832.pdf>
- Callister, Jr., W. D. (2007). *Materials Science and Engineering* (7th ed.). John Wiley & Sons, LTD.
- Cramer, C. J. (2002). *Essentials of Computational Chemistry Theories and Models*. John Wiley & Sons LTD.
- Davis, F. J. (2004). *Polymer Chemistry*. Oxford University Press.
- de Pablo, J. J., Laso, M., & Suter, U. W. (1992). Simulation of polyethylene above and below the melting point. *Teh Journal of Chemical Physics*, 2395-2403.
- Drzewinski, A., & van Leeuwen, J. M. (2006). Cross-over from reptation to Rouse dynamics in a 1-dimensional model. *Physical Review E*, 1-9.
- Duan, Y., Wu, C., Chowdhury, S., Lee, M. C., Xiong, G., Zhang, W., et al. (2003). A Point-Charge Force Field for Molecular Mechanics Simulations of Proteins Based on Condensed-Phase Quantum Mechanical Calculations. *Journal of Computational Chemistry*, 1999-2012.
- Encyclopedia Britannica. (2012). *Vulcanization*. Retrieved April 2, 2012, from Encyclopedia Britannica Online: <http://www.britannica.com.ezproxy.wpi.edu/EBchecked/topic/633433/vulcanization>
- Encyclopedia Britannica. (2012). *Elastomer*. Retrieved April 2, 2012, from Encyclopedia Britannica Online: <http://www.britannica.com.ezproxy.wpi.edu/EBchecked/topic/182081/elastomer>
- Encyclopedia Britannica. (2012). *Plastic*. Retrieved April 2, 2012, from Encyclopedia Britannica Online: <http://www.britannica.com.ezproxy.wpi.edu/EBchecked/topic/463684/plastic>
- Hunenberger, P. H. (2005). Thermostat Algorithms for Molecular Dynamics Simulations. *Advanced Polymer Science*, 105-149.
- Izaguirre, J. A., Reich, S., & Skeel, R. D. (1999). Longer time steps for molecular dynamics. *Journal of Chemical Physics*, 9853-9864.
- Jabbarzadeh, A., Atkinson, J. D., & Tanner, R. I. (2003). Effect of Molecular Shape on Rheological Properties in Molecular Dynamics Simulation of Star, H, Comb, and Linear Polymer Melts. *Macromolecules*, 5020-5031.
- Jobic, H., Smirnov, K. S., & Bougeard, D. (2001). Inelastic neutron scattering spectra of zeolite frameworks - experiment and modeling. *Chemical Physics Letters*, 147-153.
- Kamath, G., Robinson, J., & Potoff, J. J. (2005). Application of TraPPE-UA force field for determination of vapor-liquid equilibria of carboxylate esters. *Fluid Phase Equilibria*, 46-55.

- Kausik, R., Mattea, C., Fatkullin, N., & Kimmich, R. (2006). Confinement effect of chain dynamics in micrometer thick layers of a polymer melt below the critical molecular weight. *The Journal of Chemical Physics*.
- Liu, C., Wang, J., & He, J. (2002). Rheological and thermal properties of m-LLDPE blends with m-HDPE and LDPE. *Polymer*, 3811-3818.
- Marcon, V., Vehoff, T., & Ghiringhelli, L. (2007, September 19). *Force Fields*. Retrieved April 13, 2012, from Max Planck Institute for Polymer Research: http://www.mpip-mainz.mpg.de/~andrienk/journal_club/opls.pdf
- Martin, M. G., & Siepmann, J. I. (1999). Novel Configurational-Bias Monte Carlo Method for Branched Molecules. Transferable Potentials for Phase Equilibria. 2. United-Atom Description of Branched Alkanes. *The Journal of Physical Chemistry B*, 4508-4517.
- Odian, G. (2004). *Principles of Polymerization*. John Wiley & Sons LTD.
- Shorten, M. R. (2000). Running Shoe Design: Protection and Performance. *Marathon Medicine (Ed. D. Tunstall Pedoe)*, 159-169.
- Stubbs, J. M., Potoff, J. J., & Siepmann, J. I. (2004). Transferable Potentials for Phase Equilibria. 6. United-Atom Description for Ethers, Glycols, Ketones, and Aldehydes. *The Journal of Physical Chemistry B*, 17596-17605.
- The NSF Blue Ribbon Panel on Simulation-Based Engineering Science. (2006). *Revolutionizing Engineering Science through Simulation*. National Science Foundation.
- Verdejo, R., & Mills, N. (2002). Performance of EVA foam in running shoes. *The Engineering of Sport*, 580-587.
- Wade Jr., L. G. (2009). *Organic Chemistry (7th ed.)*. Pearson College Division.
- Watt, S. W., Chisholm, J. A., Jones, W., & Motherwell, S. (2004). A molecular dynamics simulation of the melting points and glass transition temperatures of myo- and neo-inositol. *The Journal of Chemical Physics*, 9565-9573.
- Wilson, J. F. (2007). Impact-induced fatigue of foamed polymers. *International Journal of Impact Engineering*, 1370-1381.
- Zhan, Y., & Mattice, W. L. (1994). Molecular Dynamics Simulation of the Collapse of Poly(1,4-trans-butadiene) to a Globule and to a Thin Film. *Macromolecules*, 7056-7062.

Appendix A

Total System Energy Plots for HDPE of Various Chain Lengths

Figure 37 through Figure 47 show the total system energy of HDPE at various chain lengths. Simulations were performed at 0atm and 300K for 1500 picoseconds. All figures in this appendix have Y-axis energy units of kcal/mol and X-axis units of time steps (0.01 picoseconds, where the end point time is 1500 picoseconds).

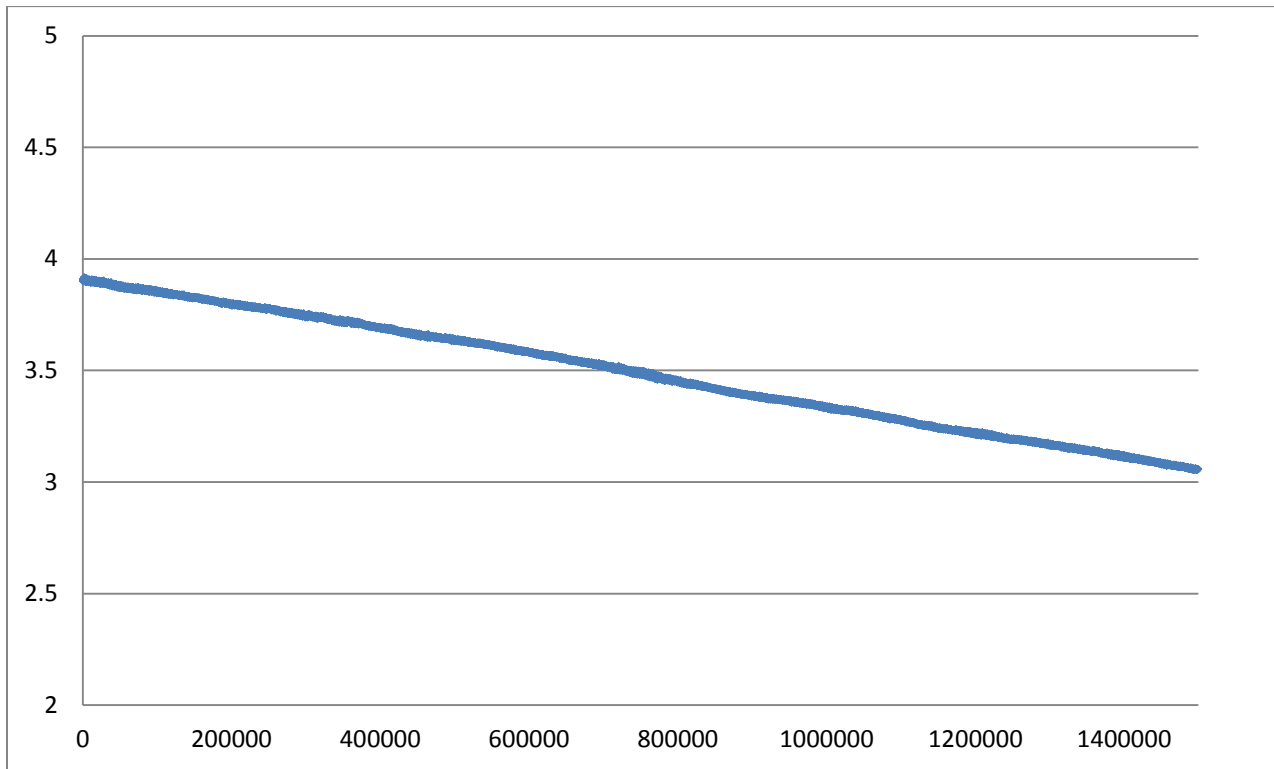


Figure 37: HDPE Chain Length 10 pseudo atoms

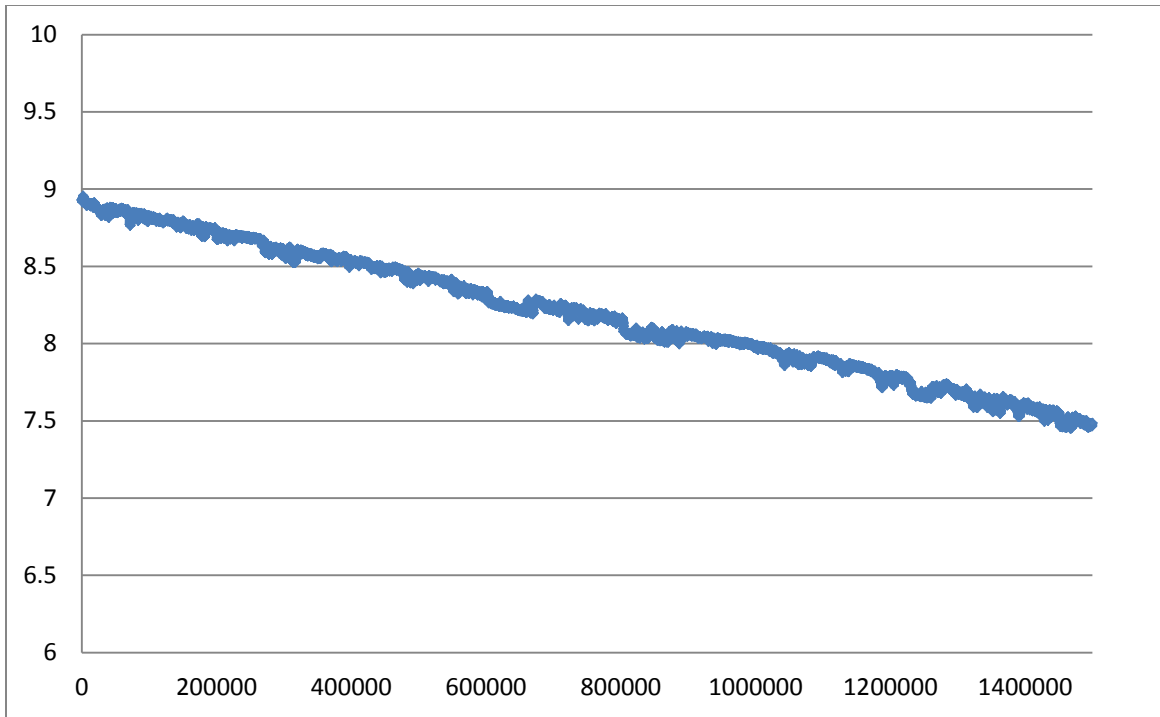


Figure 38: HDPE Chain Length 20 pseudo atoms

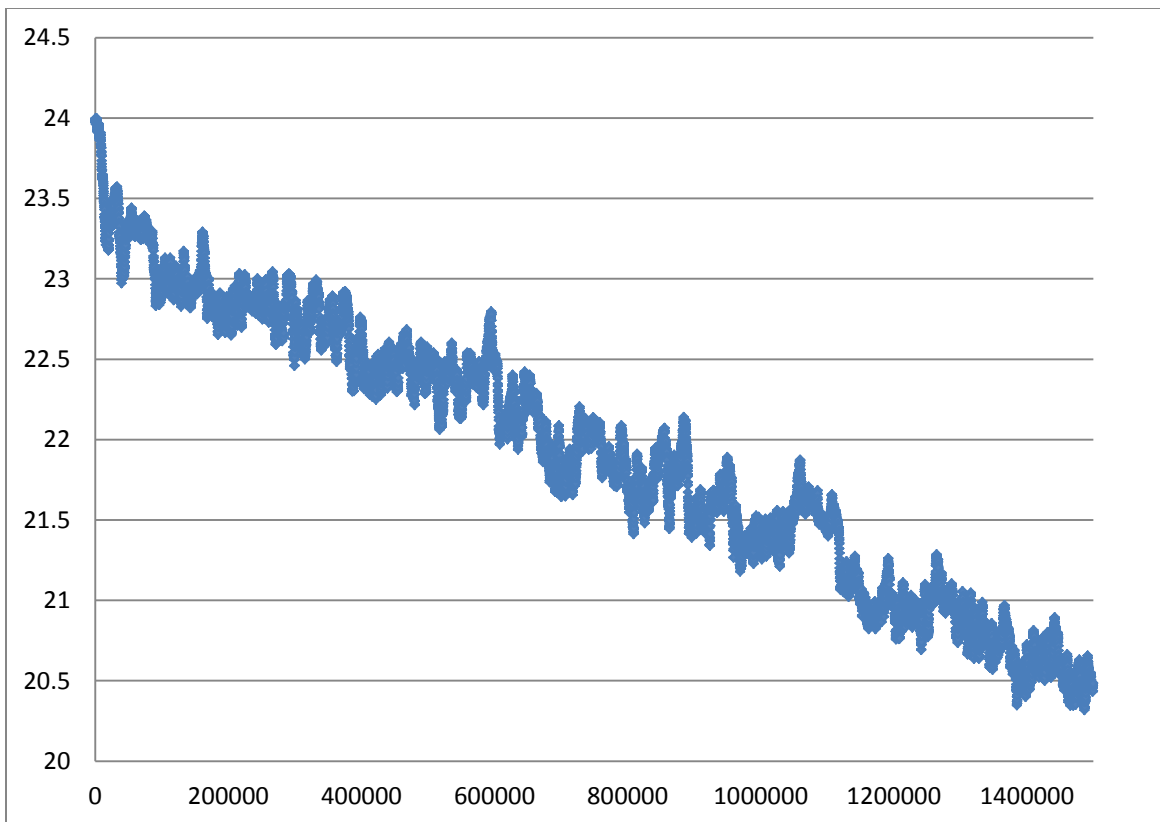


Figure 39: HDPE Chain Length 50 pseudo atoms

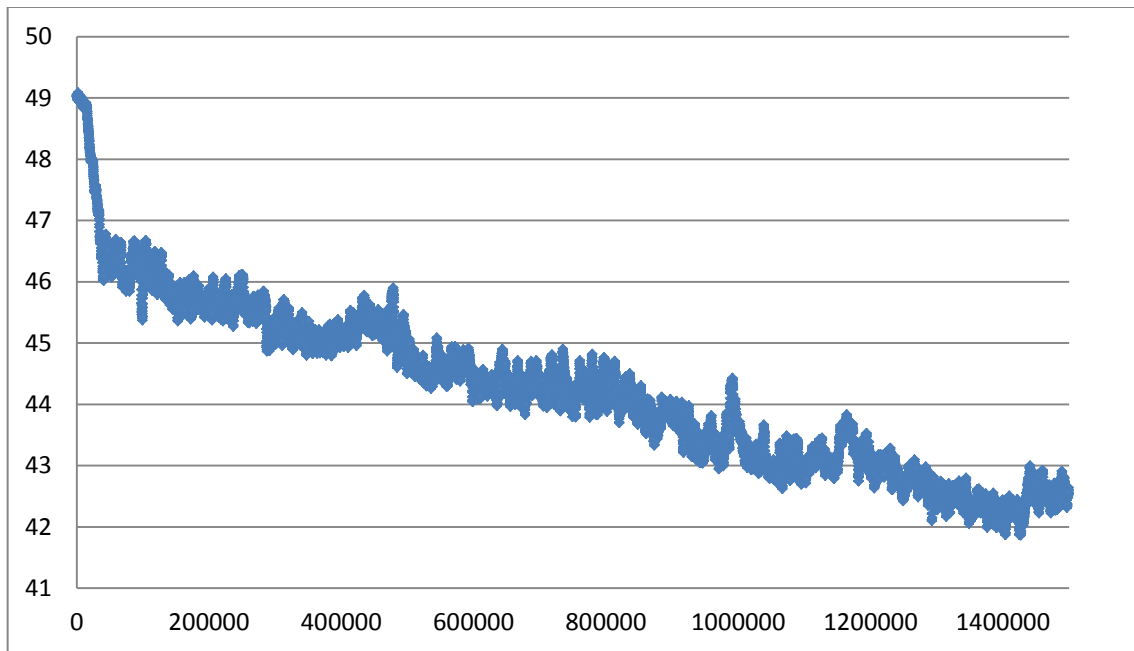


Figure 40: HDPE Chain Length 100 pseudo atoms

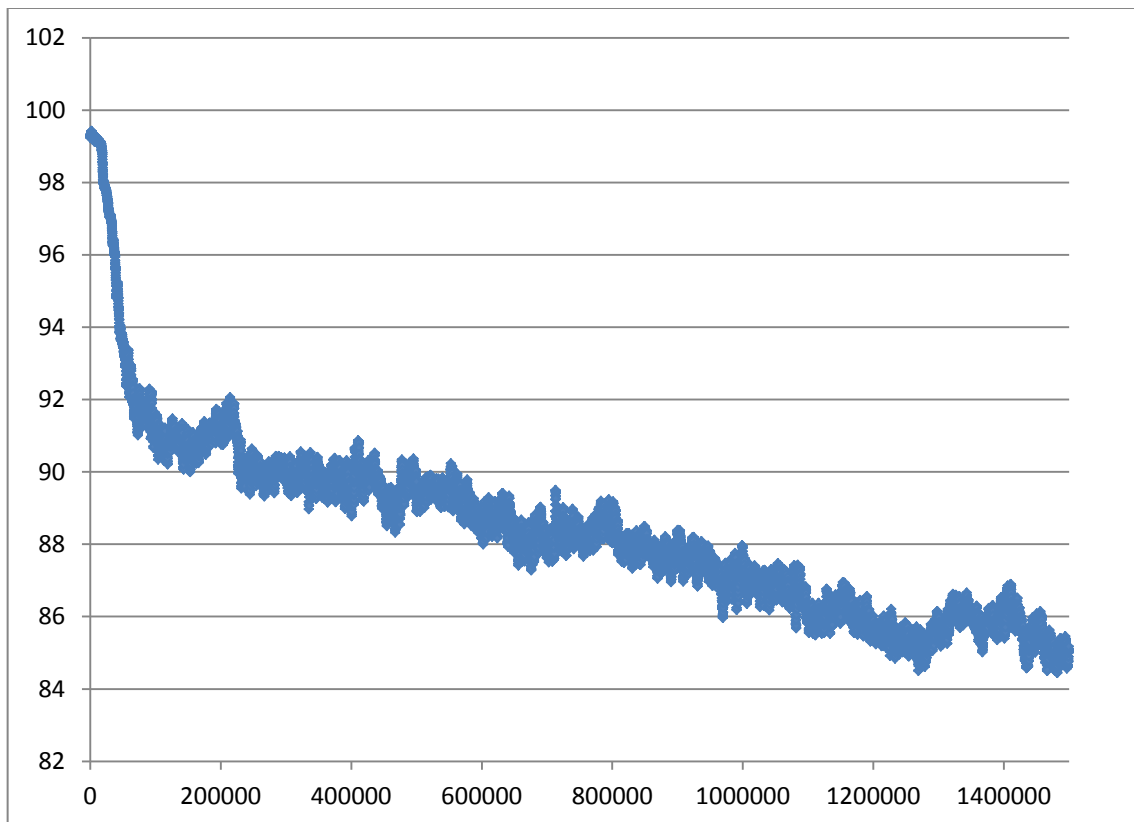


Figure 41: HDPE Chain Length 200 pseudo atoms

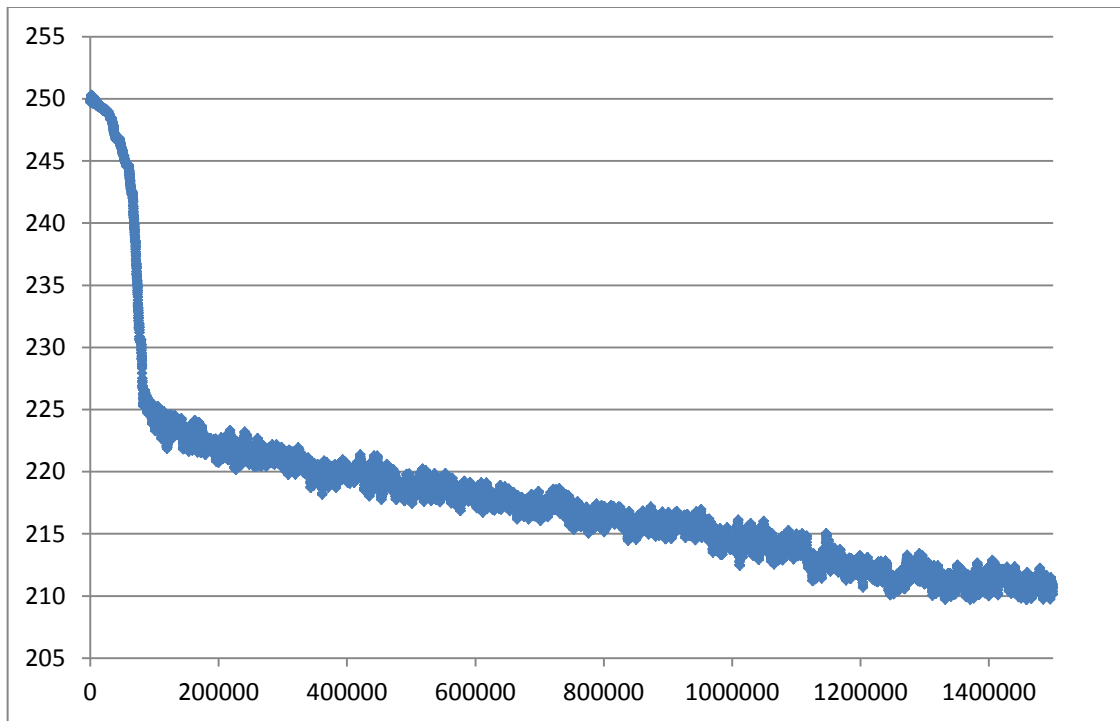


Figure 42: HDPE Chain Length 500 pseudo atoms

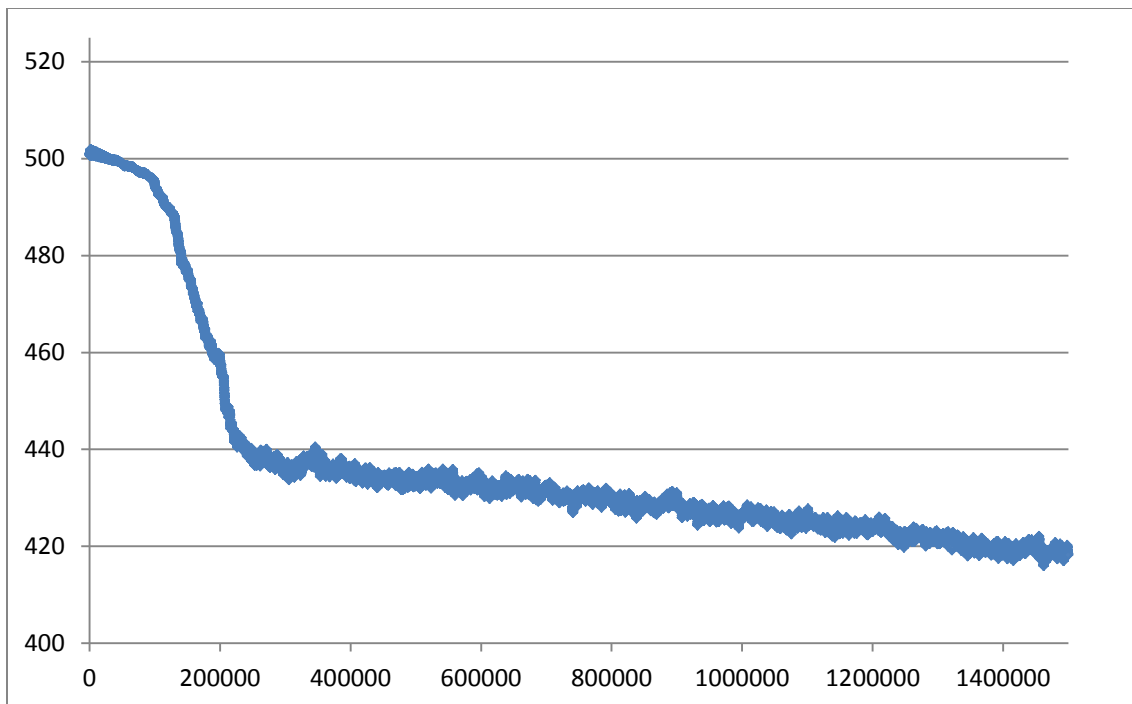


Figure 43: HDPE Chain Length 1000 pseudo atoms

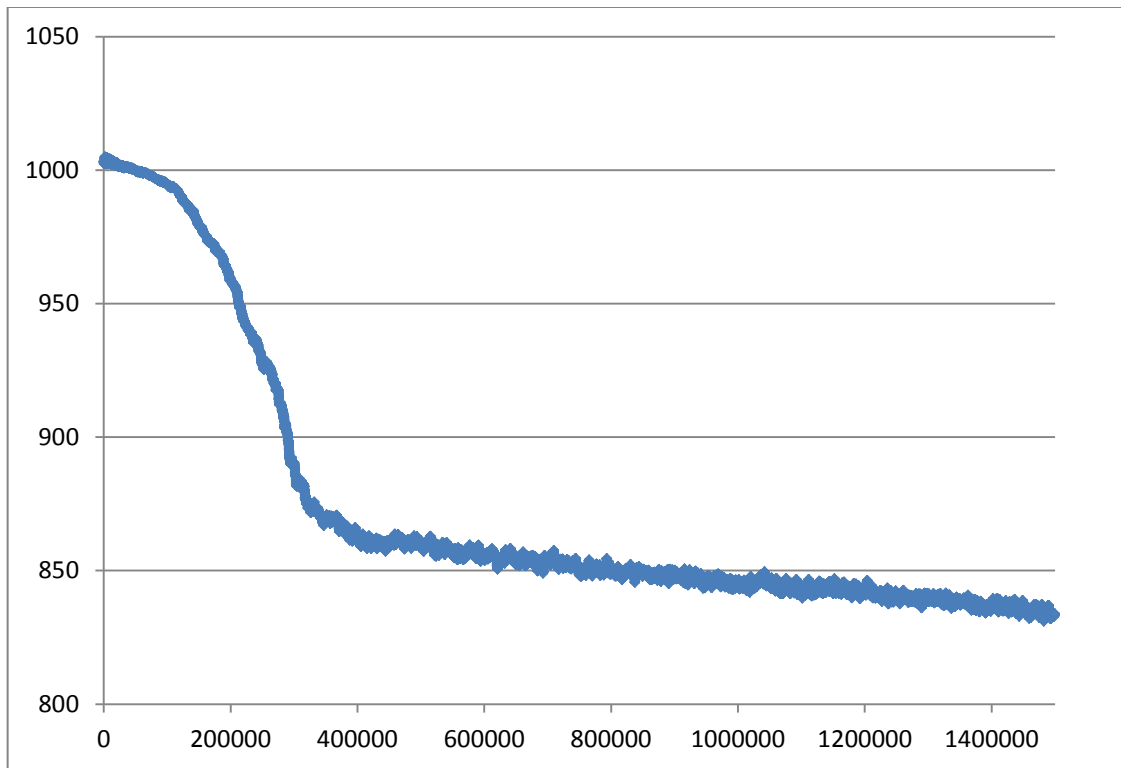


Figure 44: HDPE Chain Length 2000 pseudo atoms

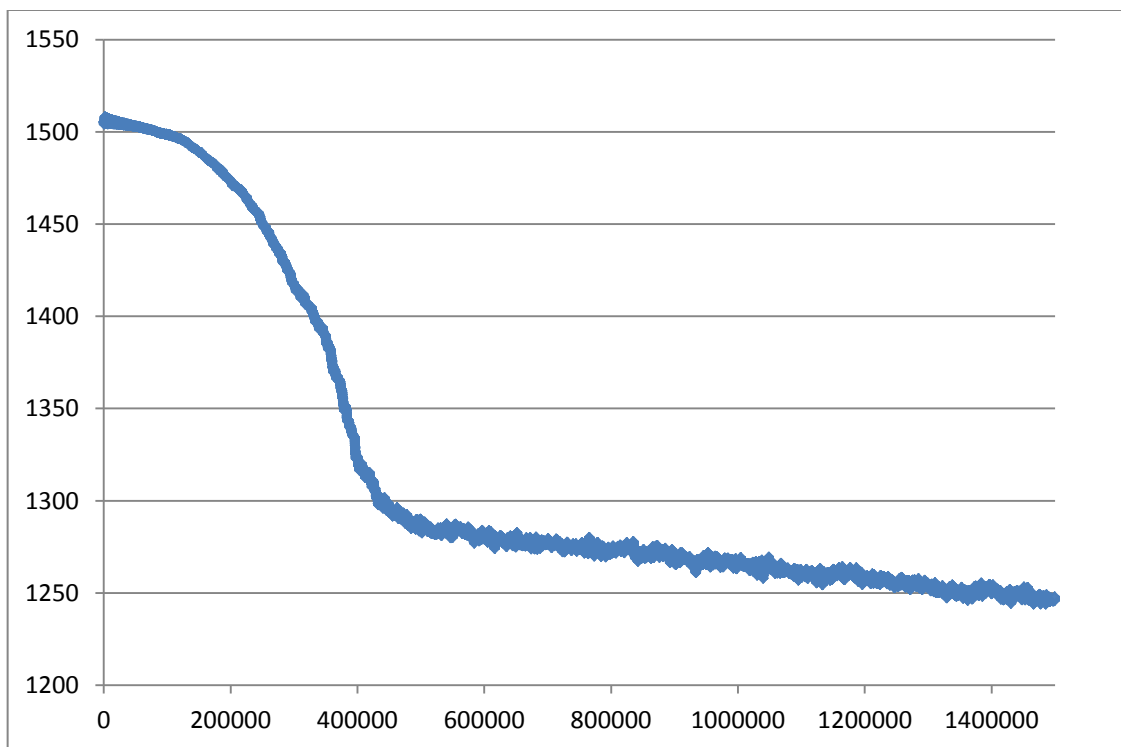


Figure 45: HDPE Chain Length 3000 pseudo atoms

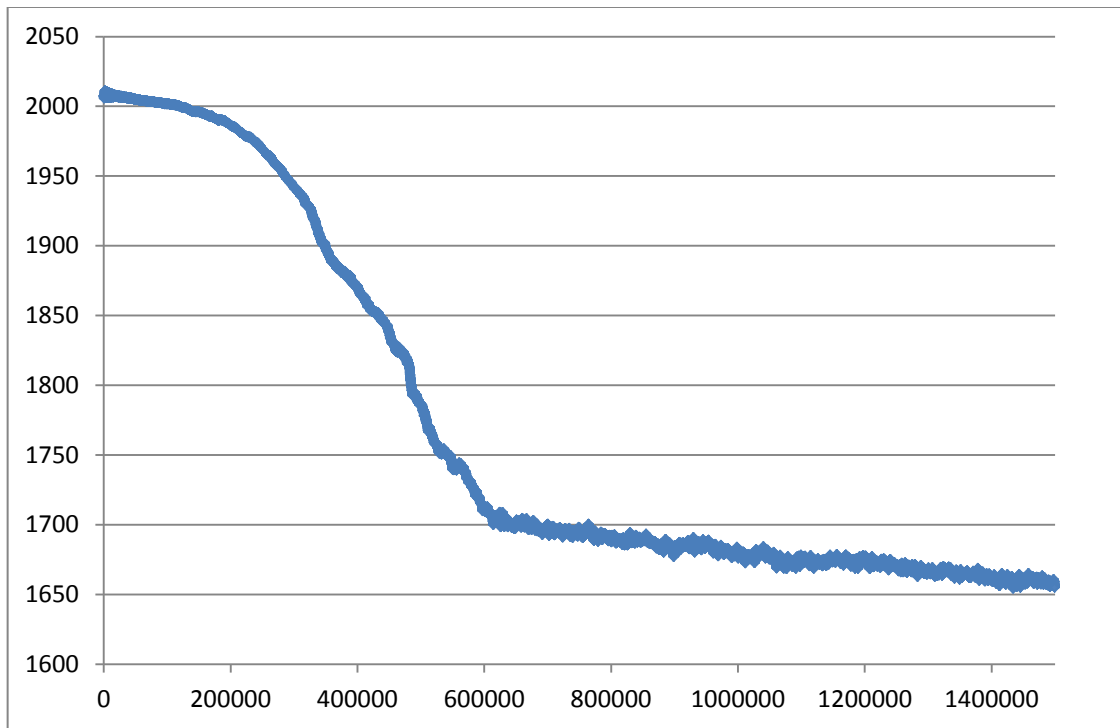


Figure 46: HDPE Chain Length 4000 pseudo atoms

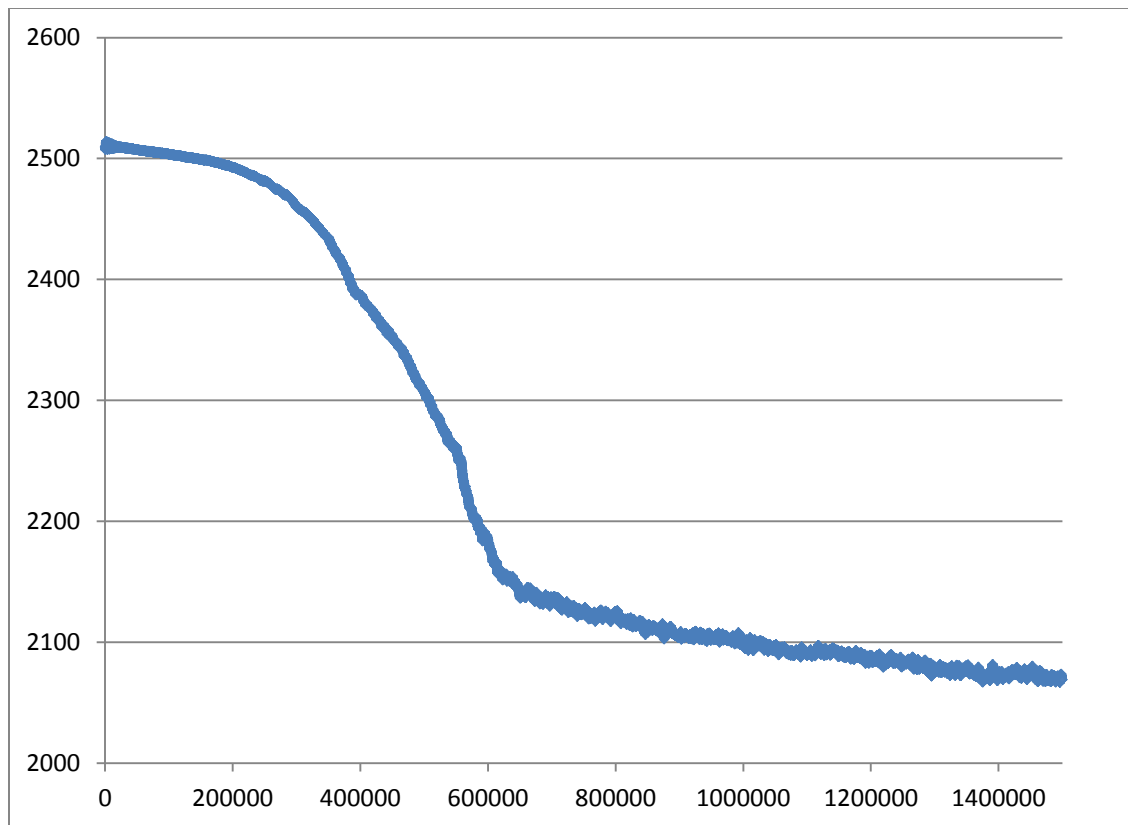


Figure 47: HDPE Chain Length 5000 pseudo atoms

Appendix B

Branching Effects of Polymer Structure

Low Density Polyethylene (LDPE)

Figure 48 through Figure 51 below, were images taken from one simulation of LDPE. Four chains of 2000 pseudo atoms in length were simulated at 0atm and 300K for 2000 picoseconds. The figures show the entanglement effects of the branching as the polymer chains form a globule over time.

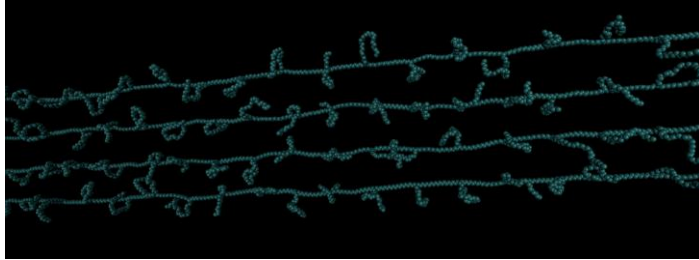


Figure 48: LDPE Initial Structure (Four Chains with Main Chain Length of 2000 pseudo atoms)

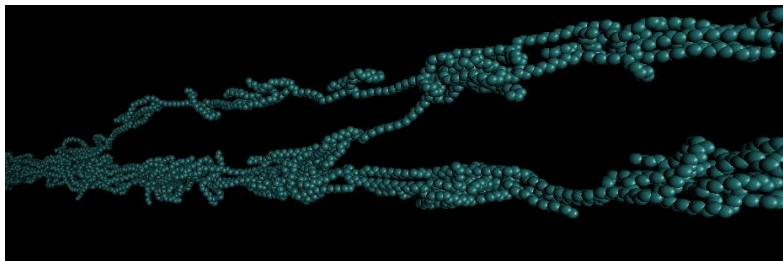


Figure 49: LDPE (60 picoseconds) (Four Chains with Main Chain Length of 2000 pseudo atoms)

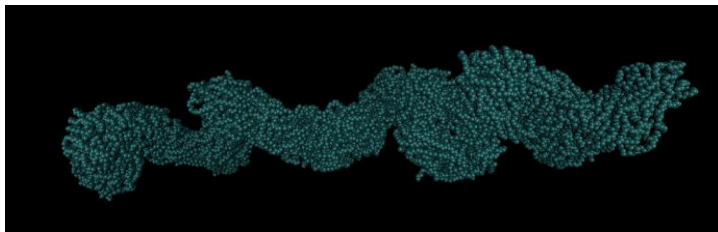


Figure 50: LDPE (310 picoseconds) (Four Chains with Main Chain Length of 2000 pseudo atoms)

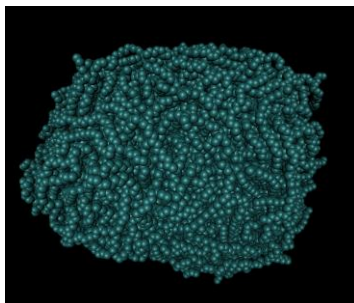


Figure 51: LDPE (2000 picoseconds) (Four Chains with Main Chain Length of 2000 pseudo atoms)

Polypropylene (PP)

The figure below was an image taken from one simulation of PP. Four chains of 2000 pseudo atoms in length were simulated at 0 atm and 300K for 3000 picoseconds. The figure shows the four straight adjacent chains beginning to interact. This demonstrates the attractive van der Waals forces.

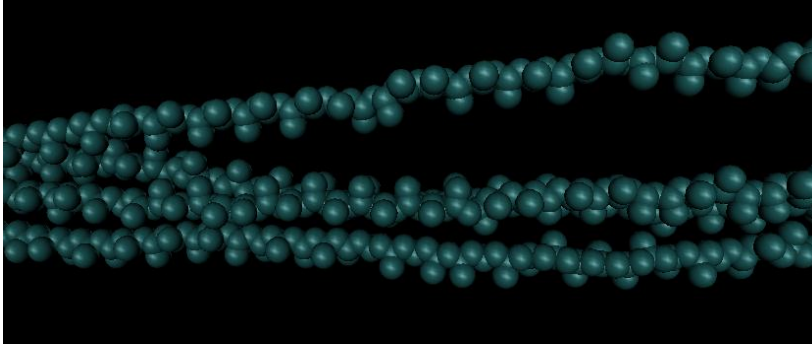


Figure 52: PP Initial Structure (Four Chains with Main Chain Length of 2000 pseudo atoms)

Appendix C

Final HDPE Temperature Variation Geometries (3000 picoseconds)

Figure 53 through Figure 60 below, show four polymer chains of 2000 pseudo atoms long at various temperatures at 3000 picoseconds. The NVT simulations were run with no periodic boundary conditions at 0 atm. The progression of temperatures ranges from 100K to 800K.

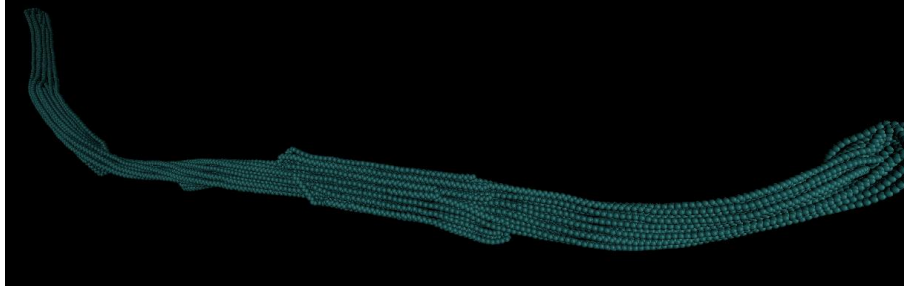


Figure 53: 100K

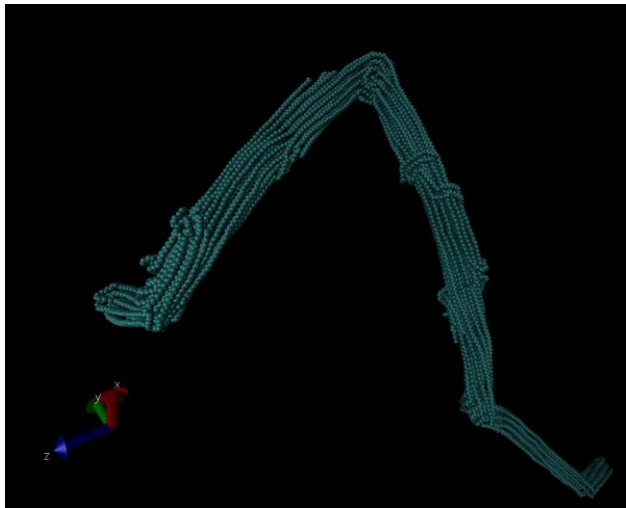


Figure 54: 200K

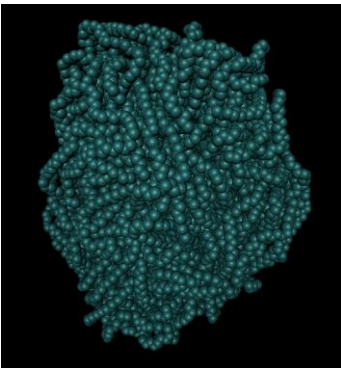


Figure 55: 300K

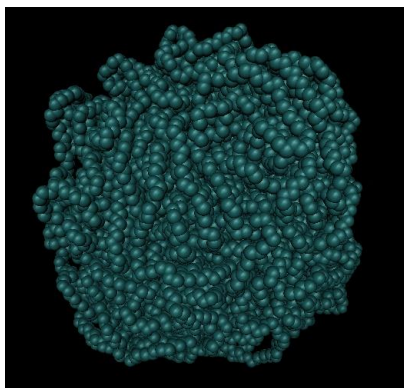


Figure 56: 350K

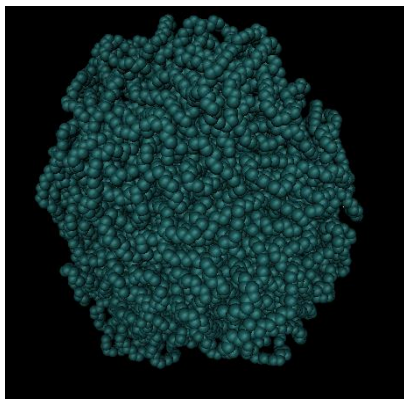


Figure 57: 400K

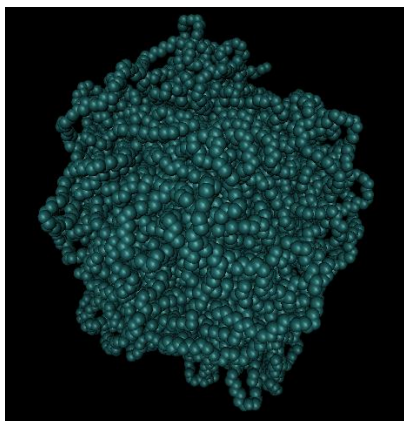


Figure 58: 500K

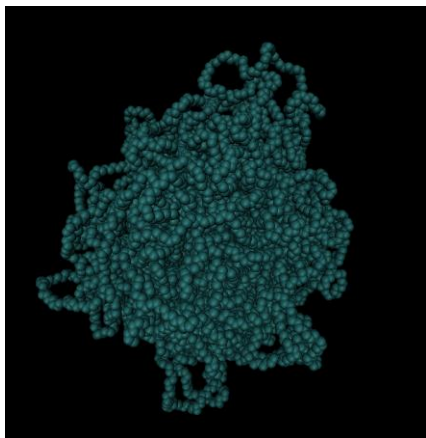


Figure 59: 600K

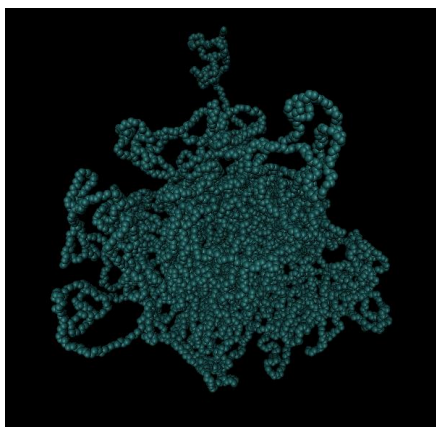


Figure 60: 800K

Appendix D

Density Calculations

Sample calculations are provided that detail how the box size values from the simulations were used to find the polymer density. Lengths of the X, Y, and Z sides of the simulation box were extracted from the REVCN file of completed NPT simulations.

Conversions

$$1 \text{ atomic mass unit} = 1.6605389217 * 10^{-30} \text{ grams}$$

$$1 \text{ picometer} = 10^{-10} \text{ centimeters}$$

$$\text{HDPE 1000} = 14028.95594 \text{ amu}$$

$$\text{Polymer Mass} = (14028.95594 \text{ amu} * 1.6605389217 * 10^{-30} \text{ g}) = 2.32956274 * 10^{-26} \text{ grams}$$

$$\text{HDPE 2000} = 28057.91188 \text{ amu}$$

$$\text{Polymer Mass} = (28057.91188 \text{ amu} * 1.6605389217 * 10^{-30} \text{ g}) = 5.3646 * 10^{-26} \text{ grams}$$

$$\text{Density} = \frac{\text{mass}}{\text{volume}}$$

Single Chain Simulations

150 Picosecond Simulation, 0atm, HDPE1000, 300K

$$\text{Polymer Volume} = (28 * 10^{-10} \text{ cm})^3 = 2.1952 * 10^{-26} \text{ cm}^3$$

$$\text{Density} = \frac{2.32956274 * 10^{-26} \text{ grams}}{2.1952 * 10^{-26} \text{ cm}^3} = 1.061 \frac{\text{g}}{\text{cm}^3}$$

1500 Picosecond Simulation, 0atm, HDPE1000, 300K

$$\text{Polymer Volume} = (29.8827 * 10^{-10} \text{ cm})^3 = 2.66845267 * 10^{-26} \text{ cm}^3$$

$$\text{Density} = \frac{2.32956274 * 10^{-26} \text{ grams}}{2.66845267 * 10^{-26} \text{ cm}^3} = 0.873 \frac{\text{g}}{\text{cm}^3}$$

1500 Picosecond Simulation, 1atm, HDPE1000, 300K

$$\text{Polymer Volume} = (29.946329 * 10^{-10} \text{ cm})^3 = 2.6855 * 10^{-26} \text{ cm}^3$$

$$\text{Density} = \frac{2.32956274 * 10^{-26} \text{ grams}}{2.6855 * 10^{-26} \text{ cm}^3} = 0.867 \frac{\text{g}}{\text{cm}^3}$$

1500 Picosecond Simulation, 0atm, HDPE2000, 300K

$$\begin{aligned} \text{Polymer Volume} &= (405278 * 10^{-10} \text{ cm})(37.5258 * 10^{-10} \text{ cm})(35.2742 * 10^{-10} \text{ cm}) \\ &= 5.3646 * 10^{-26} \text{ cm}^3 \end{aligned}$$

$$\text{Density} = \frac{4.659125 * 10^{-26} \text{ grams}}{5.3646 * 10^{-26} \text{ cm}^3} = 0.868 \frac{\text{g}}{\text{cm}^3}$$

Appendix D

Globule Formation at Various Temperatures

The figures of this appendix are images at various time intervals of HDPE simulations. Four chains of 2000 pseudo atoms long were simulated at temperatures ranging from 300K to 800K at 0atm for 3000 picoseconds.

350 Kelvin Simulation

Figure 61, Figure 62, and Figure 63 below show the structure of the four chains simulated at 350K during the formation of a globule.

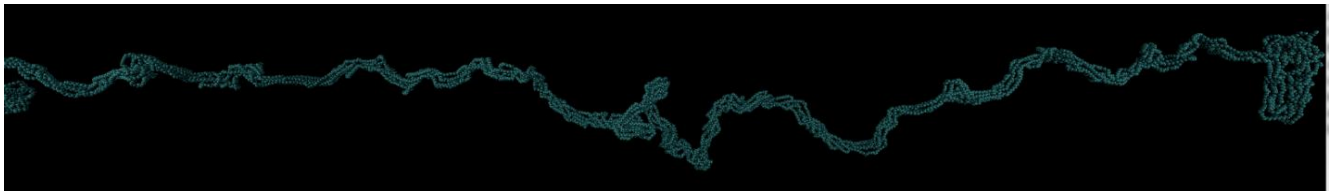


Figure 61: HDPE 350K (150 picoseconds)

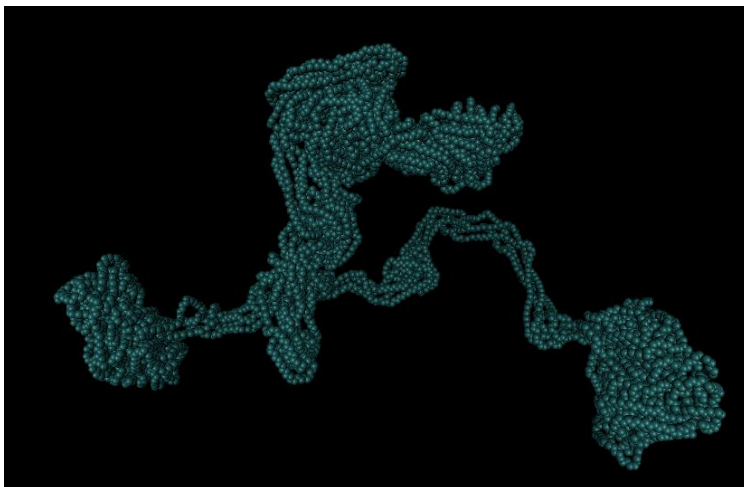


Figure 62: HDPE 350K (250 picoseconds)

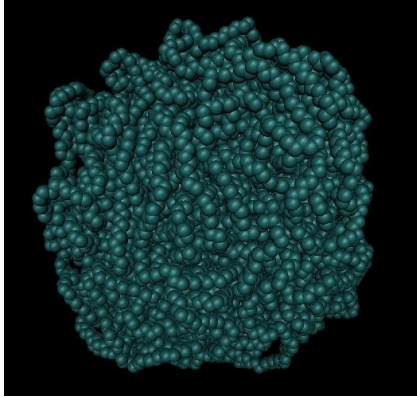


Figure 63: HDPE 350K (3000 picoseconds)

400 Kelvin Simulation

Figure 64, Figure 65, and Figure 66 below, show the structure of the four chains simulated at 400K.

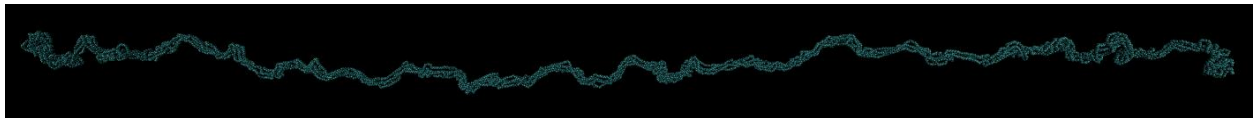


Figure 64: HDPE 400K (90 picoseconds)

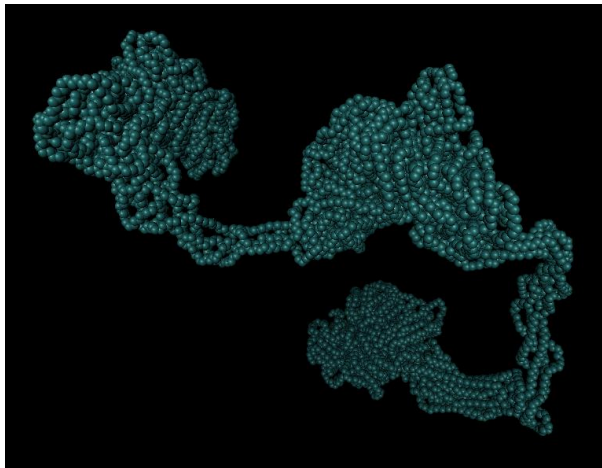


Figure 65: HDPE 400K (210 picoseconds)

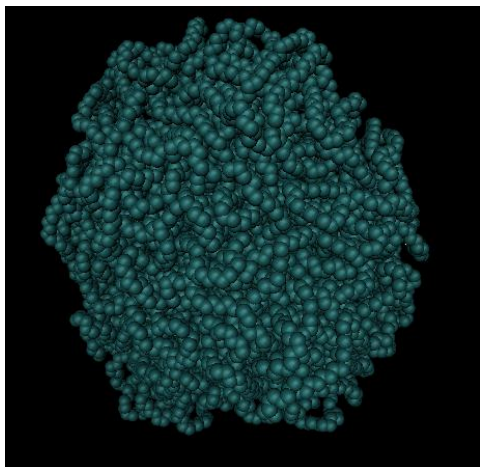


Figure 66: HDPE 400K (3000 picoseconds)

500 Kelvin Simulation

Figure 67, Figure 68, and Figure 69 below, show the structure of the four chains simulated at 500K.

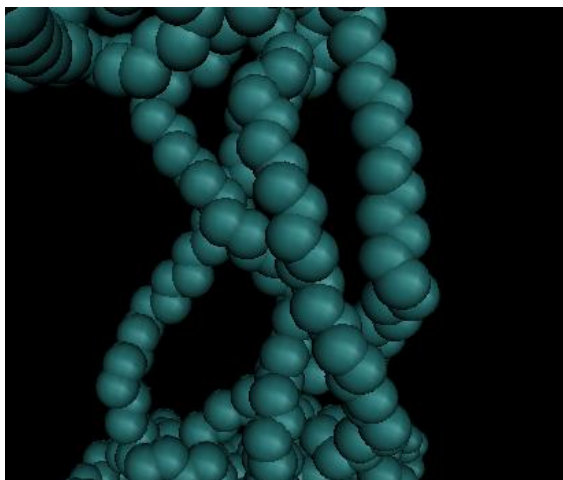


Figure 67: HDPE 500K (130 picoseconds)

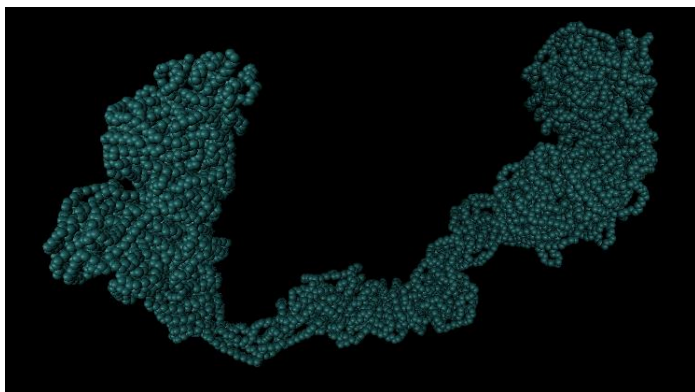


Figure 68: HDPE 500K (160 picoseconds)

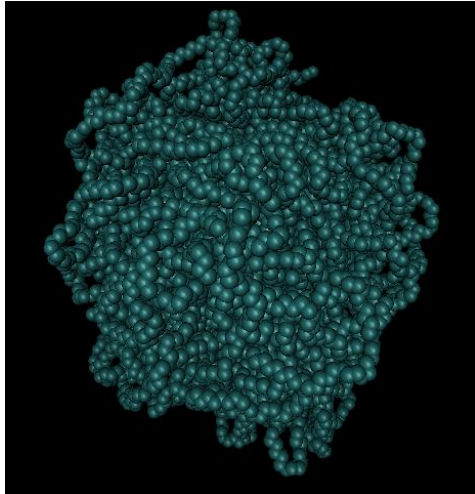


Figure 69: HDPE 500K (3000 picoseconds)

600 Kelvin Simulation

Figure 70 through Figure 74 below, show the structure of the four chains simulated at 600K. Figure 71 shows the initial point of globule formation. There is an abundance of kinetic energy in the system that prevents the globule from staying together at first pass. The momentum of the chains coming together only allows the globule to form for a brief moment before it starts to break apart. There is some oscillation between the globule state and the non-globule state as seen by the progression of Figure 70 to Figure 74.

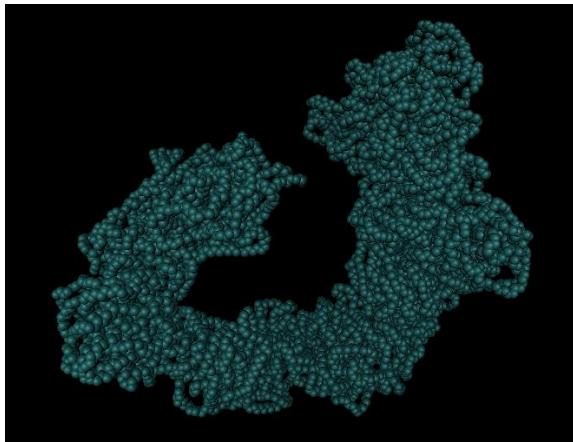


Figure 70: HDPE 600K (140 picoseconds)

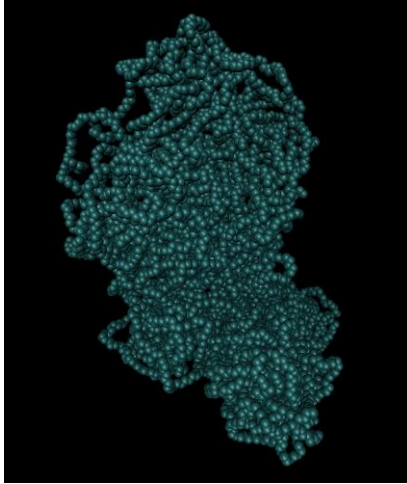


Figure 71: HDPE 600K (150 picoseconds)

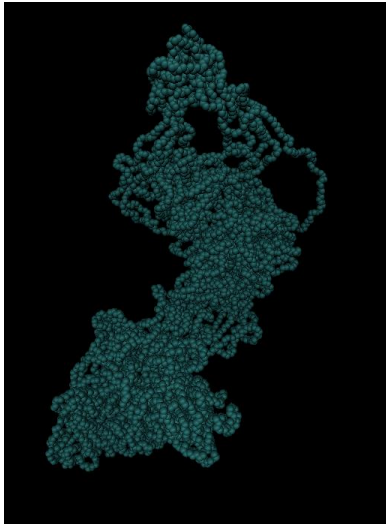


Figure 72: HDPE 600K (170 picoseconds)

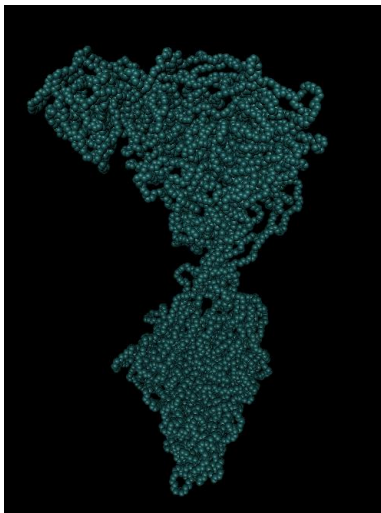


Figure 73: HDPE 600K (200 picoseconds)

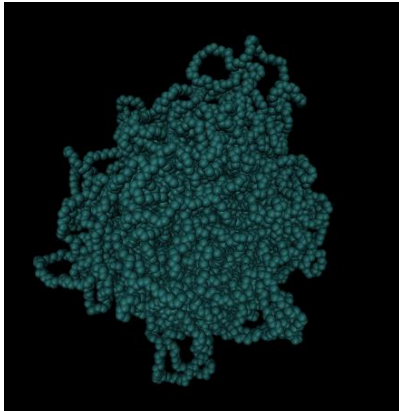


Figure 74: HDPE 600K (3000 picoseconds)

800 Kelvin Simulation

Figure 75 through Figure 78 below, show the structure of the four chains simulated at 800K. The oscillatory effect is seen as the momentum of the chains initially coming together overpowered the VDW attractive forces that hold together the globule. Figure 77 and Figure 78 depict melting as singular chains have broken away from the four adjacent chains from which they started, as well as from the globule as a whole.

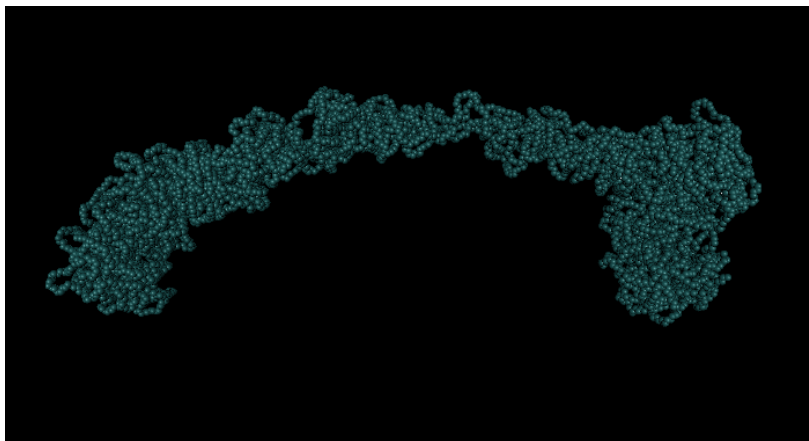


Figure 75: HDPE 800K (100 picoseconds)

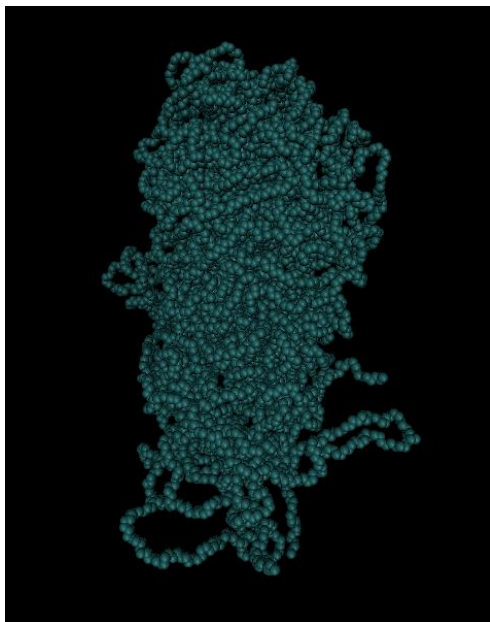


Figure 76: HDPE 800K (120 picoseconds)

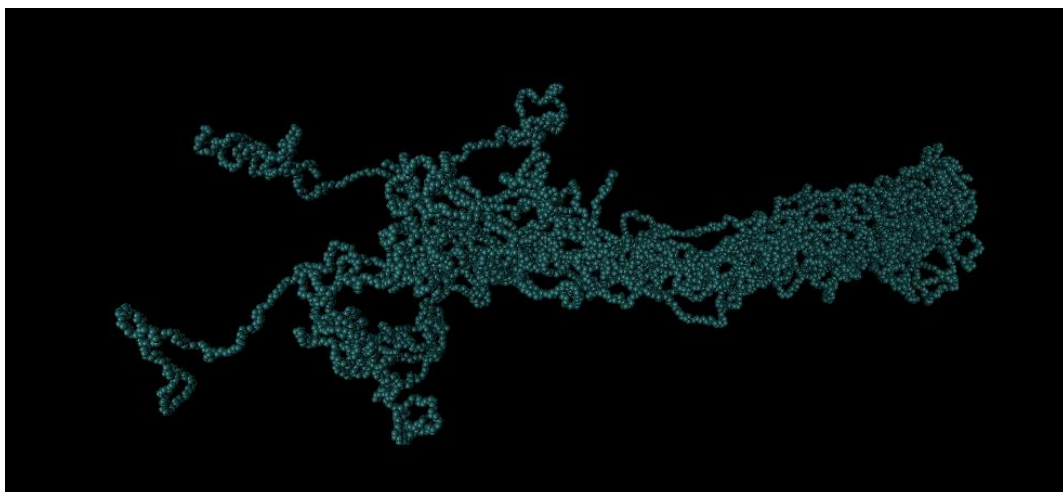


Figure 77: HDPE 800K (210 picoseconds)

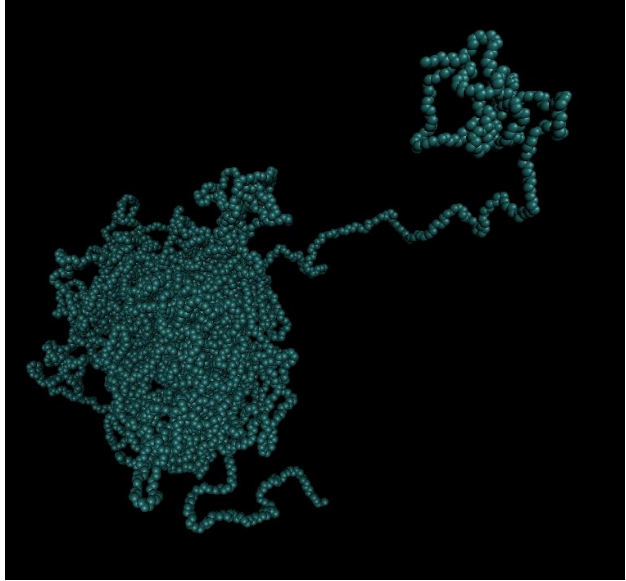


Figure 78: HDPE 800K (670 picoseconds)

Appendix E

DL_POLY2 Input Files

CONTROL, FIELD, and CONFIG input files are provided for the DL_POLY2 program below. HDPE files of one and four chain systems of 20 pseudo atoms long, PP files of a one chain system 50 pseudo atoms long, and LDPE files of a one chain system 200 pseudo atoms long were chosen.

CONTROL File

```
#zero
temperature          300 kelvin
pressure             0 katm
equilibration steps  100 steps
timestep             0.001 ps
#multiple timestep   1 steps
scale every          1 steps
shake tolerance      1.0E-5

cutoff               10.00 angstroms
#all pairs
no link
coul
rvdw                 10.00

delr                  .50 angstroms

print every          100 steps
#mxlist              2.5
rdf sampling every   100 steps
print rdf

job time             500000000 seconds
close time           1000 seconds
#ewald precision     1d-6
cap forces in equilibration mode 1000 kT/A

ensemble    nvt hoover 0.5 0.5
stats       10000
stats every 10000 steps
trajectory  nstraj=0 istraj=10000 keytrj=0
stack       100 deep
steps       3000000 steps
#restart
finish
```

FIELD Files

High Density Polyethylene (HDPE)

One Chain – 20 Pseudo Atoms Long

```
Units kcal
Molecular types 1
Molecule name test
nummols 1
atoms 20
C3      15.03470      0.00000      1      0
C2      14.02680      0.00000      1      0
C2      14.02680      0.00000      1      0
C2      14.02680      0.00000      1      0
C2      14.02680      0.00000      1      0
C2      14.02680      0.00000      1      0
C2      14.02680      0.00000      1      0
C2      14.02680      0.00000      1      0
C2      14.02680      0.00000      1      0
C2      14.02680      0.00000      1      0
C2      14.02680      0.00000      1      0
C2      14.02680      0.00000      1      0
C2      14.02680      0.00000      1      0
C2      14.02680      0.00000      1      0
C2      14.02680      0.00000      1      0
C2      14.02680      0.00000      1      0
C2      14.02680      0.00000      1      0
C2      14.02680      0.00000      1      0
C2      14.02680      0.00000      1      0
C2      14.02680      0.00000      1      0
C2      14.02680      0.00000      1      0
C3      15.03470      0.00000      1      0
CONSTRAINTS      19
  1  2  1.54000000
  2  3  1.54000000
  3  4  1.54000000
  4  5  1.54000000
  5  6  1.54000000
  6  7  1.54000000
  7  8  1.54000000
  8  9  1.54000000
  9 10  1.54000000
 10 11  1.54000000
 11 12  1.54000000
 12 13  1.54000000
 13 14  1.54000000
 14 15  1.54000000
 15 16  1.54000000
 16 17  1.54000000
 17 18  1.54000000
 18 19  1.54000000
 19 20  1.54000000
angles 18
harm   1   2   3  124.19700  112.40000
harm   2   3   4  124.19700  112.40000
harm   3   4   5  124.19700  112.40000
harm   4   5   6  124.19700  112.40000
harm   5   6   7  124.19700  112.40000
harm   6   7   8  124.19700  112.40000
harm   7   8   9  124.19700  112.40000
harm   8   9  10  124.19700  112.40000
```


C2 14.02680 0.00000 1 0
C2 14.02680 0.00000 1 0
C3 15.03470 0.00000 1 0

CONSTRAINTS 19
1 2 1.54000000
2 3 1.54000000
3 4 1.54000000
4 5 1.54000000
5 6 1.54000000
6 7 1.54000000
7 8 1.54000000
8 9 1.54000000
9 10 1.54000000
10 11 1.54000000
11 12 1.54000000
12 13 1.54000000
13 14 1.54000000
14 15 1.54000000
15 16 1.54000000
16 17 1.54000000
17 18 1.54000000
18 19 1.54000000
19 20 1.54000000

angles 18
harm 1 2 3 124.19700 112.40000
harm 2 3 4 124.19700 112.40000
harm 3 4 5 124.19700 112.40000
harm 4 5 6 124.19700 112.40000
harm 5 6 7 124.19700 112.40000
harm 6 7 8 124.19700 112.40000
harm 7 8 9 124.19700 112.40000
harm 8 9 10 124.19700 112.40000
harm 9 10 11 124.19700 112.40000
harm 10 11 12 124.19700 112.40000
harm 11 12 13 124.19700 112.40000
harm 12 13 14 124.19700 112.40000
harm 13 14 15 124.19700 112.40000
harm 14 15 16 124.19700 112.40000
harm 15 16 17 124.19700 112.40000
harm 16 17 18 124.19700 112.40000
harm 17 18 19 124.19700 112.40000
harm 18 19 20 124.19700 112.40000

dihedral 17
OPLS 1 2 3 4 0.0000000 1.41100000 -0.27100000 3.14500000 0.00000000
OPLS 2 3 4 5 0.0000000 1.41100000 -0.27100000 3.14500000 0.00000000
OPLS 3 4 5 6 0.0000000 1.41100000 -0.27100000 3.14500000 0.00000000
OPLS 4 5 6 7 0.0000000 1.41100000 -0.27100000 3.14500000 0.00000000
OPLS 5 6 7 8 0.0000000 1.41100000 -0.27100000 3.14500000 0.00000000
OPLS 6 7 8 9 0.0000000 1.41100000 -0.27100000 3.14500000 0.00000000
OPLS 7 8 9 10 0.0000000 1.41100000 -0.27100000 3.14500000 0.00000000
OPLS 8 9 10 11 0.0000000 1.41100000 -0.27100000 3.14500000 0.00000000
OPLS 9 10 11 12 0.0000000 1.41100000 -0.27100000 3.14500000 0.00000000
OPLS 10 11 12 13 0.0000000 1.41100000 -0.27100000 3.14500000 0.00000000
OPLS 11 12 13 14 0.0000000 1.41100000 -0.27100000 3.14500000 0.00000000
OPLS 12 13 14 15 0.0000000 1.41100000 -0.27100000 3.14500000 0.00000000
OPLS 13 14 15 16 0.0000000 1.41100000 -0.27100000 3.14500000 0.00000000
OPLS 14 15 16 17 0.0000000 1.41100000 -0.27100000 3.14500000 0.00000000
OPLS 15 16 17 18 0.0000000 1.41100000 -0.27100000 3.14500000 0.00000000
OPLS 16 17 18 19 0.0000000 1.41100000 -0.27100000 3.14500000 0.00000000
OPLS 17 18 19 20 0.0000000 1.41100000 -0.27100000 3.14500000 0.00000000

finish
vdw 3
C3 C3 lj 0.1947 3.7500

C2	14.02680	0.00000	1	0	1HEX
C2	14.02680	0.00000	1	0	1HEX
C2	14.02680	0.00000	1	0	1HEX
C2	14.02680	0.00000	1	0	1HEX
C2	14.02680	0.00000	1	0	1HEX
C2	14.02680	0.00000	1	0	1HEX
C2	14.02680	0.00000	1	0	1HEX
C2	14.02680	0.00000	1	0	1HEX
C2	14.02680	0.00000	1	0	1HEX
C2	14.02680	0.00000	1	0	1HEX
C2	14.02680	0.00000	1	0	1HEX
C2	14.02680	0.00000	1	0	1HEX
C2	14.02680	0.00000	1	0	1HEX
C2	14.02680	0.00000	1	0	1HEX
C2	14.02680	0.00000	1	0	1HEX
C2	14.02680	0.00000	1	0	1HEX
C3	15.03470	0.00000	1	0	1HEX

CONSTRAINTS 500

1	2	1.54000000
2	3	1.54000000
3	4	1.54000000
4	5	1.54000000
5	6	1.54000000
6	7	1.54000000
7	8	1.54000000
8	9	1.54000000
9	10	1.54000000
10	11	1.54000000
11	12	1.54000000
12	13	1.54000000
13	14	1.54000000
14	15	1.54000000
15	16	1.54000000
16	17	1.54000000
17	18	1.54000000
18	19	1.54000000
19	20	1.54000000
20	21	1.54000000
21	22	1.54000000
22	23	1.54000000
23	24	1.54000000
24	25	1.54000000
25	26	1.54000000
26	27	1.54000000
27	28	1.54000000
28	29	1.54000000
29	30	1.54000000
30	31	1.54000000
31	32	1.54000000
32	33	1.54000000
33	34	1.54000000
34	35	1.54000000
35	36	1.54000000
36	37	1.54000000
37	38	1.54000000
38	39	1.54000000
39	40	1.54000000
40	41	1.54000000
41	42	1.54000000
42	43	1.54000000
43	44	1.54000000
44	45	1.54000000
45	46	1.54000000
46	47	1.54000000

47	48	1.54000000
48	49	1.54000000
49	50	1.54000000
50	51	1.54000000
51	52	1.54000000
52	53	1.54000000
53	54	1.54000000
54	55	1.54000000
55	56	1.54000000
56	57	1.54000000
57	58	1.54000000
58	59	1.54000000
59	60	1.54000000
60	61	1.54000000
61	62	1.54000000
62	63	1.54000000
63	64	1.54000000
64	65	1.54000000
65	66	1.54000000
66	67	1.54000000
67	68	1.54000000
68	69	1.54000000
69	70	1.54000000
70	71	1.54000000
71	72	1.54000000
72	73	1.54000000
73	74	1.54000000
74	75	1.54000000
75	76	1.54000000
76	77	1.54000000
77	78	1.54000000
78	79	1.54000000
79	80	1.54000000
80	81	1.54000000
81	82	1.54000000
82	83	1.54000000
83	84	1.54000000
84	85	1.54000000
85	86	1.54000000
86	87	1.54000000
87	88	1.54000000
88	89	1.54000000
89	90	1.54000000
90	91	1.54000000
91	92	1.54000000
92	93	1.54000000
93	94	1.54000000
94	95	1.54000000
95	96	1.54000000
96	97	1.54000000
97	98	1.54000000
98	99	1.54000000
99	100	1.54000000
100	101	1.54000000
101	102	1.54000000
102	103	1.54000000
103	104	1.54000000
104	105	1.54000000
105	106	1.54000000
106	107	1.54000000
107	108	1.54000000
108	109	1.54000000
109	110	1.54000000

110	111	1.54000000
111	112	1.54000000
112	113	1.54000000
113	114	1.54000000
114	115	1.54000000
115	116	1.54000000
116	117	1.54000000
117	118	1.54000000
118	119	1.54000000
119	120	1.54000000
120	121	1.54000000
121	122	1.54000000
122	123	1.54000000
123	124	1.54000000
124	125	1.54000000
125	126	1.54000000
126	127	1.54000000
127	128	1.54000000
128	129	1.54000000
129	130	1.54000000
130	131	1.54000000
131	132	1.54000000
132	133	1.54000000
133	134	1.54000000
134	135	1.54000000
135	136	1.54000000
136	137	1.54000000
137	138	1.54000000
138	139	1.54000000
139	140	1.54000000
140	141	1.54000000
141	142	1.54000000
142	143	1.54000000
143	144	1.54000000
144	145	1.54000000
145	146	1.54000000
146	147	1.54000000
147	148	1.54000000
148	149	1.54000000
149	150	1.54000000
150	151	1.54000000
151	152	1.54000000
152	153	1.54000000
153	154	1.54000000
154	155	1.54000000
155	156	1.54000000
156	157	1.54000000
157	158	1.54000000
158	159	1.54000000
159	160	1.54000000
160	161	1.54000000
161	162	1.54000000
162	163	1.54000000
163	164	1.54000000
164	165	1.54000000
165	166	1.54000000
166	167	1.54000000
167	168	1.54000000
168	169	1.54000000
169	170	1.54000000
170	171	1.54000000
171	172	1.54000000
172	173	1.54000000

173	174	1.54000000
174	175	1.54000000
175	176	1.54000000
176	177	1.54000000
177	178	1.54000000
178	179	1.54000000
179	180	1.54000000
180	181	1.54000000
181	182	1.54000000
182	183	1.54000000
183	184	1.54000000
184	185	1.54000000
185	186	1.54000000
186	187	1.54000000
187	188	1.54000000
188	189	1.54000000
189	190	1.54000000
190	191	1.54000000
191	192	1.54000000
192	193	1.54000000
193	194	1.54000000
194	195	1.54000000
195	196	1.54000000
196	197	1.54000000
197	198	1.54000000
198	199	1.54000000
199	200	1.54000000
200	201	1.54000000
2	202	1.54000000
202	203	1.54000000
203	204	1.54000000
204	205	1.54000000
205	206	1.54000000
206	207	1.54000000
207	208	1.54000000
208	209	1.54000000
209	210	1.54000000
210	211	1.54000000
211	212	1.54000000
212	213	1.54000000
213	214	1.54000000
214	215	1.54000000
215	216	1.54000000
216	217	1.54000000
217	218	1.54000000
218	219	1.54000000
219	220	1.54000000
220	221	1.54000000
221	222	1.54000000
222	223	1.54000000
223	224	1.54000000
224	225	1.54000000
225	226	1.54000000
226	227	1.54000000
227	228	1.54000000
228	229	1.54000000
229	230	1.54000000
230	231	1.54000000
22	232	1.54000000
232	233	1.54000000
233	234	1.54000000
234	235	1.54000000
235	236	1.54000000

236	237	1.54000000
237	238	1.54000000
238	239	1.54000000
239	240	1.54000000
240	241	1.54000000
241	242	1.54000000
242	243	1.54000000
243	244	1.54000000
244	245	1.54000000
245	246	1.54000000
246	247	1.54000000
247	248	1.54000000
248	249	1.54000000
249	250	1.54000000
250	251	1.54000000
251	252	1.54000000
252	253	1.54000000
253	254	1.54000000
254	255	1.54000000
255	256	1.54000000
256	257	1.54000000
257	258	1.54000000
258	259	1.54000000
259	260	1.54000000
260	261	1.54000000
42	262	1.54000000
262	263	1.54000000
263	264	1.54000000
264	265	1.54000000
265	266	1.54000000
266	267	1.54000000
267	268	1.54000000
268	269	1.54000000
269	270	1.54000000
270	271	1.54000000
271	272	1.54000000
272	273	1.54000000
273	274	1.54000000
274	275	1.54000000
275	276	1.54000000
276	277	1.54000000
277	278	1.54000000
278	279	1.54000000
279	280	1.54000000
280	281	1.54000000
281	282	1.54000000
282	283	1.54000000
283	284	1.54000000
284	285	1.54000000
285	286	1.54000000
286	287	1.54000000
287	288	1.54000000
288	289	1.54000000
289	290	1.54000000
290	291	1.54000000
62	292	1.54000000
292	293	1.54000000
293	294	1.54000000
294	295	1.54000000
295	296	1.54000000
296	297	1.54000000
297	298	1.54000000
298	299	1.54000000

299	300	1.54000000
300	301	1.54000000
301	302	1.54000000
302	303	1.54000000
303	304	1.54000000
304	305	1.54000000
305	306	1.54000000
306	307	1.54000000
307	308	1.54000000
308	309	1.54000000
309	310	1.54000000
310	311	1.54000000
311	312	1.54000000
312	313	1.54000000
313	314	1.54000000
314	315	1.54000000
315	316	1.54000000
316	317	1.54000000
317	318	1.54000000
318	319	1.54000000
319	320	1.54000000
320	321	1.54000000
82	322	1.54000000
322	323	1.54000000
323	324	1.54000000
324	325	1.54000000
325	326	1.54000000
326	327	1.54000000
327	328	1.54000000
328	329	1.54000000
329	330	1.54000000
330	331	1.54000000
331	332	1.54000000
332	333	1.54000000
333	334	1.54000000
334	335	1.54000000
335	336	1.54000000
336	337	1.54000000
337	338	1.54000000
338	339	1.54000000
339	340	1.54000000
340	341	1.54000000
341	342	1.54000000
342	343	1.54000000
343	344	1.54000000
344	345	1.54000000
345	346	1.54000000
346	347	1.54000000
347	348	1.54000000
348	349	1.54000000
349	350	1.54000000
350	351	1.54000000
102	352	1.54000000
352	353	1.54000000
353	354	1.54000000
354	355	1.54000000
355	356	1.54000000
356	357	1.54000000
357	358	1.54000000
358	359	1.54000000
359	360	1.54000000
360	361	1.54000000
361	362	1.54000000

362	363	1.54000000
363	364	1.54000000
364	365	1.54000000
365	366	1.54000000
366	367	1.54000000
367	368	1.54000000
368	369	1.54000000
369	370	1.54000000
370	371	1.54000000
371	372	1.54000000
372	373	1.54000000
373	374	1.54000000
374	375	1.54000000
375	376	1.54000000
376	377	1.54000000
377	378	1.54000000
378	379	1.54000000
379	380	1.54000000
380	381	1.54000000
122	382	1.54000000
382	383	1.54000000
383	384	1.54000000
384	385	1.54000000
385	386	1.54000000
386	387	1.54000000
387	388	1.54000000
388	389	1.54000000
389	390	1.54000000
390	391	1.54000000
391	392	1.54000000
392	393	1.54000000
393	394	1.54000000
394	395	1.54000000
395	396	1.54000000
396	397	1.54000000
397	398	1.54000000
398	399	1.54000000
399	400	1.54000000
400	401	1.54000000
401	402	1.54000000
402	403	1.54000000
403	404	1.54000000
404	405	1.54000000
405	406	1.54000000
406	407	1.54000000
407	408	1.54000000
408	409	1.54000000
409	410	1.54000000
410	411	1.54000000
142	412	1.54000000
412	413	1.54000000
413	414	1.54000000
414	415	1.54000000
415	416	1.54000000
416	417	1.54000000
417	418	1.54000000
418	419	1.54000000
419	420	1.54000000
420	421	1.54000000
421	422	1.54000000
422	423	1.54000000
423	424	1.54000000
424	425	1.54000000

425	426	1.54000000
426	427	1.54000000
427	428	1.54000000
428	429	1.54000000
429	430	1.54000000
430	431	1.54000000
431	432	1.54000000
432	433	1.54000000
433	434	1.54000000
434	435	1.54000000
435	436	1.54000000
436	437	1.54000000
437	438	1.54000000
438	439	1.54000000
439	440	1.54000000
440	441	1.54000000
162	442	1.54000000
442	443	1.54000000
443	444	1.54000000
444	445	1.54000000
445	446	1.54000000
446	447	1.54000000
447	448	1.54000000
448	449	1.54000000
449	450	1.54000000
450	451	1.54000000
451	452	1.54000000
452	453	1.54000000
453	454	1.54000000
454	455	1.54000000
455	456	1.54000000
456	457	1.54000000
457	458	1.54000000
458	459	1.54000000
459	460	1.54000000
460	461	1.54000000
461	462	1.54000000
462	463	1.54000000
463	464	1.54000000
464	465	1.54000000
465	466	1.54000000
466	467	1.54000000
467	468	1.54000000
468	469	1.54000000
469	470	1.54000000
470	471	1.54000000
182	472	1.54000000
472	473	1.54000000
473	474	1.54000000
474	475	1.54000000
475	476	1.54000000
476	477	1.54000000
477	478	1.54000000
478	479	1.54000000
479	480	1.54000000
480	481	1.54000000
481	482	1.54000000
482	483	1.54000000
483	484	1.54000000
484	485	1.54000000
485	486	1.54000000
486	487	1.54000000
487	488	1.54000000

488	489	1.54000000
489	490	1.54000000
490	491	1.54000000
491	492	1.54000000
492	493	1.54000000
493	494	1.54000000
494	495	1.54000000
495	496	1.54000000
496	497	1.54000000
497	498	1.54000000
498	499	1.54000000
499	500	1.54000000
500	501	1.54000000

angles 509

harm	1	2	3	124.19700	112.00000
harm	2	3	4	124.19700	114.00000
harm	3	4	5	124.19700	114.00000
harm	4	5	6	124.19700	114.00000
harm	5	6	7	124.19700	114.00000
harm	6	7	8	124.19700	114.00000
harm	7	8	9	124.19700	114.00000
harm	8	9	10	124.19700	114.00000
harm	9	10	11	124.19700	114.00000
harm	10	11	12	124.19700	114.00000
harm	11	12	13	124.19700	114.00000
harm	12	13	14	124.19700	114.00000
harm	13	14	15	124.19700	114.00000
harm	14	15	16	124.19700	114.00000
harm	15	16	17	124.19700	114.00000
harm	16	17	18	124.19700	114.00000
harm	17	18	19	124.19700	114.00000
harm	18	19	20	124.19700	114.00000
harm	19	20	21	124.19700	114.00000
harm	20	21	22	124.19700	114.00000
harm	21	22	23	124.19700	112.00000
harm	22	23	24	124.19700	114.00000
harm	23	24	25	124.19700	114.00000
harm	24	25	26	124.19700	114.00000
harm	25	26	27	124.19700	114.00000
harm	26	27	28	124.19700	114.00000
harm	27	28	29	124.19700	114.00000
harm	28	29	30	124.19700	114.00000
harm	29	30	31	124.19700	114.00000
harm	30	31	32	124.19700	114.00000
harm	31	32	33	124.19700	114.00000
harm	32	33	34	124.19700	114.00000
harm	33	34	35	124.19700	114.00000
harm	34	35	36	124.19700	114.00000
harm	35	36	37	124.19700	114.00000
harm	36	37	38	124.19700	114.00000
harm	37	38	39	124.19700	114.00000
harm	38	39	40	124.19700	114.00000
harm	39	40	41	124.19700	114.00000
harm	40	41	42	124.19700	114.00000
harm	41	42	43	124.19700	112.00000
harm	42	43	44	124.19700	114.00000
harm	43	44	45	124.19700	114.00000
harm	44	45	46	124.19700	114.00000
harm	45	46	47	124.19700	114.00000
harm	46	47	48	124.19700	114.00000
harm	47	48	49	124.19700	114.00000
harm	48	49	50	124.19700	114.00000
harm	49	50	51	124.19700	114.00000

harm	50	51	52	124.19700	114.00000
harm	51	52	53	124.19700	114.00000
harm	52	53	54	124.19700	114.00000
harm	53	54	55	124.19700	114.00000
harm	54	55	56	124.19700	114.00000
harm	55	56	57	124.19700	114.00000
harm	56	57	58	124.19700	114.00000
harm	57	58	59	124.19700	114.00000
harm	58	59	60	124.19700	114.00000
harm	59	60	61	124.19700	114.00000
harm	60	61	62	124.19700	114.00000
harm	61	62	63	124.19700	112.00000
harm	62	63	64	124.19700	114.00000
harm	63	64	65	124.19700	114.00000
harm	64	65	66	124.19700	114.00000
harm	65	66	67	124.19700	114.00000
harm	66	67	68	124.19700	114.00000
harm	67	68	69	124.19700	114.00000
harm	68	69	70	124.19700	114.00000
harm	69	70	71	124.19700	114.00000
harm	70	71	72	124.19700	114.00000
harm	71	72	73	124.19700	114.00000
harm	72	73	74	124.19700	114.00000
harm	73	74	75	124.19700	114.00000
harm	74	75	76	124.19700	114.00000
harm	75	76	77	124.19700	114.00000
harm	76	77	78	124.19700	114.00000
harm	77	78	79	124.19700	114.00000
harm	78	79	80	124.19700	114.00000
harm	79	80	81	124.19700	114.00000
harm	80	81	82	124.19700	114.00000
harm	81	82	83	124.19700	112.00000
harm	82	83	84	124.19700	114.00000
harm	83	84	85	124.19700	114.00000
harm	84	85	86	124.19700	114.00000
harm	85	86	87	124.19700	114.00000
harm	86	87	88	124.19700	114.00000
harm	87	88	89	124.19700	114.00000
harm	88	89	90	124.19700	114.00000
harm	89	90	91	124.19700	114.00000
harm	90	91	92	124.19700	114.00000
harm	91	92	93	124.19700	114.00000
harm	92	93	94	124.19700	114.00000
harm	93	94	95	124.19700	114.00000
harm	94	95	96	124.19700	114.00000
harm	95	96	97	124.19700	114.00000
harm	96	97	98	124.19700	114.00000
harm	97	98	99	124.19700	114.00000
harm	98	99	100	124.19700	114.00000
harm	99	100	101	124.19700	114.00000
harm	100	101	102	124.19700	114.00000
harm	101	102	103	124.19700	112.00000
harm	102	103	104	124.19700	114.00000
harm	103	104	105	124.19700	114.00000
harm	104	105	106	124.19700	114.00000
harm	105	106	107	124.19700	114.00000
harm	106	107	108	124.19700	114.00000
harm	107	108	109	124.19700	114.00000
harm	108	109	110	124.19700	114.00000
harm	109	110	111	124.19700	114.00000
harm	110	111	112	124.19700	114.00000
harm	111	112	113	124.19700	114.00000
harm	112	113	114	124.19700	114.00000

harm	113	114	115	124.19700	114.00000
harm	114	115	116	124.19700	114.00000
harm	115	116	117	124.19700	114.00000
harm	116	117	118	124.19700	114.00000
harm	117	118	119	124.19700	114.00000
harm	118	119	120	124.19700	114.00000
harm	119	120	121	124.19700	114.00000
harm	120	121	122	124.19700	114.00000
harm	121	122	123	124.19700	112.00000
harm	122	123	124	124.19700	114.00000
harm	123	124	125	124.19700	114.00000
harm	124	125	126	124.19700	114.00000
harm	125	126	127	124.19700	114.00000
harm	126	127	128	124.19700	114.00000
harm	127	128	129	124.19700	114.00000
harm	128	129	130	124.19700	114.00000
harm	129	130	131	124.19700	114.00000
harm	130	131	132	124.19700	114.00000
harm	131	132	133	124.19700	114.00000
harm	132	133	134	124.19700	114.00000
harm	133	134	135	124.19700	114.00000
harm	134	135	136	124.19700	114.00000
harm	135	136	137	124.19700	114.00000
harm	136	137	138	124.19700	114.00000
harm	137	138	139	124.19700	114.00000
harm	138	139	140	124.19700	114.00000
harm	139	140	141	124.19700	114.00000
harm	140	141	142	124.19700	114.00000
harm	141	142	143	124.19700	112.00000
harm	142	143	144	124.19700	114.00000
harm	143	144	145	124.19700	114.00000
harm	144	145	146	124.19700	114.00000
harm	145	146	147	124.19700	114.00000
harm	146	147	148	124.19700	114.00000
harm	147	148	149	124.19700	114.00000
harm	148	149	150	124.19700	114.00000
harm	149	150	151	124.19700	114.00000
harm	150	151	152	124.19700	114.00000
harm	151	152	153	124.19700	114.00000
harm	152	153	154	124.19700	114.00000
harm	153	154	155	124.19700	114.00000
harm	154	155	156	124.19700	114.00000
harm	155	156	157	124.19700	114.00000
harm	156	157	158	124.19700	114.00000
harm	157	158	159	124.19700	114.00000
harm	158	159	160	124.19700	114.00000
harm	159	160	161	124.19700	114.00000
harm	160	161	162	124.19700	114.00000
harm	161	162	163	124.19700	112.00000
harm	162	163	164	124.19700	114.00000
harm	163	164	165	124.19700	114.00000
harm	164	165	166	124.19700	114.00000
harm	165	166	167	124.19700	114.00000
harm	166	167	168	124.19700	114.00000
harm	167	168	169	124.19700	114.00000
harm	168	169	170	124.19700	114.00000
harm	169	170	171	124.19700	114.00000
harm	170	171	172	124.19700	114.00000
harm	171	172	173	124.19700	114.00000
harm	172	173	174	124.19700	114.00000
harm	173	174	175	124.19700	114.00000
harm	174	175	176	124.19700	114.00000
harm	175	176	177	124.19700	114.00000

harm	176	177	178	124.19700	114.00000
harm	177	178	179	124.19700	114.00000
harm	178	179	180	124.19700	114.00000
harm	179	180	181	124.19700	114.00000
harm	180	181	182	124.19700	114.00000
harm	181	182	183	124.19700	112.00000
harm	182	183	184	124.19700	114.00000
harm	183	184	185	124.19700	114.00000
harm	184	185	186	124.19700	114.00000
harm	185	186	187	124.19700	114.00000
harm	186	187	188	124.19700	114.00000
harm	187	188	189	124.19700	114.00000
harm	188	189	190	124.19700	114.00000
harm	189	190	191	124.19700	114.00000
harm	190	191	192	124.19700	114.00000
harm	191	192	193	124.19700	114.00000
harm	192	193	194	124.19700	114.00000
harm	193	194	195	124.19700	114.00000
harm	194	195	196	124.19700	114.00000
harm	195	196	197	124.19700	114.00000
harm	196	197	198	124.19700	114.00000
harm	197	198	199	124.19700	114.00000
harm	198	199	200	124.19700	114.00000
harm	199	200	201	124.19700	114.00000
harm	1	2	202	124.19700	112.00000
harm	3	2	202	124.19700	112.00000
harm	2	202	203	124.19700	114.00000
harm	202	203	204	124.19700	114.00000
harm	203	204	205	124.19700	114.00000
harm	204	205	206	124.19700	114.00000
harm	205	206	207	124.19700	114.00000
harm	206	207	208	124.19700	114.00000
harm	207	208	209	124.19700	114.00000
harm	208	209	210	124.19700	114.00000
harm	209	210	211	124.19700	114.00000
harm	210	211	212	124.19700	114.00000
harm	211	212	213	124.19700	114.00000
harm	212	213	214	124.19700	114.00000
harm	213	214	215	124.19700	114.00000
harm	214	215	216	124.19700	114.00000
harm	215	216	217	124.19700	114.00000
harm	216	217	218	124.19700	114.00000
harm	217	218	219	124.19700	114.00000
harm	218	219	220	124.19700	114.00000
harm	219	220	221	124.19700	114.00000
harm	220	221	222	124.19700	114.00000
harm	221	222	223	124.19700	114.00000
harm	222	223	224	124.19700	114.00000
harm	223	224	225	124.19700	114.00000
harm	224	225	226	124.19700	114.00000
harm	225	226	227	124.19700	114.00000
harm	226	227	228	124.19700	114.00000
harm	227	228	229	124.19700	114.00000
harm	228	229	230	124.19700	114.00000
harm	229	230	231	124.19700	114.00000
harm	21	22	232	124.19700	112.00000
harm	23	22	232	124.19700	112.00000
harm	22	232	233	124.19700	114.00000
harm	232	233	234	124.19700	114.00000
harm	233	234	235	124.19700	114.00000
harm	234	235	236	124.19700	114.00000
harm	235	236	237	124.19700	114.00000
harm	236	237	238	124.19700	114.00000

harm	237	238	239	124.19700	114.00000
harm	238	239	240	124.19700	114.00000
harm	239	240	241	124.19700	114.00000
harm	240	241	242	124.19700	114.00000
harm	241	242	243	124.19700	114.00000
harm	242	243	244	124.19700	114.00000
harm	243	244	245	124.19700	114.00000
harm	244	245	246	124.19700	114.00000
harm	245	246	247	124.19700	114.00000
harm	246	247	248	124.19700	114.00000
harm	247	248	249	124.19700	114.00000
harm	248	249	250	124.19700	114.00000
harm	249	250	251	124.19700	114.00000
harm	250	251	252	124.19700	114.00000
harm	251	252	253	124.19700	114.00000
harm	252	253	254	124.19700	114.00000
harm	253	254	255	124.19700	114.00000
harm	254	255	256	124.19700	114.00000
harm	255	256	257	124.19700	114.00000
harm	256	257	258	124.19700	114.00000
harm	257	258	259	124.19700	114.00000
harm	258	259	260	124.19700	114.00000
harm	259	260	261	124.19700	114.00000
harm	41	42	262	124.19700	112.00000
harm	43	42	262	124.19700	112.00000
harm	42	262	263	124.19700	114.00000
harm	262	263	264	124.19700	114.00000
harm	263	264	265	124.19700	114.00000
harm	264	265	266	124.19700	114.00000
harm	265	266	267	124.19700	114.00000
harm	266	267	268	124.19700	114.00000
harm	267	268	269	124.19700	114.00000
harm	268	269	270	124.19700	114.00000
harm	269	270	271	124.19700	114.00000
harm	270	271	272	124.19700	114.00000
harm	271	272	273	124.19700	114.00000
harm	272	273	274	124.19700	114.00000
harm	273	274	275	124.19700	114.00000
harm	274	275	276	124.19700	114.00000
harm	275	276	277	124.19700	114.00000
harm	276	277	278	124.19700	114.00000
harm	277	278	279	124.19700	114.00000
harm	278	279	280	124.19700	114.00000
harm	279	280	281	124.19700	114.00000
harm	280	281	282	124.19700	114.00000
harm	281	282	283	124.19700	114.00000
harm	282	283	284	124.19700	114.00000
harm	283	284	285	124.19700	114.00000
harm	284	285	286	124.19700	114.00000
harm	285	286	287	124.19700	114.00000
harm	286	287	288	124.19700	114.00000
harm	287	288	289	124.19700	114.00000
harm	288	289	290	124.19700	114.00000
harm	289	290	291	124.19700	114.00000
harm	61	62	292	124.19700	112.00000
harm	63	62	292	124.19700	112.00000
harm	62	292	293	124.19700	114.00000
harm	292	293	294	124.19700	114.00000
harm	293	294	295	124.19700	114.00000
harm	294	295	296	124.19700	114.00000
harm	295	296	297	124.19700	114.00000
harm	296	297	298	124.19700	114.00000
harm	297	298	299	124.19700	114.00000

harm	298	299	300	124.19700	114.00000
harm	299	300	301	124.19700	114.00000
harm	300	301	302	124.19700	114.00000
harm	301	302	303	124.19700	114.00000
harm	302	303	304	124.19700	114.00000
harm	303	304	305	124.19700	114.00000
harm	304	305	306	124.19700	114.00000
harm	305	306	307	124.19700	114.00000
harm	306	307	308	124.19700	114.00000
harm	307	308	309	124.19700	114.00000
harm	308	309	310	124.19700	114.00000
harm	309	310	311	124.19700	114.00000
harm	310	311	312	124.19700	114.00000
harm	311	312	313	124.19700	114.00000
harm	312	313	314	124.19700	114.00000
harm	313	314	315	124.19700	114.00000
harm	314	315	316	124.19700	114.00000
harm	315	316	317	124.19700	114.00000
harm	316	317	318	124.19700	114.00000
harm	317	318	319	124.19700	114.00000
harm	318	319	320	124.19700	114.00000
harm	319	320	321	124.19700	114.00000
harm	81	82	322	124.19700	112.00000
harm	83	82	322	124.19700	112.00000
harm	82	322	323	124.19700	114.00000
harm	322	323	324	124.19700	114.00000
harm	323	324	325	124.19700	114.00000
harm	324	325	326	124.19700	114.00000
harm	325	326	327	124.19700	114.00000
harm	326	327	328	124.19700	114.00000
harm	327	328	329	124.19700	114.00000
harm	328	329	330	124.19700	114.00000
harm	329	330	331	124.19700	114.00000
harm	330	331	332	124.19700	114.00000
harm	331	332	333	124.19700	114.00000
harm	332	333	334	124.19700	114.00000
harm	333	334	335	124.19700	114.00000
harm	334	335	336	124.19700	114.00000
harm	335	336	337	124.19700	114.00000
harm	336	337	338	124.19700	114.00000
harm	337	338	339	124.19700	114.00000
harm	338	339	340	124.19700	114.00000
harm	339	340	341	124.19700	114.00000
harm	340	341	342	124.19700	114.00000
harm	341	342	343	124.19700	114.00000
harm	342	343	344	124.19700	114.00000
harm	343	344	345	124.19700	114.00000
harm	344	345	346	124.19700	114.00000
harm	345	346	347	124.19700	114.00000
harm	346	347	348	124.19700	114.00000
harm	347	348	349	124.19700	114.00000
harm	348	349	350	124.19700	114.00000
harm	349	350	351	124.19700	114.00000
harm	101	102	352	124.19700	112.00000
harm	103	102	352	124.19700	112.00000
harm	102	352	353	124.19700	114.00000
harm	352	353	354	124.19700	114.00000
harm	353	354	355	124.19700	114.00000
harm	354	355	356	124.19700	114.00000
harm	355	356	357	124.19700	114.00000
harm	356	357	358	124.19700	114.00000
harm	357	358	359	124.19700	114.00000
harm	358	359	360	124.19700	114.00000

harm	359	360	361	124.19700	114.00000
harm	360	361	362	124.19700	114.00000
harm	361	362	363	124.19700	114.00000
harm	362	363	364	124.19700	114.00000
harm	363	364	365	124.19700	114.00000
harm	364	365	366	124.19700	114.00000
harm	365	366	367	124.19700	114.00000
harm	366	367	368	124.19700	114.00000
harm	367	368	369	124.19700	114.00000
harm	368	369	370	124.19700	114.00000
harm	369	370	371	124.19700	114.00000
harm	370	371	372	124.19700	114.00000
harm	371	372	373	124.19700	114.00000
harm	372	373	374	124.19700	114.00000
harm	373	374	375	124.19700	114.00000
harm	374	375	376	124.19700	114.00000
harm	375	376	377	124.19700	114.00000
harm	376	377	378	124.19700	114.00000
harm	377	378	379	124.19700	114.00000
harm	378	379	380	124.19700	114.00000
harm	379	380	381	124.19700	114.00000
harm	121	122	382	124.19700	112.00000
harm	123	122	382	124.19700	112.00000
harm	122	382	383	124.19700	114.00000
harm	382	383	384	124.19700	114.00000
harm	383	384	385	124.19700	114.00000
harm	384	385	386	124.19700	114.00000
harm	385	386	387	124.19700	114.00000
harm	386	387	388	124.19700	114.00000
harm	387	388	389	124.19700	114.00000
harm	388	389	390	124.19700	114.00000
harm	389	390	391	124.19700	114.00000
harm	390	391	392	124.19700	114.00000
harm	391	392	393	124.19700	114.00000
harm	392	393	394	124.19700	114.00000
harm	393	394	395	124.19700	114.00000
harm	394	395	396	124.19700	114.00000
harm	395	396	397	124.19700	114.00000
harm	396	397	398	124.19700	114.00000
harm	397	398	399	124.19700	114.00000
harm	398	399	400	124.19700	114.00000
harm	399	400	401	124.19700	114.00000
harm	400	401	402	124.19700	114.00000
harm	401	402	403	124.19700	114.00000
harm	402	403	404	124.19700	114.00000
harm	403	404	405	124.19700	114.00000
harm	404	405	406	124.19700	114.00000
harm	405	406	407	124.19700	114.00000
harm	406	407	408	124.19700	114.00000
harm	407	408	409	124.19700	114.00000
harm	408	409	410	124.19700	114.00000
harm	409	410	411	124.19700	114.00000
harm	141	142	412	124.19700	112.00000
harm	143	142	412	124.19700	112.00000
harm	142	412	413	124.19700	114.00000
harm	412	413	414	124.19700	114.00000
harm	413	414	415	124.19700	114.00000
harm	414	415	416	124.19700	114.00000
harm	415	416	417	124.19700	114.00000
harm	416	417	418	124.19700	114.00000
harm	417	418	419	124.19700	114.00000
harm	418	419	420	124.19700	114.00000
harm	419	420	421	124.19700	114.00000

harm	420	421	422	124.19700	114.00000
harm	421	422	423	124.19700	114.00000
harm	422	423	424	124.19700	114.00000
harm	423	424	425	124.19700	114.00000
harm	424	425	426	124.19700	114.00000
harm	425	426	427	124.19700	114.00000
harm	426	427	428	124.19700	114.00000
harm	427	428	429	124.19700	114.00000
harm	428	429	430	124.19700	114.00000
harm	429	430	431	124.19700	114.00000
harm	430	431	432	124.19700	114.00000
harm	431	432	433	124.19700	114.00000
harm	432	433	434	124.19700	114.00000
harm	433	434	435	124.19700	114.00000
harm	434	435	436	124.19700	114.00000
harm	435	436	437	124.19700	114.00000
harm	436	437	438	124.19700	114.00000
harm	437	438	439	124.19700	114.00000
harm	438	439	440	124.19700	114.00000
harm	439	440	441	124.19700	114.00000
harm	161	162	442	124.19700	112.00000
harm	163	162	442	124.19700	112.00000
harm	162	442	443	124.19700	114.00000
harm	442	443	444	124.19700	114.00000
harm	443	444	445	124.19700	114.00000
harm	444	445	446	124.19700	114.00000
harm	445	446	447	124.19700	114.00000
harm	446	447	448	124.19700	114.00000
harm	447	448	449	124.19700	114.00000
harm	448	449	450	124.19700	114.00000
harm	449	450	451	124.19700	114.00000
harm	450	451	452	124.19700	114.00000
harm	451	452	453	124.19700	114.00000
harm	452	453	454	124.19700	114.00000
harm	453	454	455	124.19700	114.00000
harm	454	455	456	124.19700	114.00000
harm	455	456	457	124.19700	114.00000
harm	456	457	458	124.19700	114.00000
harm	457	458	459	124.19700	114.00000
harm	458	459	460	124.19700	114.00000
harm	459	460	461	124.19700	114.00000
harm	460	461	462	124.19700	114.00000
harm	461	462	463	124.19700	114.00000
harm	462	463	464	124.19700	114.00000
harm	463	464	465	124.19700	114.00000
harm	464	465	466	124.19700	114.00000
harm	465	466	467	124.19700	114.00000
harm	466	467	468	124.19700	114.00000
harm	467	468	469	124.19700	114.00000
harm	468	469	470	124.19700	114.00000
harm	469	470	471	124.19700	114.00000
harm	181	182	472	124.19700	112.00000
harm	183	182	472	124.19700	112.00000
harm	182	472	473	124.19700	114.00000
harm	472	473	474	124.19700	114.00000
harm	473	474	475	124.19700	114.00000
harm	474	475	476	124.19700	114.00000
harm	475	476	477	124.19700	114.00000
harm	476	477	478	124.19700	114.00000
harm	477	478	479	124.19700	114.00000
harm	478	479	480	124.19700	114.00000
harm	479	480	481	124.19700	114.00000
harm	480	481	482	124.19700	114.00000

harm	481	482	483	124.19700	114.00000
harm	482	483	484	124.19700	114.00000
harm	483	484	485	124.19700	114.00000
harm	484	485	486	124.19700	114.00000
harm	485	486	487	124.19700	114.00000
harm	486	487	488	124.19700	114.00000
harm	487	488	489	124.19700	114.00000
harm	488	489	490	124.19700	114.00000
harm	489	490	491	124.19700	114.00000
harm	490	491	492	124.19700	114.00000
harm	491	492	493	124.19700	114.00000
harm	492	493	494	124.19700	114.00000
harm	493	494	495	124.19700	114.00000
harm	494	495	496	124.19700	114.00000
harm	495	496	497	124.19700	114.00000
harm	496	497	498	124.19700	114.00000
harm	497	498	499	124.19700	114.00000
harm	498	499	500	124.19700	114.00000
harm	499	500	501	124.19700	114.00000
dihedral	368				
OPLS	1 2 3 4	-0.4989000	1.70390800	-0.44453000	1.753745000 0.00000000
OPLS	2 3 4 5	0.0000000	1.41100000	-0.27100000	3.145000000 0.00000000
OPLS	3 4 5 6	0.0000000	1.41100000	-0.27100000	3.145000000 0.00000000
OPLS	4 5 6 7	0.0000000	1.41100000	-0.27100000	3.145000000 0.00000000
OPLS	5 6 7 8	0.0000000	1.41100000	-0.27100000	3.145000000 0.00000000
OPLS	6 7 8 9	0.0000000	1.41100000	-0.27100000	3.145000000 0.00000000
OPLS	7 8 9 10	0.0000000	1.41100000	-0.27100000	3.145000000 0.00000000
OPLS	8 9 10 11	0.0000000	1.41100000	-0.27100000	3.145000000 0.00000000
OPLS	9 10 11 12	0.0000000	1.41100000	-0.27100000	3.145000000 0.00000000
OPLS	10 11 12 13	0.0000000	1.41100000	-0.27100000	3.145000000 0.00000000
OPLS	11 12 13 14	0.0000000	1.41100000	-0.27100000	3.145000000 0.00000000
OPLS	12 13 14 15	0.0000000	1.41100000	-0.27100000	3.145000000 0.00000000
OPLS	13 14 15 16	0.0000000	1.41100000	-0.27100000	3.145000000 0.00000000
OPLS	14 15 16 17	0.0000000	1.41100000	-0.27100000	3.145000000 0.00000000
OPLS	15 16 17 18	0.0000000	1.41100000	-0.27100000	3.145000000 0.00000000
OPLS	16 17 18 19	0.0000000	1.41100000	-0.27100000	3.145000000 0.00000000
OPLS	17 18 19 20	0.0000000	1.41100000	-0.27100000	3.145000000 0.00000000
OPLS	18 19 20 21	0.0000000	1.41100000	-0.27100000	3.145000000 0.00000000
OPLS	19 20 21 22	0.0000000	1.41100000	-0.27100000	3.145000000 0.00000000
OPLS	20 21 22 23	-0.4989000	1.70390800	-0.44453000	1.753745000 0.00000000
OPLS	21 22 23 24	-0.4989000	1.70390800	-0.44453000	1.753745000 0.00000000
OPLS	22 23 24 25	0.0000000	1.41100000	-0.27100000	3.145000000 0.00000000
OPLS	23 24 25 26	0.0000000	1.41100000	-0.27100000	3.145000000 0.00000000
OPLS	24 25 26 27	0.0000000	1.41100000	-0.27100000	3.145000000 0.00000000
OPLS	25 26 27 28	0.0000000	1.41100000	-0.27100000	3.145000000 0.00000000
OPLS	26 27 28 29	0.0000000	1.41100000	-0.27100000	3.145000000 0.00000000
OPLS	27 28 29 30	0.0000000	1.41100000	-0.27100000	3.145000000 0.00000000
OPLS	28 29 30 31	0.0000000	1.41100000	-0.27100000	3.145000000 0.00000000
OPLS	29 30 31 32	0.0000000	1.41100000	-0.27100000	3.145000000 0.00000000
OPLS	30 31 32 33	0.0000000	1.41100000	-0.27100000	3.145000000 0.00000000
OPLS	31 32 33 34	0.0000000	1.41100000	-0.27100000	3.145000000 0.00000000
OPLS	32 33 34 35	0.0000000	1.41100000	-0.27100000	3.145000000 0.00000000
OPLS	33 34 35 36	0.0000000	1.41100000	-0.27100000	3.145000000 0.00000000
OPLS	34 35 36 37	0.0000000	1.41100000	-0.27100000	3.145000000 0.00000000
OPLS	35 36 37 38	0.0000000	1.41100000	-0.27100000	3.145000000 0.00000000
OPLS	36 37 38 39	0.0000000	1.41100000	-0.27100000	3.145000000 0.00000000
OPLS	37 38 39 40	0.0000000	1.41100000	-0.27100000	3.145000000 0.00000000
OPLS	38 39 40 41	0.0000000	1.41100000	-0.27100000	3.145000000 0.00000000
OPLS	39 40 41 42	0.0000000	1.41100000	-0.27100000	3.145000000 0.00000000
OPLS	40 41 42 43	-0.4989000	1.70390800	-0.44453000	1.753745000 0.00000000
OPLS	41 42 43 44	-0.4989000	1.70390800	-0.44453000	1.753745000 0.00000000
OPLS	42 43 44 45	0.0000000	1.41100000	-0.27100000	3.145000000 0.00000000
OPLS	43 44 45 46	0.0000000	1.41100000	-0.27100000	3.145000000 0.00000000

13	14	1.54000000
14	15	1.54000000
14	16	1.54000000
16	17	1.54000000
17	18	1.54000000
17	19	1.54000000
19	20	1.54000000
20	21	1.54000000
20	22	1.54000000
22	23	1.54000000
23	24	1.54000000
23	25	1.54000000
25	26	1.54000000
26	27	1.54000000
26	28	1.54000000
28	29	1.54000000
29	30	1.54000000
29	31	1.54000000
31	32	1.54000000
32	33	1.54000000
32	34	1.54000000
34	35	1.54000000
35	36	1.54000000
35	37	1.54000000
37	38	1.54000000
38	39	1.54000000
38	40	1.54000000
40	41	1.54000000
41	42	1.54000000
41	43	1.54000000
43	44	1.54000000
44	45	1.54000000
44	46	1.54000000
46	47	1.54000000
47	48	1.54000000
47	49	1.54000000
49	50	1.54000000
50	51	1.54000000
50	52	1.54000000
52	53	1.54000000
53	54	1.54000000
53	55	1.54000000
55	56	1.54000000
56	57	1.54000000
56	58	1.54000000
58	59	1.54000000
59	60	1.54000000
59	61	1.54000000
61	62	1.54000000
62	63	1.54000000
62	64	1.54000000
64	65	1.54000000
65	66	1.54000000
65	67	1.54000000
67	68	1.54000000
68	69	1.54000000
68	70	1.54000000
70	71	1.54000000
71	72	1.54000000
71	73	1.54000000
73	74	1.54000000
74	75	1.54000000
74	76	1.54000000

angles 99

harm	1	2	3	124.19700	112.00000
harm	1	2	4	124.19700	112.00000
harm	3	2	4	124.19700	112.00000
harm	2	4	5	124.19700	114.00000
harm	4	5	6	124.19700	112.00000
harm	4	5	7	124.19700	112.00000
harm	6	5	7	124.19700	112.00000
harm	5	7	8	124.19700	114.00000
harm	7	8	9	124.19700	112.00000
harm	7	8	10	124.19700	112.00000
harm	9	8	10	124.19700	112.00000
harm	8	10	11	124.19700	114.00000
harm	10	11	12	124.19700	112.00000
harm	10	11	13	124.19700	112.00000
harm	12	11	13	124.19700	112.00000
harm	11	13	14	124.19700	114.00000
harm	13	14	15	124.19700	112.00000
harm	13	14	16	124.19700	112.00000
harm	15	14	16	124.19700	112.00000
harm	14	16	17	124.19700	114.00000
harm	16	17	18	124.19700	112.00000
harm	16	17	19	124.19700	112.00000
harm	18	17	19	124.19700	112.00000
harm	17	19	20	124.19700	114.00000
harm	19	20	21	124.19700	112.00000
harm	19	20	22	124.19700	112.00000
harm	21	20	22	124.19700	112.00000
harm	20	22	23	124.19700	114.00000
harm	22	23	24	124.19700	112.00000
harm	22	23	25	124.19700	112.00000
harm	24	23	25	124.19700	112.00000
harm	23	25	26	124.19700	114.00000
harm	25	26	27	124.19700	112.00000
harm	25	26	28	124.19700	112.00000
harm	27	26	28	124.19700	112.00000
harm	26	28	29	124.19700	114.00000
harm	28	29	30	124.19700	112.00000
harm	28	29	31	124.19700	112.00000
harm	30	29	31	124.19700	112.00000
harm	29	31	32	124.19700	114.00000
harm	31	32	33	124.19700	112.00000
harm	31	32	34	124.19700	112.00000
harm	33	32	34	124.19700	112.00000
harm	32	34	35	124.19700	114.00000
harm	34	35	36	124.19700	112.00000
harm	34	35	37	124.19700	112.00000
harm	36	35	37	124.19700	112.00000
harm	35	37	38	124.19700	114.00000
harm	37	38	39	124.19700	112.00000
harm	37	38	40	124.19700	112.00000
harm	39	38	40	124.19700	112.00000
harm	38	40	41	124.19700	114.00000
harm	40	41	42	124.19700	112.00000
harm	40	41	43	124.19700	112.00000
harm	42	41	43	124.19700	112.00000
harm	41	43	44	124.19700	114.00000
harm	43	44	45	124.19700	112.00000
harm	43	44	46	124.19700	112.00000
harm	45	44	46	124.19700	112.00000
harm	44	46	47	124.19700	114.00000
harm	46	47	48	124.19700	112.00000
harm	46	47	49	124.19700	112.00000

harm	48	47	49	124.19700	112.00000
harm	47	49	50	124.19700	114.00000
harm	49	50	51	124.19700	112.00000
harm	49	50	52	124.19700	112.00000
harm	51	50	52	124.19700	112.00000
harm	50	52	53	124.19700	114.00000
harm	52	53	54	124.19700	112.00000
harm	52	53	55	124.19700	112.00000
harm	54	53	55	124.19700	112.00000
harm	53	55	56	124.19700	114.00000
harm	55	56	57	124.19700	112.00000
harm	55	56	58	124.19700	112.00000
harm	57	56	58	124.19700	112.00000
harm	56	58	59	124.19700	114.00000
harm	58	59	60	124.19700	112.00000
harm	58	59	61	124.19700	112.00000
harm	60	59	61	124.19700	112.00000
harm	59	61	62	124.19700	114.00000
harm	61	62	63	124.19700	112.00000
harm	61	62	64	124.19700	112.00000
harm	63	62	64	124.19700	112.00000
harm	62	64	65	124.19700	114.00000
harm	64	65	66	124.19700	112.00000
harm	64	65	67	124.19700	112.00000
harm	66	65	67	124.19700	112.00000
harm	65	67	68	124.19700	114.00000
harm	67	68	69	124.19700	112.00000
harm	67	68	70	124.19700	112.00000
harm	69	68	70	124.19700	112.00000
harm	68	70	71	124.19700	114.00000
harm	70	71	72	124.19700	112.00000
harm	70	71	73	124.19700	112.00000
harm	72	71	73	124.19700	112.00000
harm	71	73	74	124.19700	114.00000
harm	73	74	75	124.19700	112.00000
harm	73	74	76	124.19700	112.00000
harm	75	74	76	124.19700	112.00000

dihedral 96

OPLS	1	2	4	5	-0.4989000	1.70390800	-0.44453000	1.753745000	0.00000000
OPLS	2	4	5	7	-0.4989000	1.70390800	-0.44453000	1.753745000	0.00000000
OPLS	4	5	7	8	-0.4989000	1.70390800	-0.44453000	1.753745000	0.00000000
OPLS	5	7	8	10	-0.4989000	1.70390800	-0.44453000	1.753745000	0.00000000
OPLS	7	8	10	11	-0.4989000	1.70390800	-0.44453000	1.753745000	0.00000000
OPLS	8	10	11	13	-0.4989000	1.70390800	-0.44453000	1.753745000	0.00000000
OPLS	10	11	13	14	-0.4989000	1.70390800	-0.44453000	1.753745000	0.00000000
OPLS	11	13	14	16	-0.4989000	1.70390800	-0.44453000	1.753745000	0.00000000
OPLS	13	14	16	17	-0.4989000	1.70390800	-0.44453000	1.753745000	0.00000000
OPLS	14	16	17	19	-0.4989000	1.70390800	-0.44453000	1.753745000	0.00000000
OPLS	16	17	19	20	-0.4989000	1.70390800	-0.44453000	1.753745000	0.00000000
OPLS	17	19	20	22	-0.4989000	1.70390800	-0.44453000	1.753745000	0.00000000
OPLS	19	20	22	23	-0.4989000	1.70390800	-0.44453000	1.753745000	0.00000000
OPLS	20	22	23	25	-0.4989000	1.70390800	-0.44453000	1.753745000	0.00000000
OPLS	22	23	25	26	-0.4989000	1.70390800	-0.44453000	1.753745000	0.00000000
OPLS	23	25	26	28	-0.4989000	1.70390800	-0.44453000	1.753745000	0.00000000
OPLS	25	26	28	29	-0.4989000	1.70390800	-0.44453000	1.753745000	0.00000000
OPLS	26	28	29	31	-0.4989000	1.70390800	-0.44453000	1.753745000	0.00000000
OPLS	28	29	31	32	-0.4989000	1.70390800	-0.44453000	1.753745000	0.00000000
OPLS	29	31	32	34	-0.4989000	1.70390800	-0.44453000	1.753745000	0.00000000
OPLS	31	32	34	35	-0.4989000	1.70390800	-0.44453000	1.753745000	0.00000000
OPLS	32	34	35	37	-0.4989000	1.70390800	-0.44453000	1.753745000	0.00000000
OPLS	34	35	37	38	-0.4989000	1.70390800	-0.44453000	1.753745000	0.00000000
OPLS	35	37	38	40	-0.4989000	1.70390800	-0.44453000	1.753745000	0.00000000
OPLS	37	38	40	41	-0.4989000	1.70390800	-0.44453000	1.753745000	0.00000000


```
OPLS 63 62 64 65 -0.4989000 1.70390800 -0.44453000 1.753745000 0.00000000
OPLS 66 65 64 62 -0.4989000 1.70390800 -0.44453000 1.753745000 0.00000000
OPLS 66 65 67 68 -0.4989000 1.70390800 -0.44453000 1.753745000 0.00000000
OPLS 69 68 67 65 -0.4989000 1.70390800 -0.44453000 1.753745000 0.00000000
OPLS 69 68 70 71 -0.4989000 1.70390800 -0.44453000 1.753745000 0.00000000
OPLS 72 71 70 68 -0.4989000 1.70390800 -0.44453000 1.753745000 0.00000000
OPLS 72 71 73 74 -0.4989000 1.70390800 -0.44453000 1.753745000 0.00000000
OPLS 75 74 73 71 -0.4989000 1.70390800 -0.44453000 1.753745000 0.00000000
```

finish

vdw 6

```
C3      C3      lj      0.1947      3.7500
C2      C3      lj      0.1334      3.8500
C1      C3      lj      0.0622      4.2150
C2      C2      lj      0.0914      3.9500
C1      C2      lj      0.0426      4.3150
C1      C1      lj      0.0199      4.6800
```

close

CONFIG Files

High Density Polyethylene

One Chain – 20 Pseudo Atoms Long

```
calc
0      0
C3
-1.920000      0.000000      0.422000
C2
-0.641000      0.000000      -0.422000
C2
0.641000      0.000000      0.422000
C2
1.920000      0.000000      -0.422000
C2
3.202000      0.000000      0.422000
C2
4.481000      0.000000      -0.422000
C2
5.763000      0.000000      0.422000
C2
7.042000      0.000000      -0.422000
C2
8.324000      0.000000      0.422000
C2
9.603000      0.000000      -0.422000
C2
10.885000      0.000000      0.422000
C2
12.164000      0.000000      -0.422000
C2
13.446000      0.000000      0.422000
C2
14.725000      0.000000      -0.422000
C2
16.007000      0.000000      0.422000
C2
17.286000      0.000000      -0.422000
C2
18.568000      0.000000      0.422000
C2
19.847000      0.000000      -0.422000
C2
21.129000      0.000000      0.422000
C3
22.408000      0.000000      -0.422000
```

Four Chains – 20 Pseudo Atoms Long

```
calc
0      0
C3
-1.920000      0.000000      0.422000
C2
```

	-0.641000	0.000000	-0.422000
C2			
	0.641000	0.000000	0.422000
C2			
	1.920000	0.000000	-0.422000
C2			
	3.202000	0.000000	0.422000
C2			
	4.481000	0.000000	-0.422000
C2			
	5.763000	0.000000	0.422000
C2			
	7.042000	0.000000	-0.422000
C2			
	8.324000	0.000000	0.422000
C2			
	9.603000	0.000000	-0.422000
C2			
	10.885000	0.000000	0.422000
C2			
	12.164000	0.000000	-0.422000
C2			
	13.446000	0.000000	0.422000
C2			
	14.725000	0.000000	-0.422000
C2			
	16.007000	0.000000	0.422000
C2			
	17.286000	0.000000	-0.422000
C2			
	18.568000	0.000000	0.422000
C2			
	19.847000	0.000000	-0.422000
C2			
	21.129000	0.000000	0.422000
C3			
	22.408000	0.000000	-0.422000
C3			
	-1.920000	5.000000	0.422000
C2			
	-0.641000	5.000000	-0.422000
C2			
	0.641000	5.000000	0.422000
C2			
	1.920000	5.000000	-0.422000
C2			
	3.202000	5.000000	0.422000
C2			
	4.481000	5.000000	-0.422000
C2			
	5.763000	5.000000	0.422000
C2			
	7.042000	5.000000	-0.422000
C2			
	8.324000	5.000000	0.422000
C2			
	9.603000	5.000000	-0.422000
C2			
	10.885000	5.000000	0.422000
C2			
	12.164000	5.000000	-0.422000
C2			
	13.446000	5.000000	0.422000

C2	14.725000	5.000000	-0.422000
C2	16.007000	5.000000	0.422000
C2	17.286000	5.000000	-0.422000
C2	18.568000	5.000000	0.422000
C2	19.847000	5.000000	-0.422000
C2	21.129000	5.000000	0.422000
C3	22.408000	5.000000	-0.422000
C3	-1.920000	10.000000	0.422000
C2	-0.641000	10.000000	-0.422000
C2	0.641000	10.000000	0.422000
C2	1.920000	10.000000	-0.422000
C2	3.202000	10.000000	0.422000
C2	4.481000	10.000000	-0.422000
C2	5.763000	10.000000	0.422000
C2	7.042000	10.000000	-0.422000
C2	8.324000	10.000000	0.422000
C2	9.603000	10.000000	-0.422000
C2	10.885000	10.000000	0.422000
C2	12.164000	10.000000	-0.422000
C2	13.446000	10.000000	0.422000
C2	14.725000	10.000000	-0.422000
C2	16.007000	10.000000	0.422000
C2	17.286000	10.000000	-0.422000
C2	18.568000	10.000000	0.422000
C2	19.847000	10.000000	-0.422000
C2	21.129000	10.000000	0.422000
C3	22.408000	10.000000	-0.422000
C3	-1.920000	15.000000	0.422000
C2	-0.641000	15.000000	-0.422000
C2	0.641000	15.000000	0.422000
C2	1.920000	15.000000	-0.422000

	3.202000	15.000000	0.422000
C2	4.481000	15.000000	-0.422000
C2	5.763000	15.000000	0.422000
C2	7.042000	15.000000	-0.422000
C2	8.324000	15.000000	0.422000
C2	9.603000	15.000000	-0.422000
C2	10.885000	15.000000	0.422000
C2	12.164000	15.000000	-0.422000
C2	13.446000	15.000000	0.422000
C2	14.725000	15.000000	-0.422000
C2	16.007000	15.000000	0.422000
C2	17.286000	15.000000	-0.422000
C2	18.568000	15.000000	0.422000
C2	19.847000	15.000000	-0.422000
C2	21.129000	15.000000	0.422000
C3	22.408000	15.000000	-0.422000

Low Density Polyethylene (LDPE)

One Chain – 200 Pseudo Atoms Long

calc	0	0	
C3	-1.920000	0.000000	0.422000
C1	-0.641000	0.000000	-0.422000
C2	0.641000	0.000000	0.422000
C2	1.920000	0.000000	-0.422000
C2	3.202000	0.000000	0.422000
C2	4.481000	0.000000	-0.422000
C2	5.763000	0.000000	0.422000
C2	7.042000	0.000000	-0.422000
C2	8.324000	0.000000	0.422000

	9.603000	0.000000	-0.422000
C2			
	10.885000	0.000000	0.422000
C2			
	12.164000	0.000000	-0.422000
C2			
	13.446000	0.000000	0.422000
C2			
	14.725000	0.000000	-0.422000
C2			
	16.007000	0.000000	0.422000
C2			
	17.286000	0.000000	-0.422000
C2			
	18.568000	0.000000	0.422000
C2			
	19.847000	0.000000	-0.422000
C2			
	21.129000	0.000000	0.422000
C2			
	22.408000	0.000000	-0.422000
C2			
	23.690000	0.000000	0.422000
C1			
	24.969000	0.000000	-0.422000
C2			
	26.251000	0.000000	0.422000
C2			
	27.530000	0.000000	-0.422000
C2			
	28.812000	0.000000	0.422000
C2			
	30.091000	0.000000	-0.422000
C2			
	31.373000	0.000000	0.422000
C2			
	32.652000	0.000000	-0.422000
C2			
	33.934000	0.000000	0.422000
C2			
	35.213000	0.000000	-0.422000
C2			
	36.495000	0.000000	0.422000
C2			
	37.774000	0.000000	-0.422000
C2			
	39.056000	0.000000	0.422000
C2			
	40.335000	0.000000	-0.422000
C2			
	41.617000	0.000000	0.422000
C2			
	42.896000	0.000000	-0.422000
C2			
	44.178000	0.000000	0.422000
C2			
	45.457000	0.000000	-0.422000
C2			
	46.739000	0.000000	0.422000
C2			
	48.018000	0.000000	-0.422000
C2			
	49.300000	0.000000	0.422000

C1	50.579000	0.000000	-0.422000
C2	51.861000	0.000000	0.422000
C2	53.140000	0.000000	-0.422000
C2	54.422000	0.000000	0.422000
C2	55.701000	0.000000	-0.422000
C2	56.983000	0.000000	0.422000
C2	58.262000	0.000000	-0.422000
C2	59.544000	0.000000	0.422000
C2	60.823000	0.000000	-0.422000
C2	62.105000	0.000000	0.422000
C2	63.384000	0.000000	-0.422000
C2	64.666000	0.000000	0.422000
C2	65.945000	0.000000	-0.422000
C2	67.227000	0.000000	0.422000
C2	68.506000	0.000000	-0.422000
C2	69.788000	0.000000	0.422000
C2	71.067000	0.000000	-0.422000
C2	72.349000	0.000000	0.422000
C2	73.628000	0.000000	-0.422000
C2	74.910000	0.000000	0.422000
C1	76.189000	0.000000	-0.422000
C2	77.471000	0.000000	0.422000
C2	78.750000	0.000000	-0.422000
C2	80.032000	0.000000	0.422000
C2	81.311000	0.000000	-0.422000
C2	82.593000	0.000000	0.422000
C2	83.872000	0.000000	-0.422000
C2	85.154000	0.000000	0.422000
C2	86.433000	0.000000	-0.422000
C2	87.715000	0.000000	0.422000
C2	88.994000	0.000000	-0.422000

	90.276000	0.000000	0.422000
C2			
	91.555000	0.000000	-0.422000
C2			
	92.837000	0.000000	0.422000
C2			
	94.116000	0.000000	-0.422000
C2			
	95.398000	0.000000	0.422000
C2			
	96.677000	0.000000	-0.422000
C2			
	97.959000	0.000000	0.422000
C2			
	99.238000	0.000000	-0.422000
C2			
	100.520000	0.000000	0.422000
C1			
	101.799000	0.000000	-0.422000
C2			
	103.081000	0.000000	0.422000
C2			
	104.360000	0.000000	-0.422000
C2			
	105.642000	0.000000	0.422000
C2			
	106.921000	0.000000	-0.422000
C2			
	108.203000	0.000000	0.422000
C2			
	109.482000	0.000000	-0.422000
C2			
	110.764000	0.000000	0.422000
C2			
	112.043000	0.000000	-0.422000
C2			
	113.325000	0.000000	0.422000
C2			
	114.604000	0.000000	-0.422000
C2			
	115.886000	0.000000	0.422000
C2			
	117.165000	0.000000	-0.422000
C2			
	118.447000	0.000000	0.422000
C2			
	119.726000	0.000000	-0.422000
C2			
	121.008000	0.000000	0.422000
C2			
	122.287000	0.000000	-0.422000
C2			
	123.569000	0.000000	0.422000
C2			
	124.848000	0.000000	-0.422000
C2			
	126.130000	0.000000	0.422000
C1			
	127.409000	0.000000	-0.422000
C2			
	128.691000	0.000000	0.422000
C2			
	129.970000	0.000000	-0.422000

C2	131.252000	0.000000	0.422000
C2	132.531000	0.000000	-0.422000
C2	133.813000	0.000000	0.422000
C2	135.092000	0.000000	-0.422000
C2	136.374000	0.000000	0.422000
C2	137.653000	0.000000	-0.422000
C2	138.935000	0.000000	0.422000
C2	140.214000	0.000000	-0.422000
C2	141.496000	0.000000	0.422000
C2	142.775000	0.000000	-0.422000
C2	144.057000	0.000000	0.422000
C2	145.336000	0.000000	-0.422000
C2	146.618000	0.000000	0.422000
C2	147.897000	0.000000	-0.422000
C2	149.179000	0.000000	0.422000
C2	150.458000	0.000000	-0.422000
C2	151.740000	0.000000	0.422000
C1	153.019000	0.000000	-0.422000
C2	154.301000	0.000000	0.422000
C2	155.580000	0.000000	-0.422000
C2	156.862000	0.000000	0.422000
C2	158.141000	0.000000	-0.422000
C2	159.423000	0.000000	0.422000
C2	160.702000	0.000000	-0.422000
C2	161.984000	0.000000	0.422000
C2	163.263000	0.000000	-0.422000
C2	164.545000	0.000000	0.422000
C2	165.824000	0.000000	-0.422000
C2	167.106000	0.000000	0.422000
C2	168.385000	0.000000	-0.422000
C2	169.667000	0.000000	0.422000

	170.946000	0.000000	-0.422000
C2			
	172.228000	0.000000	0.422000
C2			
	173.507000	0.000000	-0.422000
C2			
	174.789000	0.000000	0.422000
C2			
	176.068000	0.000000	-0.422000
C2			
	177.350000	0.000000	0.422000
C1			
	178.629000	0.000000	-0.422000
C2			
	179.911000	0.000000	0.422000
C2			
	181.190000	0.000000	-0.422000
C2			
	182.472000	0.000000	0.422000
C2			
	183.751000	0.000000	-0.422000
C2			
	185.033000	0.000000	0.422000
C2			
	186.312000	0.000000	-0.422000
C2			
	187.594000	0.000000	0.422000
C2			
	188.873000	0.000000	-0.422000
C2			
	190.155000	0.000000	0.422000
C2			
	191.434000	0.000000	-0.422000
C2			
	192.716000	0.000000	0.422000
C2			
	193.995000	0.000000	-0.422000
C2			
	195.277000	0.000000	0.422000
C2			
	196.556000	0.000000	-0.422000
C2			
	197.838000	0.000000	0.422000
C2			
	199.117000	0.000000	-0.422000
C2			
	200.399000	0.000000	0.422000
C2			
	201.678000	0.000000	-0.422000
C2			
	202.960000	0.000000	0.422000
C1			
	204.239000	0.000000	-0.422000
C2			
	205.521000	0.000000	0.422000
C2			
	206.800000	0.000000	-0.422000
C2			
	208.082000	0.000000	0.422000
C2			
	209.361000	0.000000	-0.422000
C2			
	210.643000	0.000000	0.422000

C2	211.922000	0.000000	-0.422000
C2	213.204000	0.000000	0.422000
C2	214.483000	0.000000	-0.422000
C2	215.765000	0.000000	0.422000
C2	217.044000	0.000000	-0.422000
C2	218.326000	0.000000	0.422000
C2	219.605000	0.000000	-0.422000
C2	220.887000	0.000000	0.422000
C2	222.166000	0.000000	-0.422000
C2	223.448000	0.000000	0.422000
C2	224.727000	0.000000	-0.422000
C2	226.009000	0.000000	0.422000
C2	227.288000	0.000000	-0.422000
C2	228.570000	0.000000	0.422000
C1	229.849000	0.000000	-0.422000
C2	231.131000	0.000000	0.422000
C2	232.410000	0.000000	-0.422000
C2	233.692000	0.000000	0.422000
C2	234.971000	0.000000	-0.422000
C2	236.253000	0.000000	0.422000
C2	237.532000	0.000000	-0.422000
C2	238.814000	0.000000	0.422000
C2	240.093000	0.000000	-0.422000
C2	241.375000	0.000000	0.422000
C2	242.654000	0.000000	-0.422000
C2	243.936000	0.000000	0.422000
C2	245.215000	0.000000	-0.422000
C2	246.497000	0.000000	0.422000
C2	247.776000	0.000000	-0.422000
C2	249.058000	0.000000	0.422000
C2	250.337000	0.000000	-0.422000

	251.619000	0.000000	0.422000
C2			
	252.898000	0.000000	-0.422000
C3			
	254.180000	0.000000	0.422000
C2			
	-0.709275	0.000000	-1.834738
C2			
	0.569725	0.000000	-2.678738
C2			
	0.501450	0.000000	-4.091476
C2			
	1.780450	0.000000	-4.935476
C2			
	1.712174	0.000000	-6.348214
C2			
	2.991174	0.000000	-7.192214
C2			
	2.922899	0.000000	-8.604952
C2			
	4.201899	0.000000	-9.448952
C2			
	4.133624	0.000000	-10.861690
C2			
	5.412624	0.000000	-11.705690
C2			
	5.344349	0.000000	-13.118428
C2			
	6.623349	0.000000	-13.962428
C2			
	6.555074	0.000000	-15.375166
C2			
	7.834074	0.000000	-16.219166
C2			
	7.765798	0.000000	-17.631904
C2			
	9.044798	0.000000	-18.475904
C2			
	8.976523	0.000000	-19.888642
C2			
	10.255523	0.000000	-20.732642
C2			
	10.187248	0.000000	-22.145380
C2			
	11.466248	0.000000	-22.989380
C2			
	11.397973	0.000000	-24.402118
C2			
	12.676973	0.000000	-25.246118
C2			
	12.608698	0.000000	-26.658856
C2			
	13.887698	0.000000	-27.502856
C2			
	13.819422	0.000000	-28.915594
C2			
	15.098422	0.000000	-29.759594
C2			
	15.030147	0.000000	-31.172332
C2			
	16.309147	0.000000	-32.016332
C2			
	16.240872	0.000000	-33.429070

C3	17.519872	0.000000	-34.273070
C2	24.900725	0.000000	-1.834738
C2	26.179725	0.000000	-2.678738
C2	26.111450	0.000000	-4.091476
C2	27.390450	0.000000	-4.935476
C2	27.322174	0.000000	-6.348214
C2	28.601174	0.000000	-7.192214
C2	28.532899	0.000000	-8.604952
C2	29.811899	0.000000	-9.448952
C2	29.743624	0.000000	-10.861690
C2	31.022624	0.000000	-11.705690
C2	30.954349	0.000000	-13.118428
C2	32.233349	0.000000	-13.962428
C2	32.165074	0.000000	-15.375166
C2	33.444074	0.000000	-16.219166
C2	33.375798	0.000000	-17.631904
C2	34.654798	0.000000	-18.475904
C2	34.586523	0.000000	-19.888642
C2	35.865523	0.000000	-20.732642
C2	35.797248	0.000000	-22.145380
C2	37.076248	0.000000	-22.989380
C2	37.007973	0.000000	-24.402118
C2	38.286973	0.000000	-25.246118
C2	38.218698	0.000000	-26.658856
C2	39.497698	0.000000	-27.502856
C2	39.429422	0.000000	-28.915594
C2	40.708422	0.000000	-29.759594
C2	40.640147	0.000000	-31.172332
C2	41.919147	0.000000	-32.016332
C2	41.850872	0.000000	-33.429070
C3	43.129872	0.000000	-34.273070
C2			

	50.510725	0.000000	-1.834738
C2			
	51.789725	0.000000	-2.678738
C2			
	51.721450	0.000000	-4.091476
C2			
	53.000450	0.000000	-4.935476
C2			
	52.932174	0.000000	-6.348214
C2			
	54.211174	0.000000	-7.192214
C2			
	54.142899	0.000000	-8.604952
C2			
	55.421899	0.000000	-9.448952
C2			
	55.353624	0.000000	-10.861690
C2			
	56.632624	0.000000	-11.705690
C2			
	56.564349	0.000000	-13.118428
C2			
	57.843349	0.000000	-13.962428
C2			
	57.775074	0.000000	-15.375166
C2			
	59.054074	0.000000	-16.219166
C2			
	58.985798	0.000000	-17.631904
C2			
	60.264798	0.000000	-18.475904
C2			
	60.196523	0.000000	-19.888642
C2			
	61.475523	0.000000	-20.732642
C2			
	61.407248	0.000000	-22.145380
C2			
	62.686248	0.000000	-22.989380
C2			
	62.617973	0.000000	-24.402118
C2			
	63.896973	0.000000	-25.246118
C2			
	63.828698	0.000000	-26.658856
C2			
	65.107698	0.000000	-27.502856
C2			
	65.039422	0.000000	-28.915594
C2			
	66.318422	0.000000	-29.759594
C2			
	66.250147	0.000000	-31.172332
C2			
	67.529147	0.000000	-32.016332
C2			
	67.460872	0.000000	-33.429070
C3			
	68.739872	0.000000	-34.273070
C2			
	76.120725	0.000000	-1.834738
C2			
	77.399725	0.000000	-2.678738

C2	77.331450	0.000000	-4.091476
C2	78.610450	0.000000	-4.935476
C2	78.542174	0.000000	-6.348214
C2	79.821174	0.000000	-7.192214
C2	79.752899	0.000000	-8.604952
C2	81.031899	0.000000	-9.448952
C2	80.963624	0.000000	-10.861690
C2	82.242624	0.000000	-11.705690
C2	82.174349	0.000000	-13.118428
C2	83.453349	0.000000	-13.962428
C2	83.385074	0.000000	-15.375166
C2	84.664074	0.000000	-16.219166
C2	84.595798	0.000000	-17.631904
C2	85.874798	0.000000	-18.475904
C2	85.806523	0.000000	-19.888642
C2	87.085523	0.000000	-20.732642
C2	87.017248	0.000000	-22.145380
C2	88.296248	0.000000	-22.989380
C2	88.227973	0.000000	-24.402118
C2	89.506973	0.000000	-25.246118
C2	89.438698	0.000000	-26.658856
C2	90.717698	0.000000	-27.502856
C2	90.649422	0.000000	-28.915594
C2	91.928422	0.000000	-29.759594
C2	91.860147	0.000000	-31.172332
C2	93.139147	0.000000	-32.016332
C2	93.070872	0.000000	-33.429070
C3	94.349872	0.000000	-34.273070
C2	101.730725	0.000000	-1.834738
C2	103.009725	0.000000	-2.678738
C2	102.941450	0.000000	-4.091476

	104.220450	0.000000	-4.935476
C2			
	104.152174	0.000000	-6.348214
C2			
	105.431174	0.000000	-7.192214
C2			
	105.362899	0.000000	-8.604952
C2			
	106.641899	0.000000	-9.448952
C2			
	106.573624	0.000000	-10.861690
C2			
	107.852624	0.000000	-11.705690
C2			
	107.784349	0.000000	-13.118428
C2			
	109.063349	0.000000	-13.962428
C2			
	108.995074	0.000000	-15.375166
C2			
	110.274074	0.000000	-16.219166
C2			
	110.205798	0.000000	-17.631904
C2			
	111.484798	0.000000	-18.475904
C2			
	111.416523	0.000000	-19.888642
C2			
	112.695523	0.000000	-20.732642
C2			
	112.627248	0.000000	-22.145380
C2			
	113.906248	0.000000	-22.989380
C2			
	113.837973	0.000000	-24.402118
C2			
	115.116973	0.000000	-25.246118
C2			
	115.048698	0.000000	-26.658856
C2			
	116.327698	0.000000	-27.502856
C2			
	116.259422	0.000000	-28.915594
C2			
	117.538422	0.000000	-29.759594
C2			
	117.470147	0.000000	-31.172332
C2			
	118.749147	0.000000	-32.016332
C2			
	118.680872	0.000000	-33.429070
C3			
	119.959872	0.000000	-34.273070
C2			
	127.340725	0.000000	-1.834738
C2			
	128.619725	0.000000	-2.678738
C2			
	128.551450	0.000000	-4.091476
C2			
	129.830450	0.000000	-4.935476
C2			
	129.762174	0.000000	-6.348214

C2	131.041174	0.000000	-7.192214
C2	130.972899	0.000000	-8.604952
C2	132.251899	0.000000	-9.448952
C2	132.183624	0.000000	-10.861690
C2	133.462624	0.000000	-11.705690
C2	133.394349	0.000000	-13.118428
C2	134.673349	0.000000	-13.962428
C2	134.605074	0.000000	-15.375166
C2	135.884074	0.000000	-16.219166
C2	135.815798	0.000000	-17.631904
C2	137.094798	0.000000	-18.475904
C2	137.026523	0.000000	-19.888642
C2	138.305523	0.000000	-20.732642
C2	138.237248	0.000000	-22.145380
C2	139.516248	0.000000	-22.989380
C2	139.447973	0.000000	-24.402118
C2	140.726973	0.000000	-25.246118
C2	140.658698	0.000000	-26.658856
C2	141.937698	0.000000	-27.502856
C2	141.869422	0.000000	-28.915594
C2	143.148422	0.000000	-29.759594
C2	143.080147	0.000000	-31.172332
C2	144.359147	0.000000	-32.016332
C2	144.290872	0.000000	-33.429070
C3	145.569872	0.000000	-34.273070
C2	152.950725	0.000000	-1.834738
C2	154.229725	0.000000	-2.678738
C2	154.161450	0.000000	-4.091476
C2	155.440450	0.000000	-4.935476
C2	155.372174	0.000000	-6.348214
C2	156.651174	0.000000	-7.192214

	156.582899	0.000000	-8.604952
C2			
	157.861899	0.000000	-9.448952
C2			
	157.793624	0.000000	-10.861690
C2			
	159.072624	0.000000	-11.705690
C2			
	159.004349	0.000000	-13.118428
C2			
	160.283349	0.000000	-13.962428
C2			
	160.215074	0.000000	-15.375166
C2			
	161.494074	0.000000	-16.219166
C2			
	161.425798	0.000000	-17.631904
C2			
	162.704798	0.000000	-18.475904
C2			
	162.636523	0.000000	-19.888642
C2			
	163.915523	0.000000	-20.732642
C2			
	163.847248	0.000000	-22.145380
C2			
	165.126248	0.000000	-22.989380
C2			
	165.057973	0.000000	-24.402118
C2			
	166.336973	0.000000	-25.246118
C2			
	166.268698	0.000000	-26.658856
C2			
	167.547698	0.000000	-27.502856
C2			
	167.479422	0.000000	-28.915594
C2			
	168.758422	0.000000	-29.759594
C2			
	168.690147	0.000000	-31.172332
C2			
	169.969147	0.000000	-32.016332
C2			
	169.900872	0.000000	-33.429070
C3			
	171.179872	0.000000	-34.273070
C2			
	178.560725	0.000000	-1.834738
C2			
	179.839725	0.000000	-2.678738
C2			
	179.771450	0.000000	-4.091476
C2			
	181.050450	0.000000	-4.935476
C2			
	180.982174	0.000000	-6.348214
C2			
	182.261174	0.000000	-7.192214
C2			
	182.192899	0.000000	-8.604952
C2			
	183.471899	0.000000	-9.448952

C2	183.403624	0.000000	-10.861690
C2	184.682624	0.000000	-11.705690
C2	184.614349	0.000000	-13.118428
C2	185.893349	0.000000	-13.962428
C2	185.825074	0.000000	-15.375166
C2	187.104074	0.000000	-16.219166
C2	187.035798	0.000000	-17.631904
C2	188.314798	0.000000	-18.475904
C2	188.246523	0.000000	-19.888642
C2	189.525523	0.000000	-20.732642
C2	189.457248	0.000000	-22.145380
C2	190.736248	0.000000	-22.989380
C2	190.667973	0.000000	-24.402118
C2	191.946973	0.000000	-25.246118
C2	191.878698	0.000000	-26.658856
C2	193.157698	0.000000	-27.502856
C2	193.089422	0.000000	-28.915594
C2	194.368422	0.000000	-29.759594
C2	194.300147	0.000000	-31.172332
C2	195.579147	0.000000	-32.016332
C2	195.510872	0.000000	-33.429070
C3	196.789872	0.000000	-34.273070
C2	204.170725	0.000000	-1.834738
C2	205.449725	0.000000	-2.678738
C2	205.381450	0.000000	-4.091476
C2	206.660450	0.000000	-4.935476
C2	206.592174	0.000000	-6.348214
C2	207.871174	0.000000	-7.192214
C2	207.802899	0.000000	-8.604952
C2	209.081899	0.000000	-9.448952
C2	209.013624	0.000000	-10.861690

	210.292624	0.000000	-11.705690
C2			
	210.224349	0.000000	-13.118428
C2			
	211.503349	0.000000	-13.962428
C2			
	211.435074	0.000000	-15.375166
C2			
	212.714074	0.000000	-16.219166
C2			
	212.645798	0.000000	-17.631904
C2			
	213.924798	0.000000	-18.475904
C2			
	213.856523	0.000000	-19.888642
C2			
	215.135523	0.000000	-20.732642
C2			
	215.067248	0.000000	-22.145380
C2			
	216.346248	0.000000	-22.989380
C2			
	216.277973	0.000000	-24.402118
C2			
	217.556973	0.000000	-25.246118
C2			
	217.488698	0.000000	-26.658856
C2			
	218.767698	0.000000	-27.502856
C2			
	218.699422	0.000000	-28.915594
C2			
	219.978422	0.000000	-29.759594
C2			
	219.910147	0.000000	-31.172332
C2			
	221.189147	0.000000	-32.016332
C2			
	221.120872	0.000000	-33.429070
C3			
	222.399872	0.000000	-34.273070
C2			
	229.780725	0.000000	-1.834738
C2			
	231.059725	0.000000	-2.678738
C2			
	230.991450	0.000000	-4.091476
C2			
	232.270450	0.000000	-4.935476
C2			
	232.202174	0.000000	-6.348214
C2			
	233.481174	0.000000	-7.192214
C2			
	233.412899	0.000000	-8.604952
C2			
	234.691899	0.000000	-9.448952
C2			
	234.623624	0.000000	-10.861690
C2			
	235.902624	0.000000	-11.705690
C2			
	235.834349	0.000000	-13.118428

C2	237.113349	0.000000	-13.962428
C2	237.045074	0.000000	-15.375166
C2	238.324074	0.000000	-16.219166
C2	238.255798	0.000000	-17.631904
C2	239.534798	0.000000	-18.475904
C2	239.466523	0.000000	-19.888642
C2	240.745523	0.000000	-20.732642
C2	240.677248	0.000000	-22.145380
C2	241.956248	0.000000	-22.989380
C2	241.887973	0.000000	-24.402118
C2	243.166973	0.000000	-25.246118
C2	243.098698	0.000000	-26.658856
C2	244.377698	0.000000	-27.502856
C2	244.309422	0.000000	-28.915594
C2	245.588422	0.000000	-29.759594
C2	245.520147	0.000000	-31.172332
C2	246.799147	0.000000	-32.016332
C2	246.730872	0.000000	-33.429070
C3	248.009872	0.000000	-34.273070

Polypropylene

One Chain – 50 Pseudo Atoms Long

calc	0	0	
C3	-1.920000	0.000000	0.422000
C1	-0.641000	0.000000	-0.422000
C3	-0.641000	0.000000	-1.962000
C2	0.641000	0.000000	0.422000
C1	1.920000	0.000000	-0.422000
C3	1.920000	0.000000	-1.962000
C2			

	3.202000	0.000000	0.422000
C1			
	4.481000	0.000000	-0.422000
C3			
	4.481000	0.000000	-1.962000
C2			
	5.763000	0.000000	0.422000
C1			
	7.042000	0.000000	-0.422000
C3			
	7.042000	0.000000	-1.962000
C2			
	8.324000	0.000000	0.422000
C1			
	9.603000	0.000000	-0.422000
C3			
	9.603000	0.000000	-1.962000
C2			
	10.885000	0.000000	0.422000
C1			
	12.164000	0.000000	-0.422000
C3			
	12.164000	0.000000	-1.962000
C2			
	13.446000	0.000000	0.422000
C1			
	14.725000	0.000000	-0.422000
C3			
	14.725000	0.000000	-1.962000
C2			
	16.007000	0.000000	0.422000
C1			
	17.286000	0.000000	-0.422000
C3			
	17.286000	0.000000	-1.962000
C2			
	18.568000	0.000000	0.422000
C1			
	19.847000	0.000000	-0.422000
C3			
	19.847000	0.000000	-1.962000
C2			
	21.129000	0.000000	0.422000
C1			
	22.408000	0.000000	-0.422000
C3			
	22.408000	0.000000	-1.962000
C2			
	23.690000	0.000000	0.422000
C1			
	24.969000	0.000000	-0.422000
C3			
	24.969000	0.000000	-1.962000
C2			
	26.251000	0.000000	0.422000
C1			
	27.530000	0.000000	-0.422000
C3			
	27.530000	0.000000	-1.962000
C2			
	28.812000	0.000000	0.422000
C1			
	30.091000	0.000000	-0.422000

C3	30.091000	0.000000	-1.962000
C2	31.373000	0.000000	0.422000
C1	32.652000	0.000000	-0.422000
C3	32.652000	0.000000	-1.962000
C2	33.934000	0.000000	0.422000
C1	35.213000	0.000000	-0.422000
C3	35.213000	0.000000	-1.962000
C2	36.495000	0.000000	0.422000
C1	37.774000	0.000000	-0.422000
C3	37.774000	0.000000	-1.962000
C2	39.056000	0.000000	0.422000
C1	40.335000	0.000000	-0.422000
C3	40.335000	0.000000	-1.962000
C2	41.617000	0.000000	0.422000
C1	42.896000	0.000000	-0.422000
C3	42.896000	0.000000	-1.962000
C2	44.178000	0.000000	0.422000
C1	45.457000	0.000000	-0.422000
C3	45.457000	0.000000	-1.962000
C2	46.739000	0.000000	0.422000
C1	48.018000	0.000000	-0.422000
C3	48.018000	0.000000	-1.962000
C2	49.300000	0.000000	0.422000
C1	50.579000	0.000000	-0.422000
C3	50.579000	0.000000	-1.962000
C2	51.861000	0.000000	0.422000
C1	53.140000	0.000000	-0.422000
C3	53.140000	0.000000	-1.962000
C2	54.422000	0.000000	0.422000
C1	55.701000	0.000000	-0.422000
C3	55.701000	0.000000	-1.962000
C2			

C1	56.983000	0.000000	0.422000
C3	58.262000	0.000000	-0.422000
C2	58.262000	0.000000	-1.962000
C1	59.544000	0.000000	0.422000
C3	60.823000	0.000000	-0.422000
C3	60.823000	0.000000	-1.962000
C3	62.105000	0.000000	0.422000